Development of DPP-IV inhibitors for the treatment of type 2 diabetes

A thesis submitted to the University of Strathclyde for the Degree of Master of Philosophy by

Salha M Tawati

March, 2011

Strathclyde Institute of Pharmacy and Biomedical Science
University of Strathclyde
Glasgow

"This thesis is the result of the author's original research. It has been composed by the author and has not been previously submitted for examination which has led to award of a degree".

Author's signature:

Date:

Table of contents

List of Figures

List of Tables

Abbreviations

ADA-bp	Deaminase binding protein
Ala	ALanine
AMC	7-Amido-4-methylcoumarin
Arg	Arginine
Asn	Asparagine
Asp	Aspartate
ATR	Attenuated total reflection mode
°C	Celsius
cAMP	Cyclic adenosine monophosphate
$CDCl_3$	Deuterated chloroform
CHN	Carbon, hydrogen and nitrogen elemental analysis
CI	Chemical impact
^{13}C NMR	Carbon nuclear magnetic resonance
d	Doublet
DCM	Dichloromethane
dd	doublet of doublet
DDP	Drug Discovery Portal
DMF	Dimethylformamide
DMSO-d6	Deuterated dimethyl Sulfoxide
DPP-IV	Dipeptidyl peptidase –IV
DS	Discovery Studio
EI	Electron impact
EtOAc	Ethylacetate
FAB	Fast atom bombardment ionizations
FDA	Food and Drug Administration
FTIR	Fourier transform infrared spectroscopy
GIP	Glucose-dependent insulinotropic peptid
GLP-1	Glucagon-like peptide-1
Glu	Glutamic acid
Gly	Glycine
GOLD	Genetic optimization for ligand docking
1H NMR	Proton Nuclear Magnetic Resonance
HbALC	Glycosylated haemoglobin
His	Histidine
HRMS	High resolution mass spectroscopy
HTS	High Throughput Screening
Hz	Hertz
IC_{50}	Half maximal (50%) inhibitory concentration of a substance
IR	Infrared
J	Coupling constant
KBr	potassium bromide
kDa	Kilo-Delton
Ki	The binding affinity of the inhibitor

Km	Affinity of the substrate for the enzyme
M	Mole
m	Multiplet
mg	Milligram
$MgSO_4$	Magnesium sulphate
MHZ	Megahertz
ml	Milliter
µ M	Micromolar
Mpt	melting point
MR	Melting Range
MS	mass spectroscopy
MSD	Merck, Sharpe and Dohme
m/z	mass over charge
NA	not active
NaCl	sodium chloride
NEt_3	Triethylamine
NH_4Cl	Amoniun chloride
s	Singlet
S	Substrate concentration.
SAR	structure activity relationship
Ser	Serine
SIDR	Strathclyde Innovations Drug Research
PDB	Protein Data Bank
Phe	Phenylalanine
POP	Prolyloligopeptidase
ppm	Part per million
Pro	Proline
q	Quartet
t	Triplet
THF	Tetrahydrofurane
TMS	Tetramethylsilane
Trp	Tryptophan
Tyr	Tyrosine
Val	Valine
WHO	World Health Organization

Acknowledgement

First of all, I would like to express my deepest sense of gratitude to my first supervisor, Prof. Simon Mackay, for his guidance, encouragement and excellent advice throughout this project. I am also deeply grateful to second my supervisor, Dr. Oliver Sutcliffe, for his detailed and constructive comments, and for his important support throughout this work.

I am most thankful to Dr. Murray Robertson for his help in learning the laboratory skills. I am also deeply thankful for his help with the docked poses of all the compounds and for his invaluable guidance toward writing of my thesis.

I would like to thank Prof Alan Harvey and Ms. Louise Young of the Strathclyde Innovations in Drug Research for conducting the biological assay testing and Dr Tong Zhang for providing mass spec analysis. I also thank Mr Steve Steer for the help he gave me in the use of the IR instruments.

Many thanks to Dr. Judith Huggan, Dr. Fang Wang and my other colleagues at SIBS 3.12, Murad, Bilal, Hasan, Azra, Jessica, Giacomo, James, and Sabin; thank you all for your help and your invaluable advice to me.

To my husband (Elbibani) thank you for your unconditional support in completing my Mphil, for always believing in me and making me feel that anything is achievable.

To my mother thank you for being such wonderful mother and to my sisters and brothers, especially my sister Mabrouka thanks a lot for your encouragement, love and caring.

To my lovely son (Almontiser) you are a precious gift from Allah. I am so grateful for you and I am very regretful for giving you so little time throughout my Mphil. Lastly, I offer my regards and blessings to all friends who supported me in many respects during my study.

Dedication

In loving memory of my father and my brother(**Almontiser**) , who encourage my curiosity toward science , I'm so sorry that even I have not got the chance to say thanks for you. I know that you would love to see me getting my postgraduate degree; I had always imagined giving a copy to you. Also, I dedicate this thesis in memory of my sister (Nafesa) and my aunt (Sharifa). Also, I dedicate this work to my lovely country Libya.

Abstract

Type 2 diabetes mellitus is a worldwide chronic disorder which is characterised by insulin resistance and high blood glucose levels. The treatment of type 2 diabetes involves the use of traditional oral antidiabetic agents, such as sulphonylurea or glibenclamide, metformin, and/or insulin. However, incidence of the disease is increasing in many parts of the world which means novel antidiabetic agents are needed.

Recently, new types of oral antidiabetic agents that inhibit DPP-IV have been developed and one has been approved for medical use. A collaboration between Strathclyde Innovations in Drug Research (SIDR) and the Drug Discovery Portal (DDP) using a combination of virtual and high throughput screening identified a novel hit (AM11) against DPP-IV. The aim of this project was to modify AM11 to see if inhibition against DPP-IV could be improved.

Compounds with a range of activities against DPP-IV were prepared, but all had comparable or lower activity than AM11. Docking studies were performed to explain the structure-activity relationship profiles of the different libraries prepared.

Chapter 1: Introduction

1.1 Diabetes

Diabetes mellitus (or diabetes) is a metabolic disorder prevalent worldwide. There are two types of diabetes: type 1 (insulin-dependent) and type 2 (non-insulin-dependent). It has been predicted that by the year 2025, about 333 million people will be diagnosed with the disease and approximately 90% - 95% of these patients will suffer from type 2 diabetes. Diabetes is characterised by the deterioration in carbohydrate, protein, and fat metabolism due to total or partial suppression of insulin secretion and/or insulin action (Wu *et al.*, 2009).

1.1.1 Type 1 Diabetes

Type 1 diabetes affects about 3% of the adult population in the UK. It arises from the deterioration of insulin producing β-cells in the pancreas with subsequent low or no blood insulin levels (Holt and Hanley, 2007).

Treatment involves the use of insulin injections as a replacement for the depleted body insulin. In the UK, there are four major types of insulin used to control type 1 diabetes: 1-rapid acting insulin, 2- intermediate-acting insulin, 3- short or regular insulin and 4- long-acting insulin (American Diabetes Association, 2007).

1.1.2 Type 2 Diabetes

Type 2 diabetes is a chronic disease that develops as a consequence of increasing insulin resistance that can no longer be compensated by increasing insulin secretion. It is characterised by a number of pathological defects, such as insulin resistance and progressive β-cell dysfunction (Ludvik *et al.*, 2003). With insulin resistance, glucose production from the liver and uptake from the muscle cannot be controlled by insulin due to several mechanisms including abnormal, absent, or decreased numbers of insulin receptors (Huang and Czech, 2007). Progressive β-cell dysfunction is a complex phenomenon that is caused by the uncontrolled increase of blood glucose level (glucotoxicity) and the formation of free radicals. As a consequence, this leads to the gradual decrease of β-cell numbers (Guillausseau *et al.*, 2008). Type 2 diabetes patients may suffer from several additional complications such as renal disease,

neuropathy, retinopathy, and peripheral vascular insufficiencies as long term complications (Wu *et al.,* 2009).

1.1.3 Management of Type 2 Diabetes

The treatment of type 2 diabetes involves the use of oral antidiabetic agents, such as glibenclamide, metformin, and/or insulin. According to the American Diabetes Association, the first line of treatment for type 2 diabetes is metformin along with lifestyle changes. Second line treatments, such as sulphonylureas and thiazolidines, may be employed to manage glycemia uncontrolled by first line therapy or to replace metformin in cases of contraindications. Although the pharmacological treatment is widely used, attention to diet should be observed (Prisant, 2004). Although there are a number of treatments available, the progress of the disease remains uncontrolled in many parts of the world.

This is due to the progressive nature of the disease and poor patient compliance with continuous monitoring and increased dosages. Also, some oral diabetic agents such as sulphonylurea, may lose their ability to control glycemia because long term use causes damage to β-cells. In addition, using some of these agents may be associated with undesirable side-effects or decreased effectiveness over time (see Table 1.1) (Wu *et al.,* 2009). Although metformin has the ability to control glycemia, it unfortunately can cause deterioration of β-cell function in some patients (Koo *et al.,* 2007).

Despite the great efforts that have been made to understand and manage type 2 diabetes, insulin resistance and diabetes-related complications, such as nerve damage (neuropathy), retinopathy (eye disease), heart disease, and vascular disease (arteriosclerosis), are still a major concern. Type 2 diabetes is a progressive disorder and the patient may eventually have to begin insulin injections (Covington, 2001).

Novel treatments for type 2 diabetes are required to overcome these problems. The development of oral antihyperglycemic drugs that have the ability to enhance glycemic control and preserve pancreatic islet function has been of great interest to researchers. The development of new drugs that specifically target dipeptidyl

peptidase-IV (DPP-IV) has shown great promise as potential therapies as they can prevent the degradation of the incretin hormone, glucagon-like peptide-1 (GLP-1), which can promote the release of insulin and increase glucose uptake in diabetic patients (Wu *et al.*, 2009).

Table 1.1: Common side effects of some oral type 2 antidiabetic drugs.

Class	Example	Mechanism of Action	Adverse Effects
Sulphonylurea First-generation Agents Second-generation Agents	Tolbutamide Glyburide (Micronase), Glipizide (Glucotrol), and Glimepiride (Amaryl)	1-Stimulates insulin release from the β-cells of the pancreas. 2-Slightly improves insulin resistance in peripheral target tissues (muscle, fat).	Hypoglycemia, weight gain, nausea, vomiting, and hypersensitivity reactions.
Biguanide	Metformin (Glucophage)	1-Reduces hepatic glucose output. 2-Enhances insulin sensitivity in hepatic and peripheral tissues.	Metallic taste, diarrhea, nausea, lactic acidosis and vomiting.
α-Glucosidase Inhibitor	Acarbose (Precose) and Miglitol (Glycet)	1-Prevents the enzyme αglucosidase from the digestion of dietary carbohydrates in the small intestine. 2- Inhibits the breakdown and subsequent absorption of carbohydrates, except glucose, from the gut following meals.	Gastrointestinal effects, including abdominal discomfort, bloating, flatulence, and diarrhea.
Meglitinides Non-sulfonylurea Insulin Secretagogue Agent	Repaglinide (Prandin) Nateglinide (Starlix)	1-Stimulates the release of insulin from the pancreatic β-cells.	Weight gain and hypoglycemia.
Thiazolidinedione	Rosiglitazone (Avandia) Pioglitazone (Actos) Troglitazone (Rezulin)	1-Increases insulin sensitivity in both muscle and adipose tissue 2-Prevents hepatic glucose production. 3- Enhance insulin resistance.	Anemia, detrimental cardiac effect, and weight gain.
Insulin	Insulin	Replaces/supplements endogenous insulin hormone to correct deficiency	Hypoglycemia and weight gain.

(Luna and Felinglos, 2001).

1.2 Incretin Hormones and Insulin Secretion

1.2.1 Role of GLP-1 in Regulating Insulin Secretion

The incretin theory was first established in 1930 by LaBarre and Still to explain why orally administered glucose was associated with a greater increase in systemic insulin secretion when compared to glucose given intravenously (Brubaker and Drucker, 2002). Unger and Eisentraut (1969) (Unger and Eisentraut, 1969) and Creutzfeldt (1979) (Creutzfeldt, 1979) further developed this concept to describe incretin as a gut hormone secreted in response to food ingestion, which stimulates glucose-dependent insulin secretion (Brubaker and Drucker, 2002).

Glucose-dependent insulinotropic peptid (GIP) was discovered in 1965. It was the first duodenal incretin hormone discovered that could stimulate insulin secretion. Twenty years later, GLP-1 was identified as another major incretin hormone. Several studies on the insulinotropic actions of GIP and GLP-1 have now shown that both hormones regulate the majority of the observed incretin effects, following ingestion of a meal, and that both contribute equally to this effect (Kieffer and Habener, 1999).

Recently, the biological role of the incretins has been widely investigated. It has been found that there is an increase in blood glucose levels following food ingestion, which leads to an increase in insulin secretion. As a consequence, this stimulates the release of incretin gut hormones, particularly GIP and GLP-1, and, in turn, has a positive impact on increasing the secretion and activity of insulin (Yip and Wolfe, 2000).

GIP is peptide that consists of 42 amino acids. It is secreted by duodenal intestinal K cells, but it has a lesser insulinotropic effect than GLP-1; therefore, GIP does not have an important role in type 2 diabetes and its treatment. GLP-1 is a peptide of about 30 amino acids. It is secreted by T-cells in the gut and mucosa in response to food intake. Both carbohydrates and lipids effectively stimulate its secretion. GLP-1 is responsible for about 50 – 70% of the insulin secretion in response to an oral

glucose load (Idris and Donnelly, 2007). Both GIP and GLP-1 are inactivated by DPP-IV.

1.2.2 Mechanism of Action of GLP-1

The hormone plays a crucial role in regulating insulin secretion by interacting with the g-protein coupled receptor located on the pancreatic β-cell membrane. This mechanism of action is glucose dependent and will only occur when the systemic glucose concentrations are high. When activated, GLP1 stimulates the adenyl cyclase pathway resulting in an accumulation of cyclic adenosine monophosphate (cAMP) inside the cell. The production of cAMP activates protein kinase A, which in turn elevates the intracellular calcium concentration and, subsequently, mobilises insulin granules that lead to the stimulation of insulin secretion (Ding *et al.,* 1997; Gromada *et al.,* 1998).

1.2.3 The role of incretin hormones in type-2 diabetes

In individuals suffering from type 2 diabetes, the incretin effect is partially or totally impaired either due to a reduction in the secretion of GLP-1, but GIP secretion is normal, or due to a reduction in pancreatic response to GIP while the response of GLP-1 is normal. It has been found that both GIP and GLP-1 are important in the pathogenesis of diabetes. Recent studies have shown that up to 70% of insulin secretion is due to the effect of these incretin hormones (Vilsbøll and Knop, 2007).

GLP-1 has an important role in maintaining several biological mechanisms, such as the stimulation of glucose–dependent insulin secretion by its direct effect on the β-cells of the pancreas. It also inhibits glucagon release from pancreatic α-cells. In addition, the role of GLP-1 in the management of patients with type 2 diabetes includes the following:

- Reduces body weight as a consequence of reduced appetite and food intake,
- Decreases gastric motility, and
- Promotes β-cell function.

Due to the fact that the insulinotropic effect of GLP-1 is preserved in type 2 diabetic patients, GLP-1 has become the target for the development of new antidiabetic agents (Mulakayala *et al.,* 2010). There are two possible mechanisms for the development of antidiabetic effects based on the role of prolonging the action of GLP-1. This can be done by developing long acting analogues of GLP-1 or by developing inhibitors for DPP-IV, which is responsible for the degradation of GLP-1 (Idris and Donnelly, 2007).

1.2.4 Effect of GLP-1on β-cells

Positive impacts of GLP-1 on pancreatic β-cells involve enhancement of β-cells neogenesis from progenitor cells in the pancreatic duct epithelium. It also improves proliferation and prevents apoptosis of β-cell (Drucker, 2003). Furthermore, the tropic effect of GLP-1 leads to prevention of progressive β-cell deterioration and failure that appears in type -2 diabetes patients. This has resulted in the clinical theory that the administration of drugs or molecules that improve circulating GLP-1 concentration might improve, maintain, and reactivate β-cells function (Ahren *et al.,* 2005).

1.3 Dipeptidyl peptidase-IV (DPP-IV)

1.3.1 Definition and distribution of DPP-IV

DPP-IV, also known as CD26T-cell activating antigen or adenosine deaminase binding protein (ADA-bp), is a well known pharmaceutical target in the treatment of type 2 diabetes (Engel *et al.,* 2006). DPP-IV is a serine protease that selectively cleaves two amino acid sequences from the *N*-terminal of peptide sequences containing proline or alanine (Figure 1.1). DPP-IV contains 766 amino acid residues and is classified as a type II transmembrane glycoprotein that belongs to the prolyloligopeptidase (POP) family (Lambeir *et al.,* 2003). It consists of six cytoplasmic residues, a 22 residue transmembrane spanning region, and a 738 residue extracellular domain. The 110 kDa DPP-IV is secreted as a mature monomer, but requires (in contrast to POP) dimerisation for normal proteolytic activity. It is expressed by a variety of cells including differential epithelial cells, endothelial cells,

lymphocytes, the capillary bed of the gut mucosa (where most GLP-1 is inactivated locally) where it is located in a membrane associated peptidase form, although it is also available in a soluble form in the plasma and urine (Flatt *et al.*, 2008).

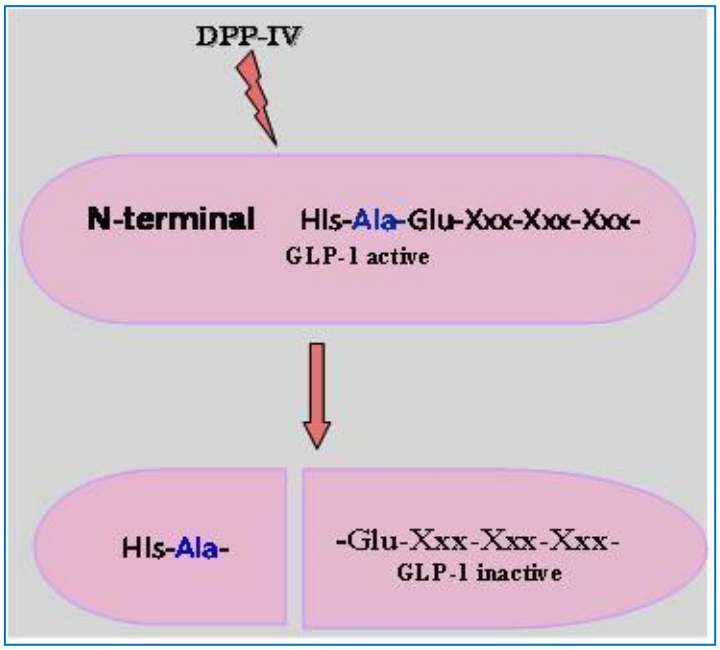

Figure 1.1: DPP-IV cleaves two amino acids from the N-terminal end of peptides, such as GLP-1.

1.3.2. The crystal structure of DPP-IV enzyme:

The first crystal structure of DPP-IV (Figure 1.2) was published as the free form in 2003 (Engel *et al.*, 2003; Oefner *et al.*, 2003; Rasmussen *et al.*, 2003; Hiramatsu *et al.*, 2003: Thoma *et al.*, 2003). Since then, a number of crystal structures of DPP-IV in complexes with small molecules inhibitors have been published (Engel *et al.*, 2006).

There are a number of key structural features in the protein:

- all of the published crystal structures of DPP-IV have described the enzyme as a dimeric or tetrameric structure;
- the enzyme exhibits a tetrameric structure with an almost square central core about which the four monomer units are arranged. Additionally, within each dimeric structure (formed through both hydrophobic and hydrophilic

interactions) there are two loops located at the dimer interface (Chien *et al.*, 2004);

- each DPP-IV monomer has two domains: a *C*-terminal α/β-hydrolase domain and an *N*-terminal 8-bladed β-propeller domain; each blade is formed of a four-strand antiparallel
- β-sheet;
- the propeller domain packs next to the hydrolase domain and the catalytic triad that contains residues (Ser 630, Asp 708, and His 740) that is located within 140 residues of the *C*-terminal region (Ogata *et al.*, 1992);
- the two domains enclose an internal core that contains the active site which has two channels: the propeller opening and side opening channel provide access for the substrates to the active site (Aertgeerts *et al.*, 2004);
- the active site (a deep lipophilic S_1 pocket combined with several exposed aromatic side chains for achieving high affinity small molecule binding) lies between these two domains (Aertgeerts *et al.*, 2004).

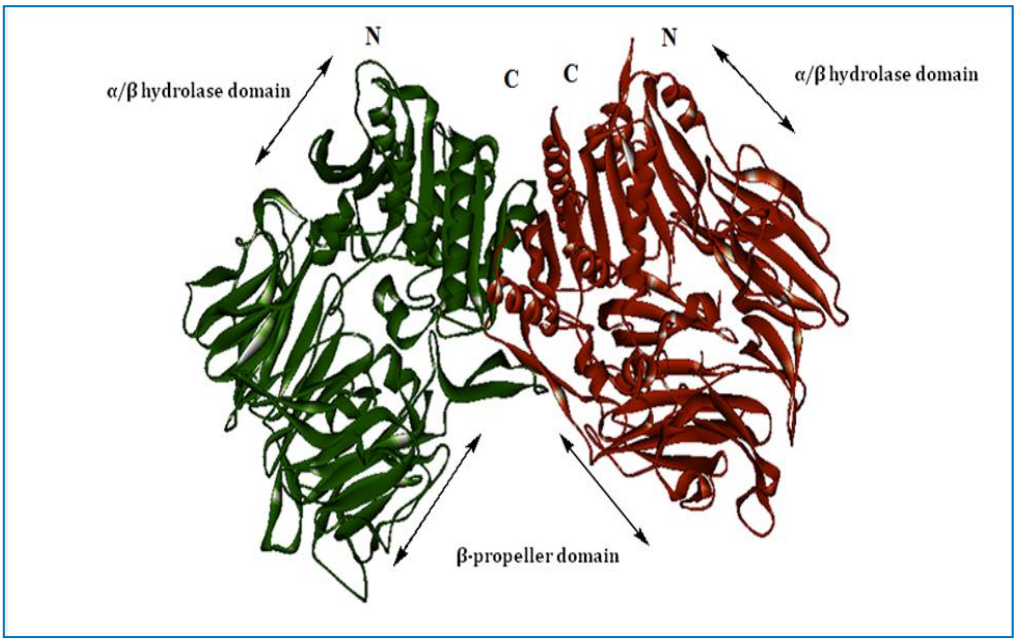

Figure 1.2: Structure of human DPP-IV. The two monomers of DPP-IV are labelled with two different colours; green and orange. The figure was drawn using DS Visualizer (Protein Data Bank: 1N1M) (Rasmussen *et al.*, 2003).

1.3.3 The binding site of dipeptidyl peptidase (DPP-IV)

The active site of DPP-IV (Figure 1.3) has the following features:

- a well-defined hydrophobic S_1 pocket that contains residues Trp 656, Tyr 662, Tyr 631, Val 659, Val 711 and Tyr 666 that determine specificity;
- the hydrophobic S_1 pocket is occupied optimally by an Ala residue or a Pro residue which gives it the unique ability to recognize and cleave peptides that have these amino acids in the penultimate position (Senten *et al.*, 2003);
- the S_2 pocket is hydrophobic and characterized by the presence of Phe 357, Tyr 547, Pro 550, Arg 125. This sub-site can recognize large hydrophobic and aromatic side chains;
- the α, β-hydrolase has a catalytic triad consisting of His 740, Asp 708, and Ser 630. The hydroxyl group of Ser 630 can interact with small molecules and inhibitors containing an electrophilic group (Aertgeerts *et al.*, 2004);
- the two negatively charged Glu 205 and Glu 206 residues at the end of an *α*-helical segment that projects from the β-propeller domain into the active site of the enzyme are negatively charged and form a salt bridge or hydrogen bond with the substrate (Abbott *et al.*, 1999).

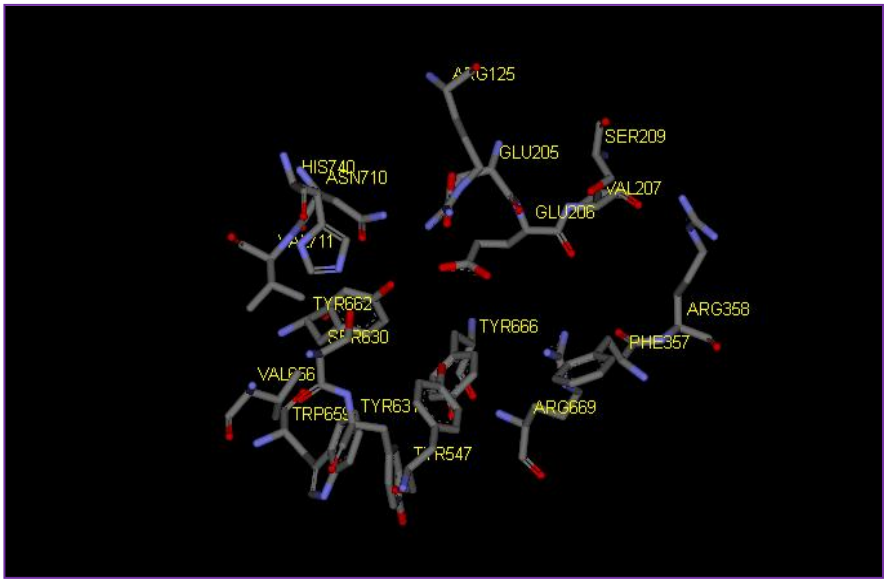

Figure 1.3: Active site of DPP-IV. The figure was drawn using DS Visualizer (Protein Data Bank: 2BUC) (Nordhoff *et al.*, 2006).

1.3.4 Physiological role of DPP-IV

Physiologically, DPP-IV plays an important role in a variety of regulatory processes. It has been found that the presence of alanine at the *N*- terminal of amino acid sequences of GLP-1 and GIP peptides made both incretin hormones optimal substrates for DPP-IV. In addition to cleaving GLP-1, DPP-IV may play a role in the cleavage of other substrates with accessible the amino-terminal Xaa- Pro- or Xaa-Ala- dipeptide sequences. Potential DPP-IV substrates include growth hormone releasing peptide, neuropeptide Y, peptide YY, substance P, bradykinin, gastrin chemokines, stromal cell-derived factor, and macrophage-derived chemokines (Augustyns *et al.*, 2005 ; Geldern and Trevillyan, 2006). Besides its role in type 2 diabetes, DPP-IV is involved in a variety of other diseases, such as obesity, tumour growth, and HIV infection (Geldern and Trevillyan, 2006).

1.4. Inhibition of DPP-IV as a treatment of type-2 diabetes

1.4.1 History of development

The serine protease DPP-IV was first discovered in 1967 and became subject of interest for many researchers. Inhibition of DPP-IV has been utilised to identify the functional importance of the enzyme (Wiedeman, 2007). In the late 1980s, the first inhibitors were discovered by Dr. John Eng, an endocrinologist at the Bronx VA Medical Center in New York, who found that venom from a lizard called the Gila Monster stimulated the production of insulin. Animal models of type 2 diabetes were first tested with a DPP-IV inhibitor in the late 1990s (Goke *et al.*, 1993). One of the early studies by Merck established that oral administration of the proline mimic P32/98 enhanced glucose tolerance in Zucker fatty rats. Further development of P32/98 was not carried out due to toxicity (Figure 1.4) (Flatt *et al.*, 2008; Mulakayala *et al.*, 2010).

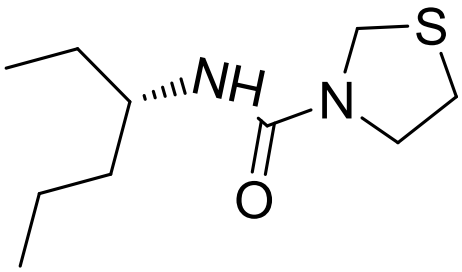

1

Figure 1.4: Chemical structure of P32/98.

After 1995, cyanopyrrolidines were first developed as DPP-IV inhibitors; vildagliptin (LAF237, NVP-LAF237) and saxagliptin (BMS-477118) by Novartis and Bristol-Myers Squibb, respectively, are potent cyanopyrrolidines inhibitors of DPP-IV (Table1.2). In 2004 and 2005 both vildagliptin and saxagliptin entered Phase III clinical trials (Petres, 2007).

Table 1.2: DPP-IV inhibitors.

DPP-IV inhibitor	Company	Structure	Clinical phase
Sitagliptin (Januvia^{TM})	Merck Sharp & Dohme	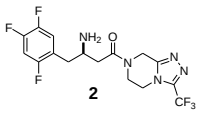 **2**	Available
Vildagliptin (LAF237, NVP-LAF237)	Novartis	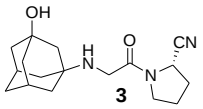 **3**	Approved
Saxagliptin (BMS-477118)	Bristol-Myers Squibb	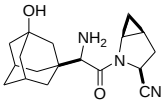 **4**	FDA approved in 2009.
Alogliptin (SYR-322)	TakedaGlobal Research & Development Center, Inc (Syrrx)	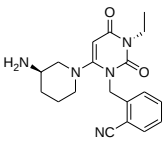 **5**	Phase III
Denagliptin (GW823093)	GlaxoSmithKline	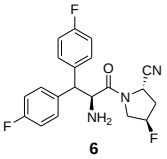 **6**	Phase III
Dutogliptin tartrate (PHX1149**)**	Phenomix	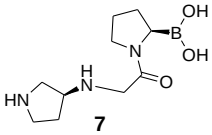 **7**	Phase II
ABT-279	Global pharmaceutical R&D	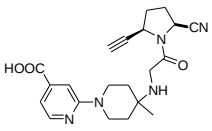 **8**	Phase II

(Wu *et al.,* 2009; Vilsbøll and Knop, 2007; Mulakayala *et al.,* 2010; Flatts *et al.,* 2008)

Sitagliptin was identified by Merck, Sharpe and Dohme (MSD) and was approved in 2006 by the Food and Drug Administration (FDA) for use in monotherapy, and in combination with metformin (or thiazolidinedione) (Miller *et al*., 2008). Following

its approval, other combination therapies with sitagliptin were released and approved, which included sitagliptin-sulphonylurea and sitagliptin-sulphonylurea-metformin. The structurally related inhibitor, vildagliptin (Novartis), has also been approved as a mono- and combination therapy (Geldern and Trevillyan, 2006). Sitagliptin and vildagliptin have been reported to be highly effective oral anti-diabetic agents that have the ability to reduce glycosylated hemoglobin (HbALC) and fasting plasma glucose levels in diabetes patients (Wu *et al*., 2009).

The early work by Merck and Novartis helped to confirm that DPP-IV was a major enzyme involved in the regulation of the incretin hormone GLP-1 and hence led to it becoming a validated clinical target in diabetes therapy. The research confirmed the hypothesis that, in animal models, DPP-IV inhibition resulted in higher levels of circulating active GLP-1, enhanced insulin secretion and improved glucose tolerance. These findings prompted several other pharmaceutical companies to initiate programmes aimed at the identification of DPP-IV inhibitors (Geldern and Trevillyan, 2006). In 2009, saxagliptin was approved by FDA under the trade name Onglyza (Shubrook *et al*., 2009). In addition to these therapies, there are a number of other DPP-IV inhibitors currently in development, and in Phase II (pre-clinical) or Phase III (clinical) trials (Table1.2) (Wu *et al*., 2009).

1.4.2 Mechanism of action of DPP-IV inhibitors

1) Increase insulin secretion

Patients with type 2 diabetes mellitus have an insufficient amount of insulin for the regulation of glucose homeostasis. Therefore, the inhibition of GLP-1 inactivation via DPP-IV inhibitors may stabilize the GLP-1 at a physiological level that is adequate to achieve a physiological insulinotropic effect (Figure1.5) (Farooqi *et al.*, 2010). A non-physiological high concentration of GLP-1 (about 60pmole/l) is associated with some side effects such as delayed gastric emptying, nausea and vomiting. In contrast, the role of DPP-IV inhibitors is to increase the percentage of active GLP-1 after a meal to about 30 p mole/l rather than the total GLP-1 concentration. As a consequence, DPP-IV inhibitors do not induce the GLP-1 side effects (Mest and Mentlein, 2005).

In addition, using DPP IV as antidiabetic agents for type 2 diabetes mellitus patients will produce therapeutic effects without demonstrating any hypoglycemic side effects due to the improvement of insulin secretion in a glucose-dependent manner. In contrast, drugs like the sulphonylurea are used for the treatment of type 2 diabetes based on the enhancement of insulin secretion in a glucose-independent manner, which eventually leads to hypoglycemia and obesity as major side effects (Mest and Mentlein, 2005). In animals that are genetically deficient in DPP-IV, or after a pharmacological treatment with a DPP-IV inhibitor, increasingly active GLP-1, GIP and improved glucose tolerance were observed (Kim *et al.*, 2005).

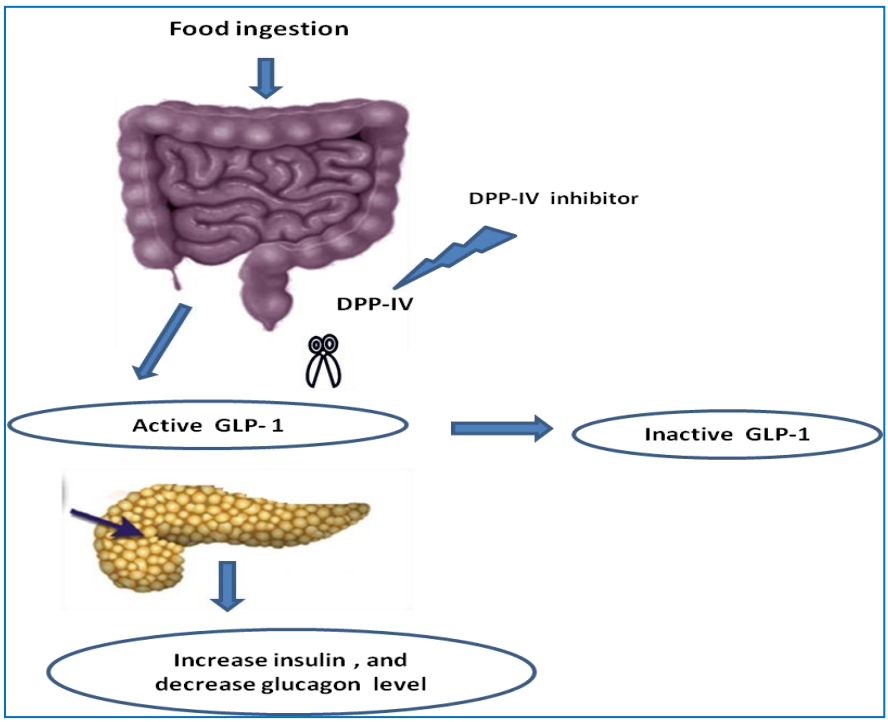

Figure 1.5: Shows mechanism of action of DPP-IV.

2) Decreased glucagon secretion

After a meal, active endogenous GLP-1 and GIP concentrations are increased two- to threefold by DPP-IV inhibitors. This action leads not only to an increase in insulin secretion as long as hyperglycemia is present, but also to a suppression of glucagon secretion. Increased insulin and decreased glucagon levels were also observed in DPP-IV-deficient mice and, after pharmacological treatment with inhibitors, in rodents and humans, consistent with the role of this enzyme in incretin regulation

and metabolic control. DPP-IV inhibitors do not improve glucose tolerance in mice deficient in both GLP-1 and GIP receptors, indicating that these incretins are exclusively responsible for the improved glucose tolerance observed in these animals (Thornberry and Gallwitz, 2009). Idris and Donnelly (2007) concluded that the therapeutic action of DDP-IV inhibitors was because of the suppression of glucose either directly by the action of DDP-IV on pancreatic cells or indirectly.

1.5 Classification of DPP-IV inhibitors

Extensive studies of structure activity relationships (SARs) in many different laboratories have resulted in the identification of a number of potent, competitive DPP-IV inhibitors. Based on structural diversity, the reported DPP-IV inhibitors were classified into two major distinctive classes: peptidomimetic and non-peptidomimetic DPP-IV inhibitors (Havale and Pal, 2009; Mulakayala *et al.*, 2010). The peptidomimetic series (Figure 1.6) can be subdivided into two subclasses: (a) glycine-based (*α*-series) and (b) β-alanine-based (β-series) inhibitors. SAR studies reported that although both series have a common pyrrolidine ring, every series has a different pattern of interaction with the DPP-IV active site (Havale and Pal, 2009; Mulakayala *et al.*, 2010).

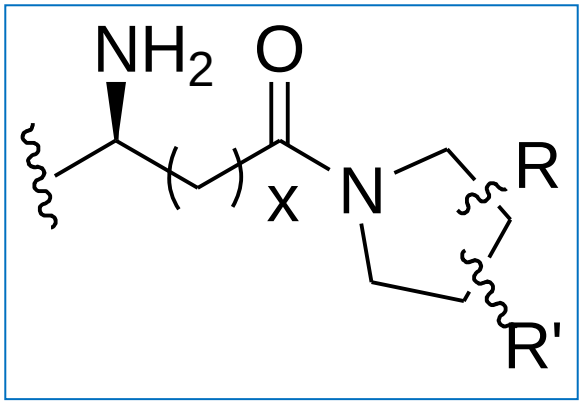

X= 0, α-series or X=1, β-series, R=H , R'=CN

Figure 1.6: General structure of the peptidomimetic series of DPP-IV inhibitors.

1.5.1 The peptidomimetic series

1.5.1.1 Glycine-based (α-series) inhibitors

Subclasses

In general, the α-series can be subdivided into two major classes based on the differences in the R group located at C2 of the pyrrolidine ring: (a) reversible DPP-IV inhibitors when the R is boronic acid [$B(OH)_2$], nitrile (CN) or hydrogen and (b) irreversible inhibitors when the R is the diphenylphosphonate ester [$eP(O)(OPh)_2$] or O-acylhydroxamic acid (CONHOCOR') (Snow and Bachovchin, 1995; Senten *et al.*, 2003; Demuth *et al.*, 1988).

General structural activity relationship (SAR) of α-series

In terms of the SAR of the α-series, several studies relied on molecular modeling and the crystal structure of DPP-IV and reported two possible ways of interaction between α-series inhibitors and the DPP-IV active site (Figure1.7) (Havale and Pal, 2009) :

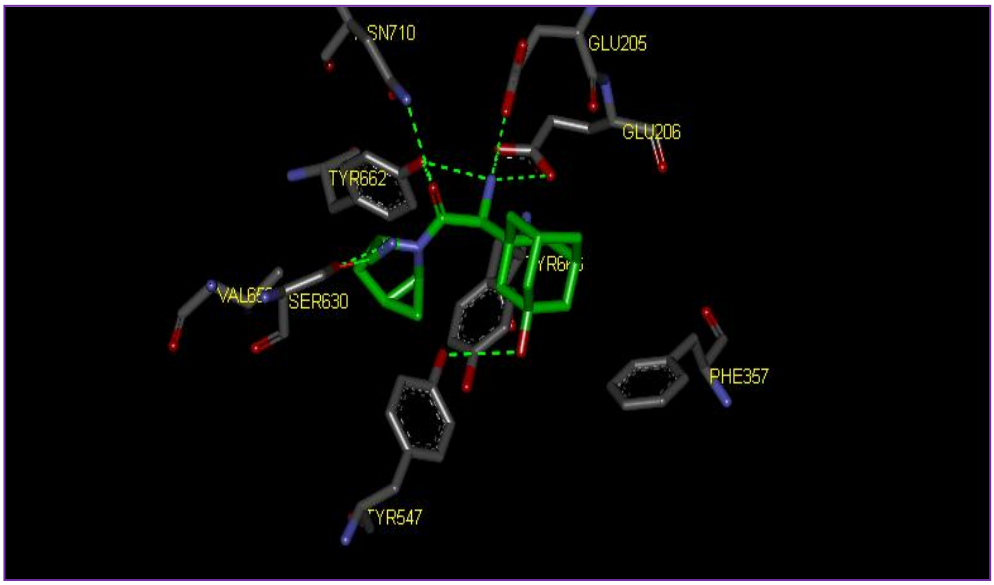

Figure 1.7: Key Interactions of compound 4 with the DDP-IV active site (Protein Data Bank: 3BJM) (Metzler *et al,* 2008).

- The free amino group adjacent to carbonyl group formed a salt bridge with the negatively charged Glu 205 and/or Glu 206 residues.

- A hydrogen bond formed between the carbonyl group and Arg125.

Furthermore, a number of important SARs for α-series inhibitors were identified:

- Irreversible inhibitors that included an electrophile such as a nitrile group at C2 of the pyrrolidine ring (compound **3**) (Table 1.2), showed optimum potency due to the formation of a covalent bond with the active site Ser 630 (Villhauer *et al.*, 2003).
- Replacement of the pyrrolidine ring with piperidine or oxazolidine markedly decreased the activity. However, the addition of a thiazolidine, such as compound **1** (Figure1.4) instead of a pyrrolidine ring had a positive impact on the stability and provided moderate potency (Ahn, 2005).
- Modification of the pyrrolidine ring, such as fusing the pyrrolidine ring with a cyclopropyl ring, afforded enhanced chemical stability and the high inhibitory potency (compound **4**) (Table 1.2) (Magnin *et al.*, 2004 ; Augeri *et al.*, 2005).

1.5.1.2 2-Cyano pyrrolidine-based inhibitors

This class of inhibitors contains a proline mimic ring and a nitrile group and have been shown to interact with the DPP-IV complex through the same two key interactions that are characteristic of the glycine-based (α-series) inhibitors. In addition, the 2-cyanopyrrolidide group presents a rapid and reversible inhibition of DPP-IV. The first 2-cyano pyrrolidine-based inhibitor to be developed was compound **3** with an IC_{50} = 34 nM (Table 1. 2) (Villhauer *et al.*, 2003).

Based on this inhibitor, a number of important SARs of cyanopyrrolidine-type inhibitors were identified:

- The pyrrolidine ring can accept minor modifications that can interact with the hydrophobic S_1 pocket with high affinity.
- A nitrile group on the pyrrolidine ring is essential for maximum potency. Removal of the nitrile group from the pyrrolidine ring increases stability but lowers potency as in compound **1** (IC_{50} = 320 nM) (Sorbera *et al.*, 2001).

- Addition of the alkyne group at C2 of the pyrrolidine ring in place of the nitrile group affords compound **8** (Table 1.2) with good potency (IC_{50}=1.0 nM) and is associated with superior selectivity against DPP-7, DPP-8 and DPP- 9 (Mulakayala *et al.,* 2010).
- Incorporation of a fluoro substituent at the C-4 position of the pyrrolidine ring introduces a new series of potent DPP-IV inhibitors such as compound **6** (Table 1.2) which is a potent, stable and selective inhibitor (IC_{50}= 22 nM) that prolongs the duration of action in both rat and dog (Haffner *et al.,* 2003).
- The presence of a bulky substituent such the adamantyl group (compound **4**) (IC_{50} = 26 nM) or 4-cyanopyridine (compound **5**) **(**IC_{50} = 4 nM) introduces ring constraints that provide good inhibition with increased selectivity (Tsai *et al.,* 2006).
- A boronic acid moiety at the 2-position of the pyrrolidine ring, such as compound **7** (Table 1.2) (IC_{50} = 320 nM), provides effective inhibition of DPP-IV associated with moderate selectivity (Burkey *et al.,* 2008).

1.5.1.3 Alanine-based inhibitors or β-series

Other types of DPP-IV inhibitors are structurally different from cyanopyrroldine - based compounds and usually have an aromatic ring that occupies the S_1 pocket instead of the proline mimetic ring that is involved in covalent bond interactions. The majority of the initial DDP-IV inhibitors in this class were α- amino acids such as the phenylalanine derivatives (Table 1.2). However, more recent novel DDP-IV inhibitors incorporating β-amino acids have been developed. For example, sitagliptin (compound **2**) (Table 1.2) is also known as a non-substrate like inhibitor. Compound **2** (IC_{50} = 18 nM) was the first DPP-IV inhibitor to receive FDA approval for the treatment of type 2 diabetes (Kowalchick *et al.,* 2007). Unlike the cyanopyrroline-based inhibitors, compound **2** contains a bicyclic heterocycle and a β-amino acid within its structure (Edmondson *et al.,* 2007).

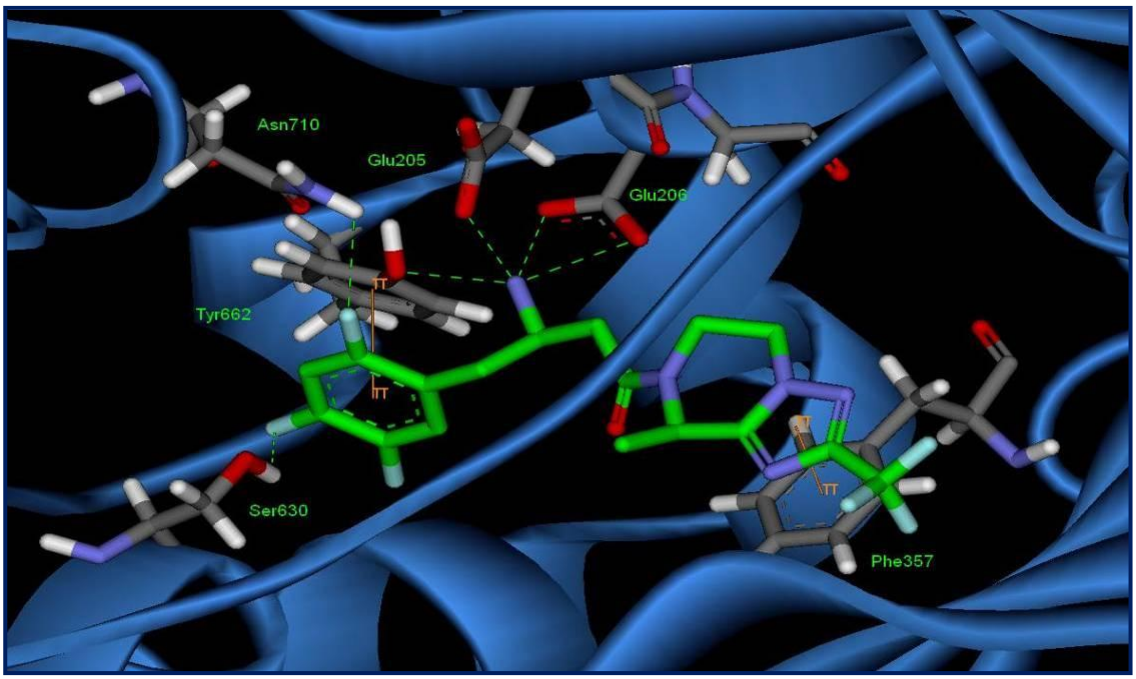

Figure 1.8: The crystal structure of compound 2 co-crystallised in DPP-IV. The hydrogen bonds shown as dashed green lines and π-π interactions as continuous orange lines (Protein Data Bank: 2QOE) (Kowalchick *et al.*, 2007).

In terms of SAR, it has been found that the trifluorophenyl, amino and trifluoromethyl moieties are essential for activity (Figure1.8). The S_1 pocket was occupied by the trifluorophenyl group through π-stacking interactions between the aromatic ring of compound **2** and the aromatic side chain of Tyr 662. A salt bridge is formed between the amino group and Tyr 662 and two glutamate residues, Glu 205 and Glu 206. Fluorine atoms of the trifluorophenyl group form hydrogen bonds with residues Ser 630 and Asn 710, and the triazolopiperazine core has been shown to interact with residue Phe 357 via π-stacking (Edmondson *et al.*, 2007). Orientation of compound **2** within the active site through these interactions provides reversible, non-covalent binding with DPP-IV. Recently, through superimposing the X-ray structures of α-series derivatives and β-series compounds, it has been found that the fluoropyrrolidine amide moiety of the α-series and the fluorobenzyl group of the β-series occupied the same pocket in the DPP-IV active site (Liang *et al.*, 2008).

1.5.2 Non-peptidomimetic inhibitors

Non-peptidomimetic inhibitors have a different structure from the traditional α-series or β-series. Despite differences in the chemical structure, the non-peptidomimetic inhibitors have similar key interactions with the DPP-IV active site as the peptidomimetic inhibitors (Figure 1.9) (Havale and Pal, *2009*). This class of DPP-IV inhibitor is exemplified by compound **5** (Table 1.2), which has been recently introduced by Syrrx as a potent and selective inhibitor (IC_{50}= 4 nM).

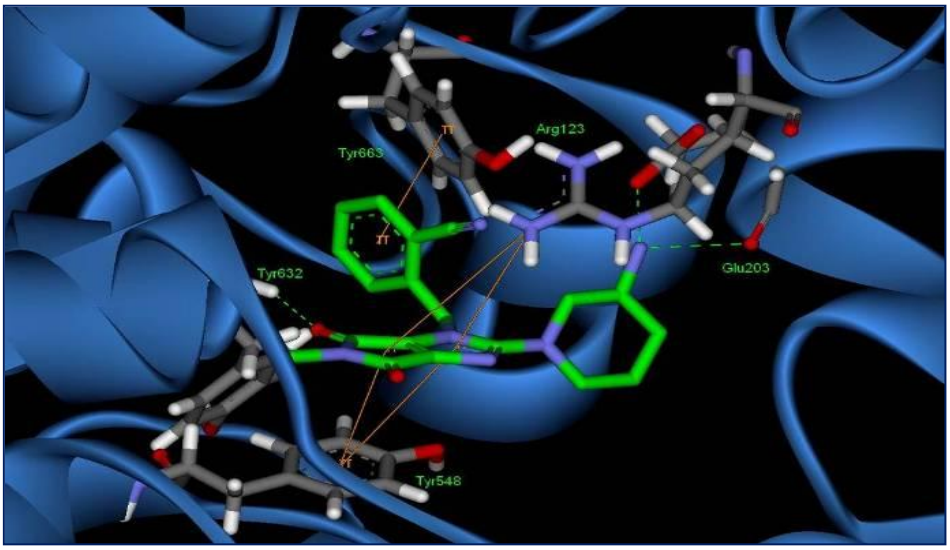

Figure1.9: Key Interactions of compound 5 with the DDP-IV active site (Protein Data Bank: 2I3Z) (Kurukulasuriya *et al.*, 2006).

The X-ray crystal structure of compound **5** co-crystallised in DPP-IV revealed that the amino group at C3 of the piperidine ring formed a salt bridge with Glu 203 and Glu 204. The uracil moiety was oriented to form a π-stacking interaction with Tyr 548 and another a π-stacking interaction was found between the benzyl group and Tyr 663. Moreover, the carbonyl group of the uracil ring formed hydrogen bonds with Tyr 632 (Kurukulasuriya *et al.*, 2006).

1.6 Pharmacology of DPP-IV inhibitors

The pharmacokinetic and pharmacodynamic properties, efficacy, safety and tolerability of a numbers of DPP-IV inhibitors been assessed in several clinical studies. Sitagliptin, alogliptin, saxagliptin and vildagliptin competitively inhibit DPP-IV with high affinity. Sitagliptin and vildagliptin show clinical efficacy for the treatment of type 2 diabetes in both monotherapy and in combination with traditional oral anti-glycemic agents, including metformin in studies lasting at least 6 months and up to 2 years for sitagliptin. Recent studies have showed that both sitagliptin and vildagliptin possess low susceptibility for drug–drug interactions, especially with other anti-diabetic oral drugs (Geldern and Trevillyan, 2006).

1.7 Advantages of DPP-IV inhibitors:

DPP-IV inhibitors have significant advantages over currently available antidiabetic drugs. By improving the concentration of biologically active GLP-1, insulin will be released and glucagon production inhibited in a strictly glucose-dependent manner, which is expected to have a lower risk of hypoglycemia. Moreover, no weight gain was anticipated with DPP-IV inhibitors (Nauck *et al.,* 2007). Interest in this class was also driven by an emerging body of evidence that DPP-IV inhibitors have a long term beneficial impact on the β- cell mass and function (Geldern and Trevillyan, 2006). Diabetes type 2 patients have only 50% of the normal mass of islet cells due to accelerated apoptosis, and DPP-IV inhibitors may reverse loss of β-cell function, particularly with early diagnosis. Recent studies on mice and rats showed that there was stimulation of β-cell proliferation, induction of islet neogenesis, and inhibition of β-cell apoptosis leading to a larger β-cell mass (Pospisilik *et al.,* 2003).

1.8 Summary

DPP-IV inhibitors are considered one of the most promising treatments of type 2 diabetes. Inhibition of the DPP-IV enzyme increases the half life and improves the activity of incretin hormones that play a crucial role in the regulation of insulin secretion and blood glucose (Green *et al.,* 2006). Type 2 diabetes is a chronic metabolic disease characterized by pancreatic β-cell dysfunction, deficiency in insulin secretion, insulin resistance and/or increased hepatic glucose production. DPP-IV inhibitors are capable of controlling glycemia without inducing hypoglycemia and weight gain. Furthermore, DPP-IV inhibitors to date have the advantage of being orally active and have few gastrointestinal side effects. In addition, inhibition of DPP-IV may preserve or reverse the decrease β-cell function that is characteristic of type2 diabetic patients. It seems clear that DPP-IV inhibitors are going to be an effective therapy for patients with type 2 diabetes and further studies are required to elucidate whether this class of drugs are capable of modifying the progression of those diseases associated with type 2 diabetes (Vilsbøll and Knop, 2007).

1.9 Aims and Objectives

This project is based on the previous work by Strathclyde Innovations in Drug Research (SIDR) and the Drug Discovery Portal (DDP) at the University of Strathclyde. Originally, 14,000 compounds (Maybridge Hit Finder V7) were evaluated for activity *in vitro*, via an established High Throughput Screening (HTS) method developed within SIDR. In conjunction with this, the DPP set out to produce a virtual model of DPP-IV that would enrich the percentage of actives in future selections of compounds. Ideally, with a validated model, virtual screening can improve hit rates by over 100-fold; typically, HTS produces 0.1 % enrichment, whereas virtual screening aims for 10% (Shoichet, 2006).

One of the active hits identified from the Maybridge collection using this approach against porcine DPP-IV was SB1072 (Figure 1.10) which had a K_i value of 2.4 μM. The absolute geometry of the double bond was not defined by the supplier, and was therefore treated as a racemic mixture. SB1072 has a chemical structure that is a

unique in comparison with other DPP-IV inhibitors. The synthesis of pure *E* and *Z* isomers of SB1072 by a previous researcher established that the *Z* conformation was the active form, and that the *E* conformation showed no activity at all (Table 1.3).

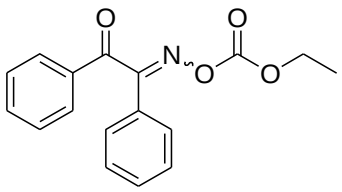

9

Figure 1.10: Chemical structure of the racemic hit SB1072.

Table 1.3: Summary of the original library and its biological activities against porcine DPP-IV.

Codes	Structures	K_i
AM10	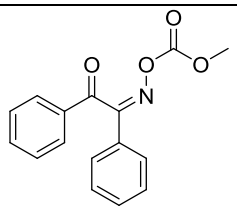	1.5 μM
AM11	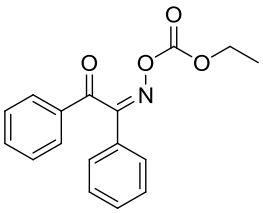	0.5 μM
AM14	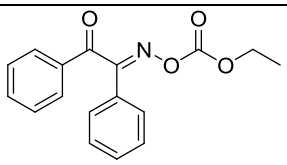	>30 μM
AM20	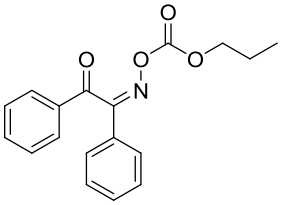	0.8 μM
AM21	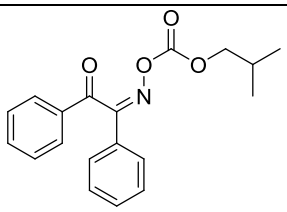	4 μM
AM22	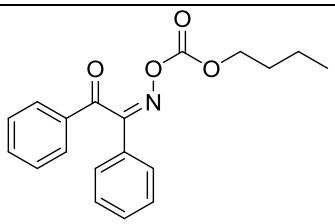	>30 μM

The aim of this project was to develop a series of compounds based on AM11 that includes an investigation of the impact of different modifications on the interactions with DPP-IV aided by molecular modeling.

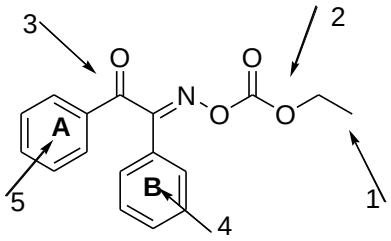

Figure 1.11: Modifications on AM11.

The specific objectives were as follows (Figure 1.11):

1. To investigate the effect of different side chains on the interaction with DPP-IV.
2. To determine the effect of removing the oxygen atom and investigating the chemical stability and interaction with DPP-IV.
3. To determine the importance of the carbonyl group in the potency of AM11.
4. To explore the effect of hydrophobic substitutions (halogens) on the two phenyl rings, and their relative positions on Ring A and Ring B.
5. To determine the effect of a hydrophilic group on the phenyl rings.

Chapter 2: Results and discussion

2.1 Synthetic Strategy (Scheme 2.1)

Library 1: Expansion of the chloroformate derived series. As the original set of active compounds came from this library, further investigation of the formate moiety was initiated via the introduction of halogenated and unsaturated formate side chains – expansion was limited by the fact that we had already demonstrated that AM09 (Figure 2.1) and AM22 (Table1.3) were inactive.

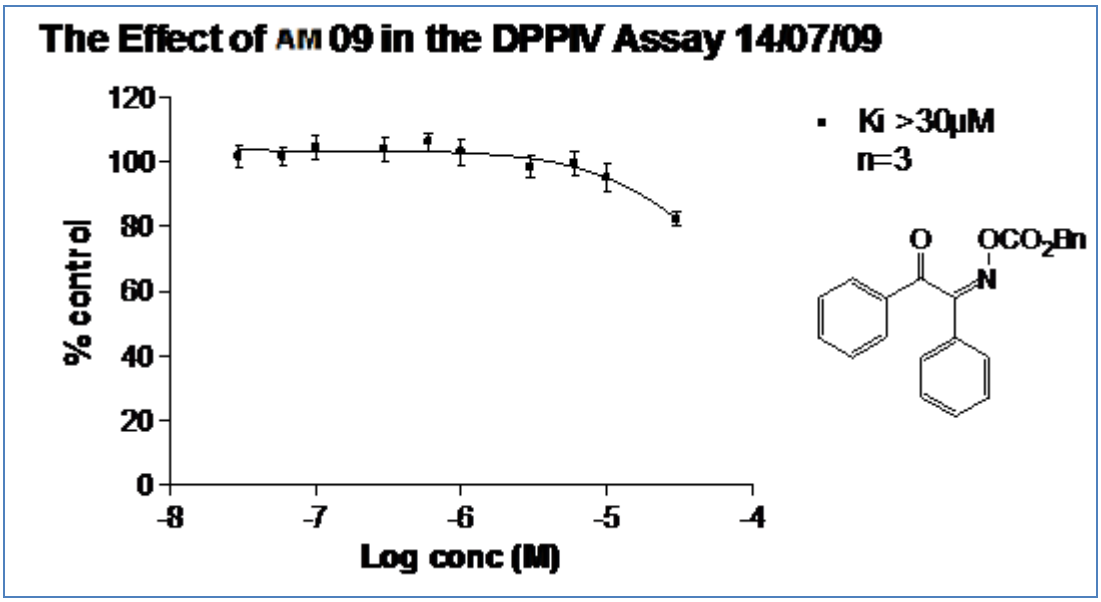

Figure 2.1: DPP-IV Assay results for compound AM09.

Library 2: Synthesis of acid chloride derived series. Substituting the chloroformates with acid chlorides would allow us to explore the effect of replacing the oxygen of the side chain with a carbon atom. This would help to determine the importance of the binding interactions of the oxygen on the outer edge of the pocket.

Library 3: Determining the importance of the carbonyl group. A small library of compounds was synthesized to establish the importance of the carbonyl group in binding to the enzyme active site and its effect on the orientation of the molecule within the binding site.

Library 4: Halogen substitutions on the phenyl ring. Introducing halogens into the phenyl ring at *para*- or *meta*-positions would allow us to investigate possible new interactions and provide a handle for further extensions to the molecule.

Library 5: Halogens at different sites on the benzoyl group. As shown by Haffner *et al* (2003), the addition of halogens into the ring that occupies the S_1 pocket increases hydrophobicity, selectivity, and potency toward DPP-IV.

Library 6: Substituents in both aromatic rings. The final approach was to substitute both rings at the *para* position with a methoxy group to investigate the effect of a hydrophilic substituent on activity.

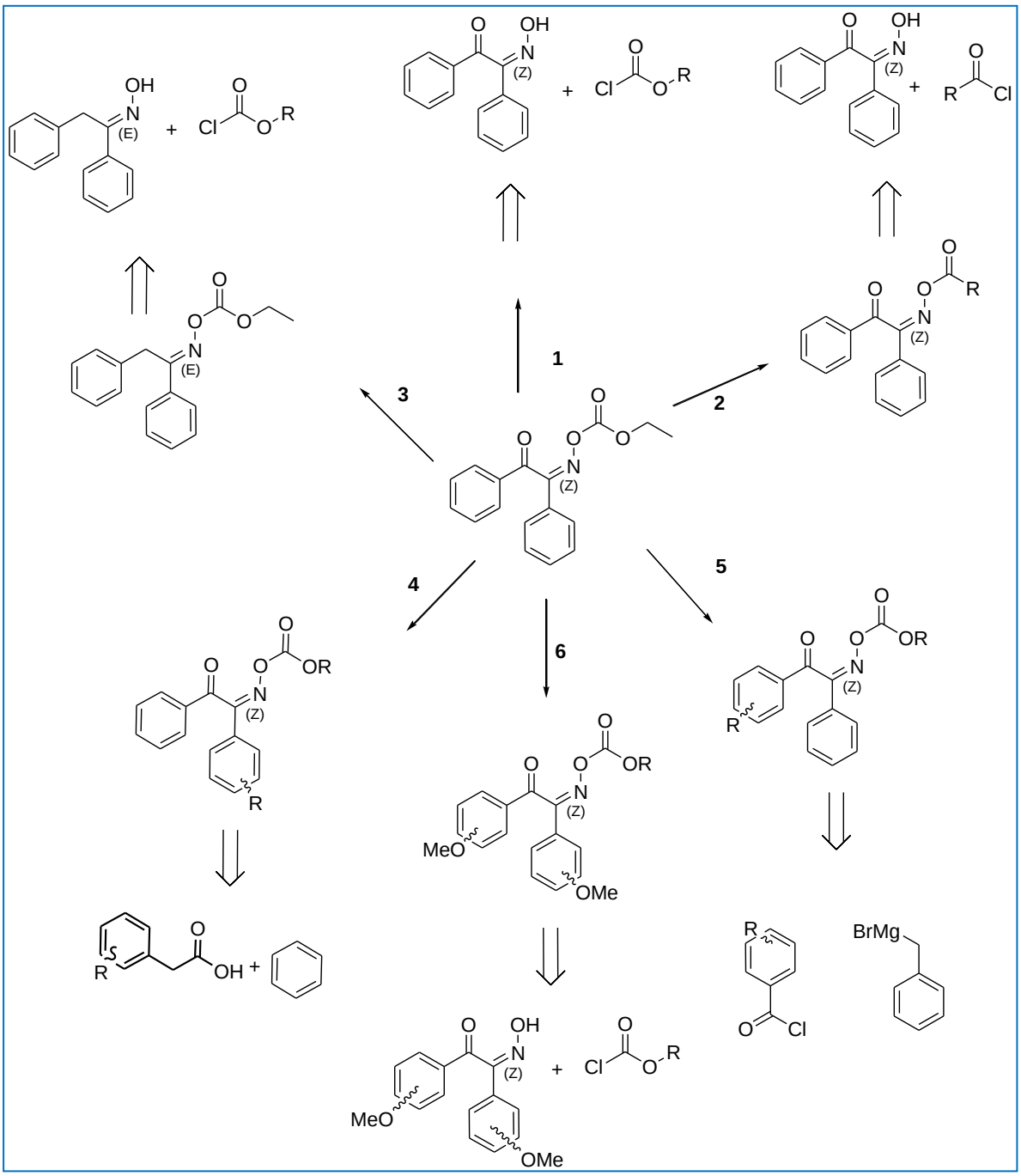

Scheme 2.1: General synthetic strategies where numbers 1-6 refer to the libraries described on the previous page.

2.2 Library 1: Expansion of the chloroformate-derived series

Derivatization of compound **10** with ethyl chloroformate to produce the most active compound AM 11 (K_i =0.5 μM), in association with the results of those compounds

with larger substituents at this position for which there was no activity against DPP-IV (e.g. AM22) suggested that we should prepare compounds with small side chains.

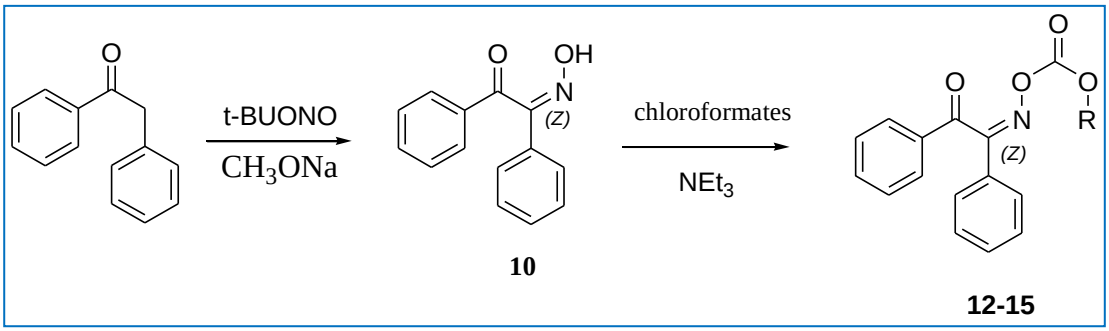

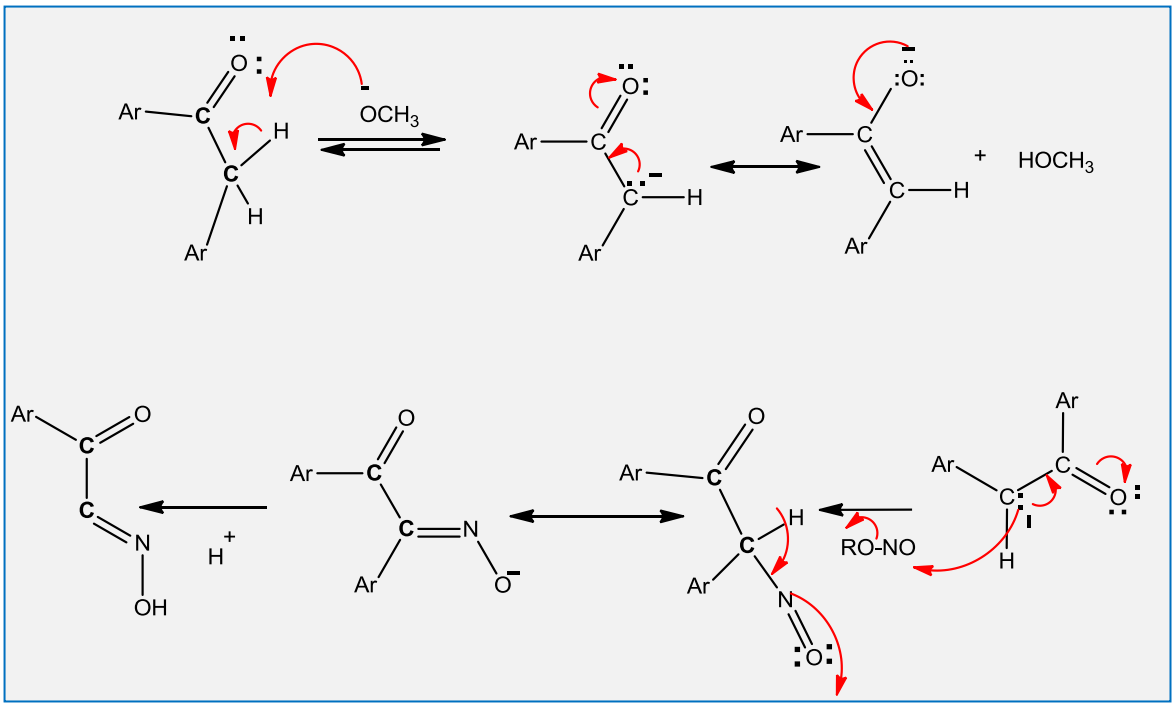

Scheme 2.2: Preparation and mechanism for the synthesis of 2-(hydroximino)-1, 2-diphenylethanone (10-11).

San Martín *et al*. (1995) reported that a racemic mixture of compounds (**10**) and (**11**) could be synthesized from 1,2-diphenylethanone using *tert*-butyl nitrile and sodium methoxide. Mechanistically, in the presence of sodium methoxide which acts as strong base, a nitrosonium ion directly attacks the ketone enolate, followed by tautomerization of the obtained nitroso compound to ketoxime (Scheme 2.2) (Iglesias

and Williams, 1989). The proton NMR of the crude product displayed separate **OH** proton signals due to both ***Z*** and ***E*** isoforms being formed (Figure 2.2), with the ***E*** isomer having a more deshielded proton (**δ 12.47** ppm) compared with the ***Z*** isomer at δ **11.76** ppm (Kileinspehn *et al.*, 1967).

Replication of the techniques to separate the geometric isomers previously developed within the group proved troublesome. A new reproducible and robust method was achieved and modified for the various derivatives produced during this work as follows: the concentrated dichloromethane (DCM) extract was mixed with hot toluene, and the undissolved solid removed by filtration to isolate the ***E*** isomer as an off-white solid (compound **11**). Recrystalization of the remaining crude product from the organic mixture using diethyl layer afforded the **Z** isomer (compound **10**) as a white solid. This separation was confirmed by proton NMR (Figure 2.2), where only one singlet was detected for the **OH** of the ***Z*** ketoxime at **δ11.76** ppm and one for the ***E*** ketoxime at **12.47** ppm. The carbon NMR spectrum supported these findings.

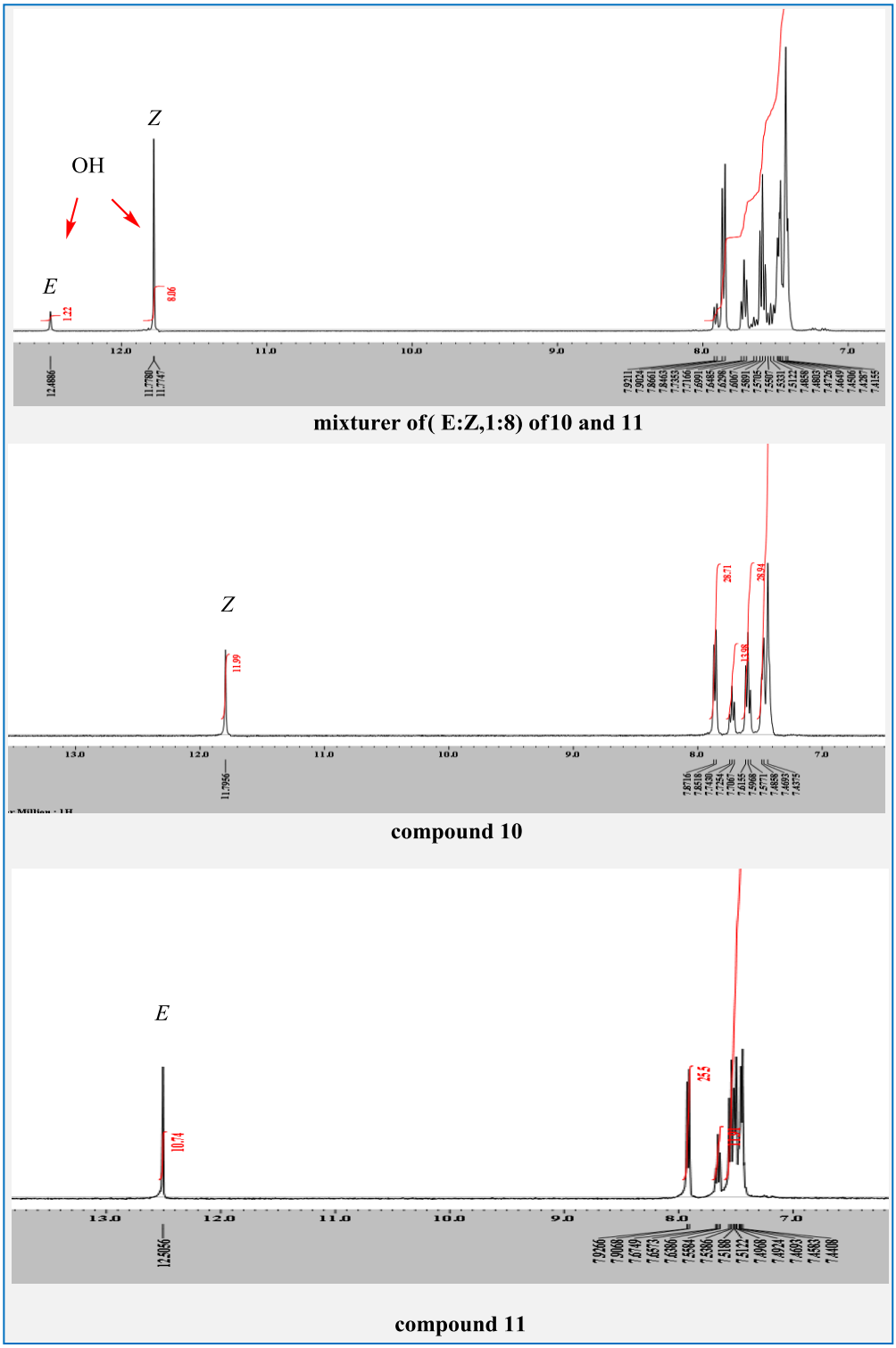

Figure 2.2: Separation of two isomers compounds (10) and (11).

2.2.1 Synthesis of further formate derivatives.

As previously shown, compounds with butyl- and isobutyl formate (Table1.3) side chains were inactive. Smaller side chains were therefore introduced (isopropyl, allyl, cholоromethyl and 2-bromoethyl formate) to expand the original series by reacting with compound **10** under anhydrous conditions and in the presence of triethylamine (Table 2.1).

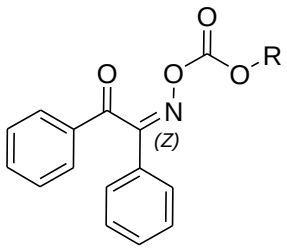

Table 2.1: The structure and the biological results for the first library.

Compound	R	Yield %	K_i (µM)*
12		57.2	NA
13	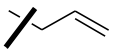	29.2	102
14	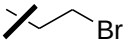	29.9	11.7
15		14.1	5.8

K_i values are the average of two readings.

2.2.2 Docking results and biological results.

The crystal structure of DPP-IV used for the docking studies was porcine DPP-IV. The crystal structure (2BUC) (Nordhoff *et al.*, 2006) was downloaded from the Protein Data Bank (PDB). Compounds were docked using GOLD (UPC) Version 4.1, and visualized using Discovery Studio Visualizer (Accerlys) to predict the binding of the synthesized compounds with the active site of DPP-IV. Docking of AM11 in the active site of the DPP-IV enzyme showed that it had a unique orientation inside the active site that was different from other DPP-IV inhibitors, although the key interactions are similar to that of sitagliptin (Figure 1.8), such as the formation of hydrogen bonding with the same amino acid residues. AM11 represents the hit compound, particularly when the resolved compound showed a significant increase in the K_i value from 2.4 μM for the commercially purchased SB1072 to 0.5 μM for AM11. The enhanced activity of AM11, along with its unique orientation inside the active site, provided the evidence that the *Z* isomer is the active isomer.

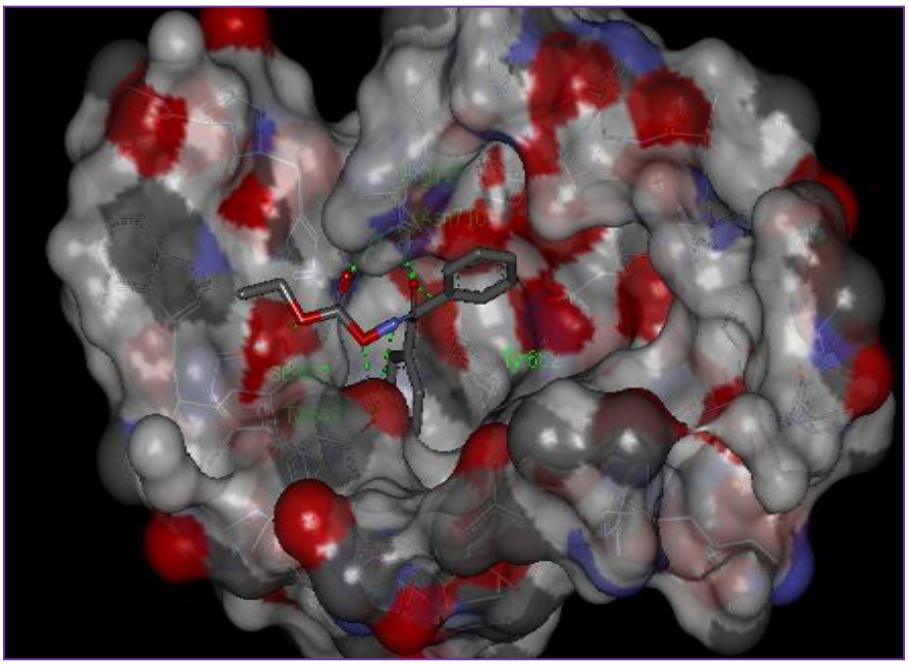

Figure 2.3: docked AM11 in the active site of DPP-IV.

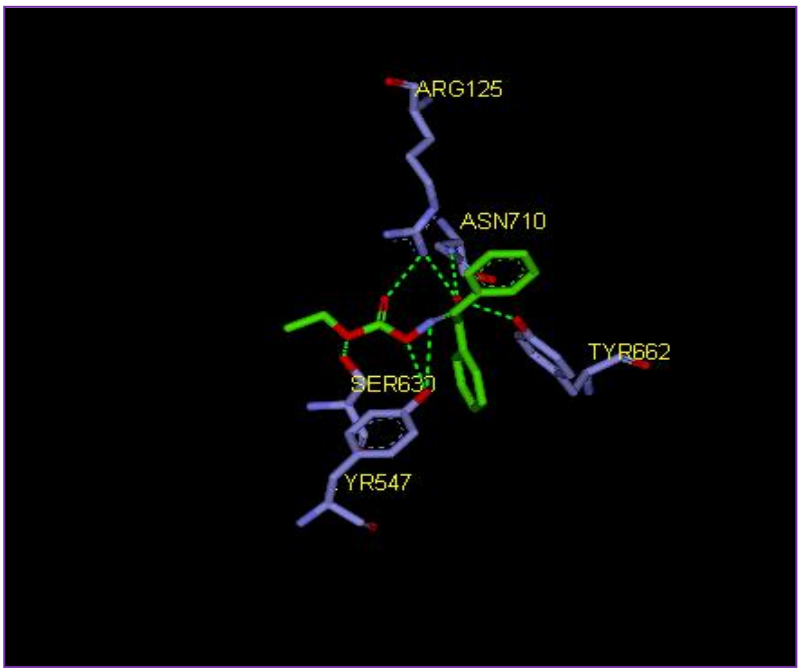

Figure 2.4: key interactions of AM11 in the active site of DPP-IV.

Figure 2.4 shows that seven hydrogen bonds may be essential for the activity of AM11: the carbonyl group adjacent to phenyl ring forms three hydrogen bonds with Arg 125, Asn 710, and Tyr 662; two hydrogen bonds are formed between Tyr 547 and the oxygen and the nitrogen of the oxime; the carbonyl group of the formate side chain forms a hydrogen bond with Arg 125; and the final hydrogen bond is between the oxygen of the formate side chain and Ser 630. Moreover, the aromatic ring adjacent to the carbonyl group occupies the hydrophobic S_1 pocket, while the other aromatic ring is in the S_2 pocket. The pose of AM11 suggests the alkyl side chain is orientated at the outer edge of the pocket (Figure 2.4).

As it can be seen in Table 1.3, replacement of the ethyl formate by the propyl formate showed good inhibition of DPP-IV. However, introducing a branched side chain such as the isopropyl formate (compound **12**) led to no inhibition (Table 2.1; Figures 2.5 and 2.6).

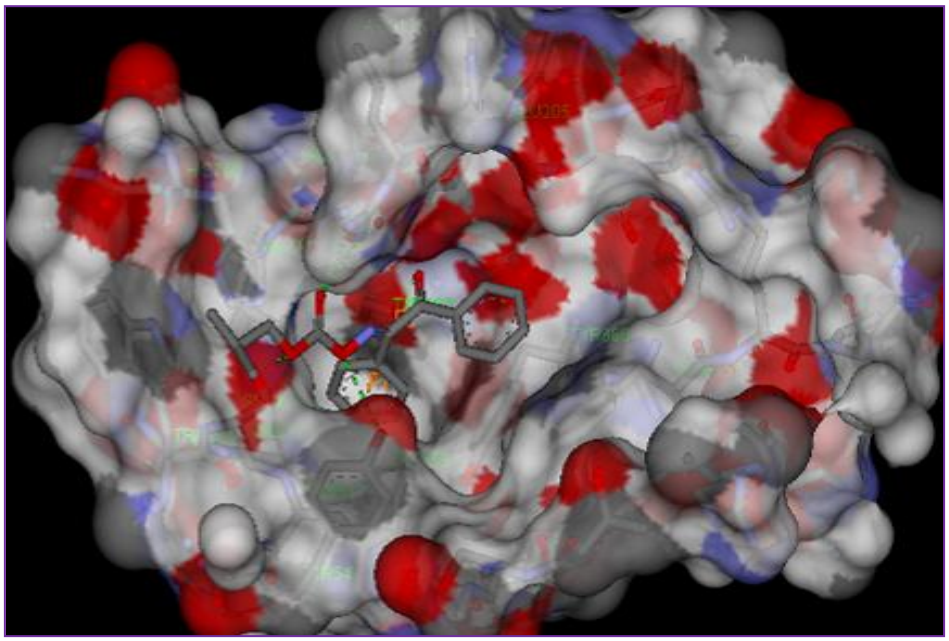

Figure 2.5: docked compound 12 in the active site of DPP-IV.

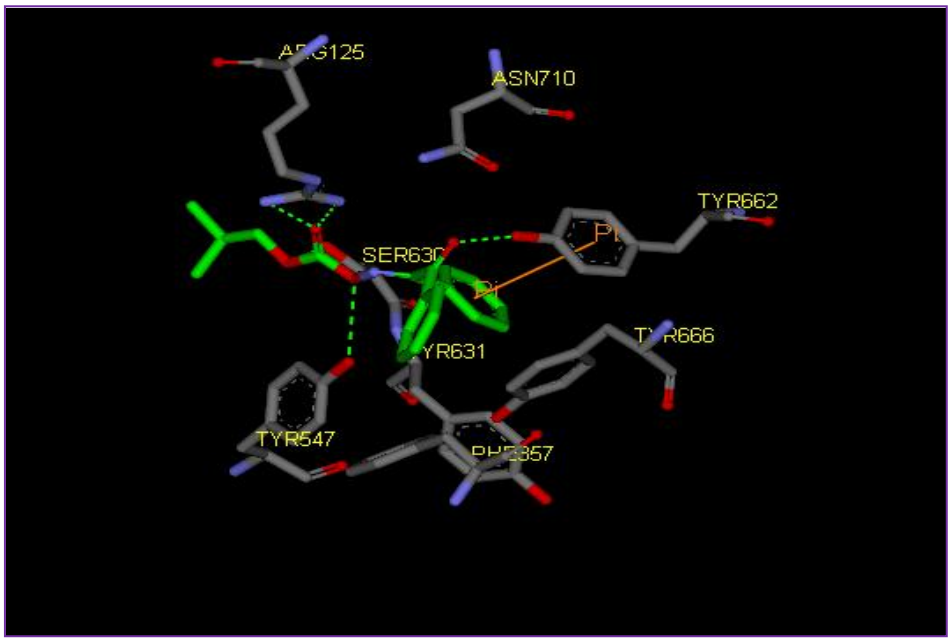

Figure 2.6: key interactions of compound 12 in the active site of DPP-IV.

Docking studies with compound **12** suggest that the isopropyl side chain appears to cause twisting of the molecule with the two aromatic rings rotating about the carbonyl group and inverting their positions.

Figure 2.6 shows that hydrogen bonds observed between the carbonyl group and residues Asn 710 and Arg 125 seen with AM11 are no longer present, but the

hydrogen bond with Tyr 662 is maintained. Two alternative hydrogen bonds between the carbonyl group of the formate and Arg 125 are evident, and the oxygen of the oxime forms only one hydrogen bond with Tyr 547. The biological results listed in Table 2.1 demonstrate that there is no activity for compound **12**. The docked pose (Figure 2.5) suggests that the inactivity of compound **12** could be due to the loss of the two hydrogen bonds formed by the carbonyl group and the consequent reorientation to accommodate the more bulky isopropyl group leading to reduced binding affinity and activity.

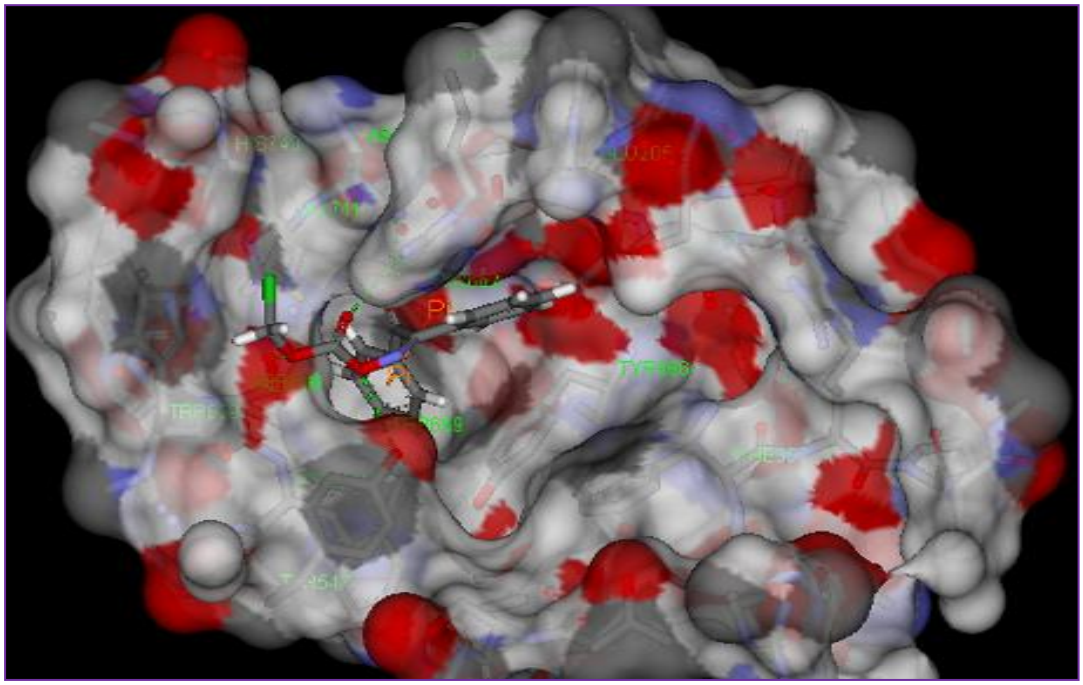

Figure 2.7: docked compound 15 in the active site of DPP-IV.

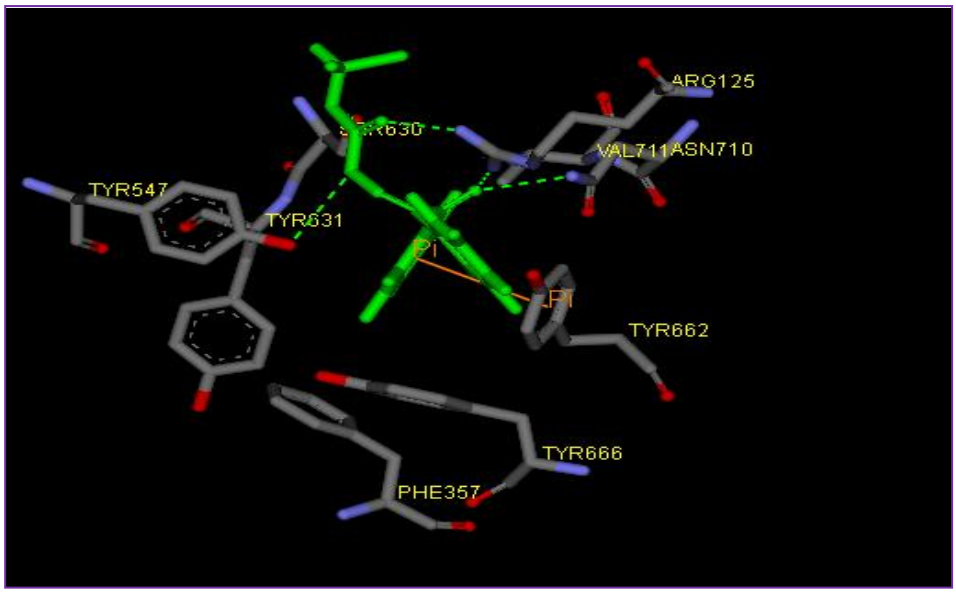

Figure 2.8: key interactions of compound 15 in the active site of DPP-IV.

In contrast, compound **15** with the chloromethyl side chain showed good inhibition of DPP-IV with K_i value of 5.8 μM (Table 2.1). According to our docking study, compound **15** interacts with key residues in the DPP-IV active site in a way that restores the same orientation observed for AM11. Hydrogen bonds are formed between the carbonyl group and residues Asn 710 and Arg 125 (Figures 2.7 and 2.8), although the hydrogen bond with Try 662 is lost. The π-π interaction with Tyr 662 is retained, but there is only one hydrogen bond between the carbonyl group of the formate side chain and Arg 125, instead of the two hydrogen bonds seen with the docked pose of compound **12.**

The chloromethyl side chain, which is equivalent to ethyl side chain, can provide flexibility so the molecule orientates similarly to AM11. The ethyl group is the appropriate size for inhibition and branching or substituting the alkyl side chain appears to markedly reduce activity.

2.3 Library 2: Synthesis of acid chloride derived series.

To confirm the importance of oxygen in the formate side chains for binding with residues at the outer edge of the pocket, the formates were replaced by acyl side chains. An additional consequence of this modification would also be improved chemical stability compared with the formates.

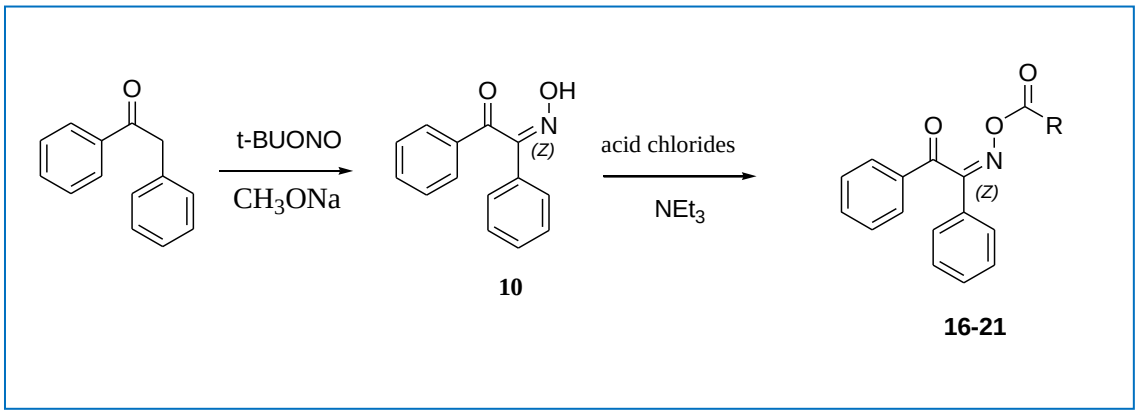

Scheme2.3: Synthesis of the acyl library.

Compound **10** as the pure ***Z*** isomer was reacted with different acyl chlorides under anhydrous conditions and in the presence of triethylamine (Scheme 2.3) to produce the library listed in Table 2.2.

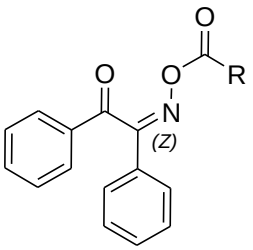

Table 2.2: The biological results for the acyl-based library (16-21).

Compound	R	Yield %	K_i (μM)*
16		50.1	NA
17		45.6	NA
18	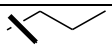	45.2	5.9
19	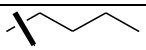	21.8	>30
20		22	NA
21		45.2	NA

*K_i values are the average of two readings.

2.3.1 Docking and biological results

All compounds with the exception of compound **18** were inactive against DPP-IV (Table 2.2). Docking studies suggest that removal of this oxygen will lead to a loss of a number of hydrogen bonds. Compound **18** showed good activity (K_i = 5.9 μM) and has a similar orientation and interaction to that of AM11 within the S_1 pocket. However, absence of the formate oxygen means the hydrogen bond with Ser 360 is lost, which could account for the 11.8-fold decrease in activity compared to AM11 **(**Figures 2.9 and 2.10).

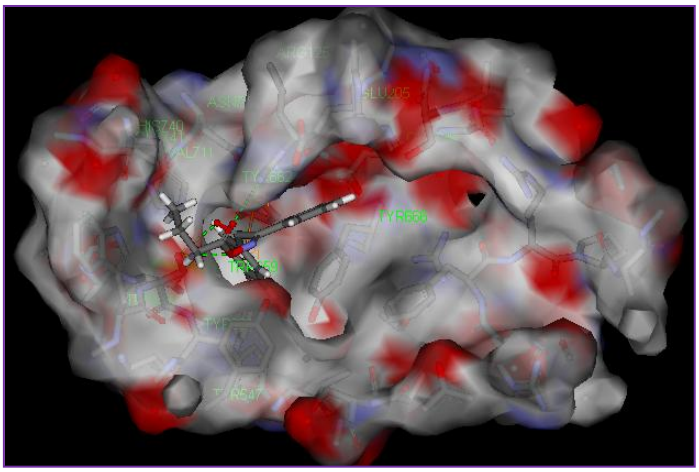

Figure 2.9: docked compound 18in the active site of DPP-IV.

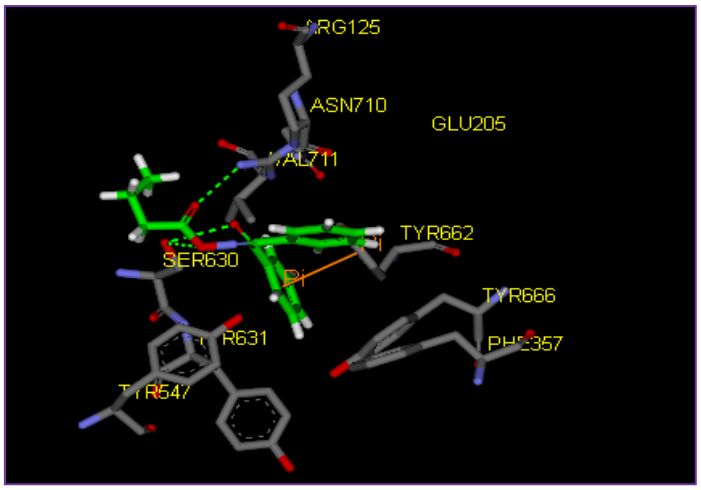

Figure 2.10: key interactions of compound 18 in the active site of DPP-IV.

Compound **19** (Figures 2.11 and 2.12) was docked for comparison against compound **18**, and clearly showed that there is a difference in both the orientation and interactions. Inactivity of this compound could be due to rotation about the double bond of the oxime, so that the butyl formate side chain now occupies the S_2 pocket without the formation of any interactions with key residues. Moreover, the carbonyl group of the acyl side chain faces down the pocket, reducing its ability to form hydrogen bonds with any of the amino acid residues inside the active site. Furthermore, the hydrogen bonds observed between the carbonyl group and residues Asn 710 and Arg 125 seen for for AM11 and compound **18** are reduced to only one hydrogen bond with Arg 125.

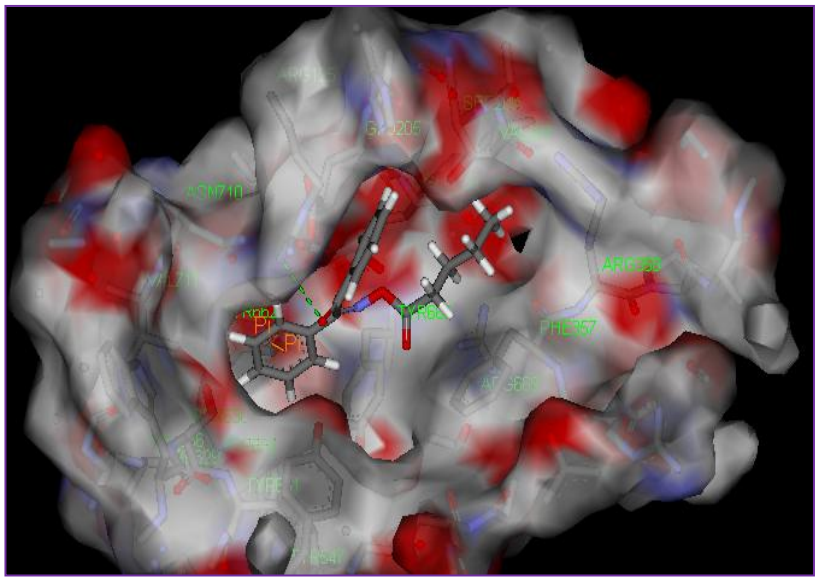

Figure 2.11: docked compound 19 in the active site of DPP-IV.

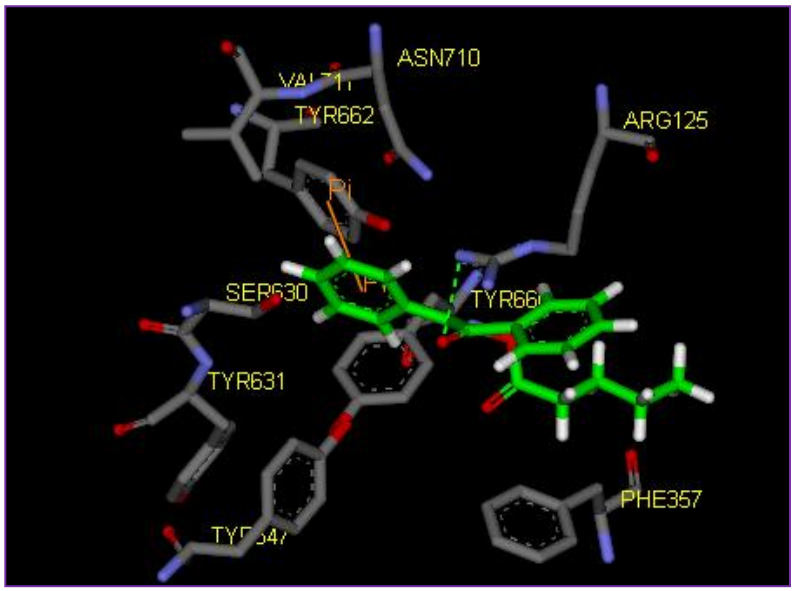

Figure 2.12: Key interactions of compound 19 in the active site of DPP-IV.

This presence of an extra CH_2 in the formate side chain of compound **19** appears to cause it to interact differently with key residues within the binding site and orientate differently within the pocket leading to a loss in activity.

It would therefore appear that a small formate rather than an acyl side chain is preferable for activity.

2.4 Library 3: Determining the importance of the carbonyl group

Synthesis of a library of compounds without a carbonyl group from diphenylethanone was to test the importance of a hydrogen bond acceptor in the benzoyl moiety of the molecule.

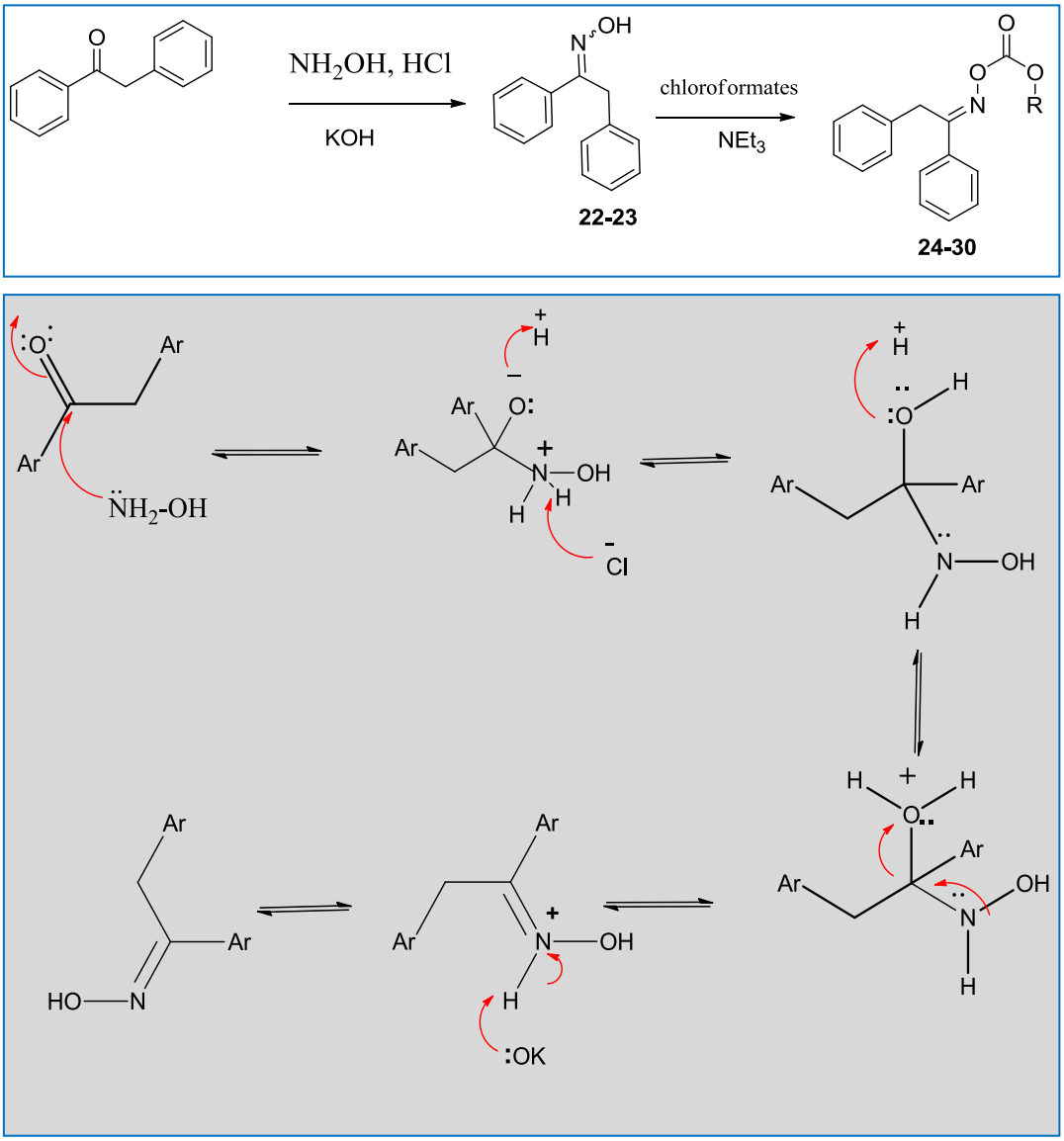

Scheme 2.4: Mechanism of the synthesis of *N*-Hydroxy-1,2-diphenylethanimine (22- 23) (Morrison and Boyde, 1983).

Diphenylethanone was converted to the oxime (compounds **22-23**) using the method of Ooi *et al.* (2002), with hydroxylamine hydrochloride and potassium hydroxide to yield a 3:1 mixture of ***E*** and ***Z*** isomers (Scheme 2.4). The mechanism involves the nucleophilic addition of hydroxylamine to the carbonyl group, followed by protonation and dehydration to afford the imine. The proton NMR of the crude product showed a singlet at δ10.8 ppm for the **OH** of the ***Z*** isomer and at 11.50 ppm for the **OH** of the ***E*** isomer (Figure 2.13).

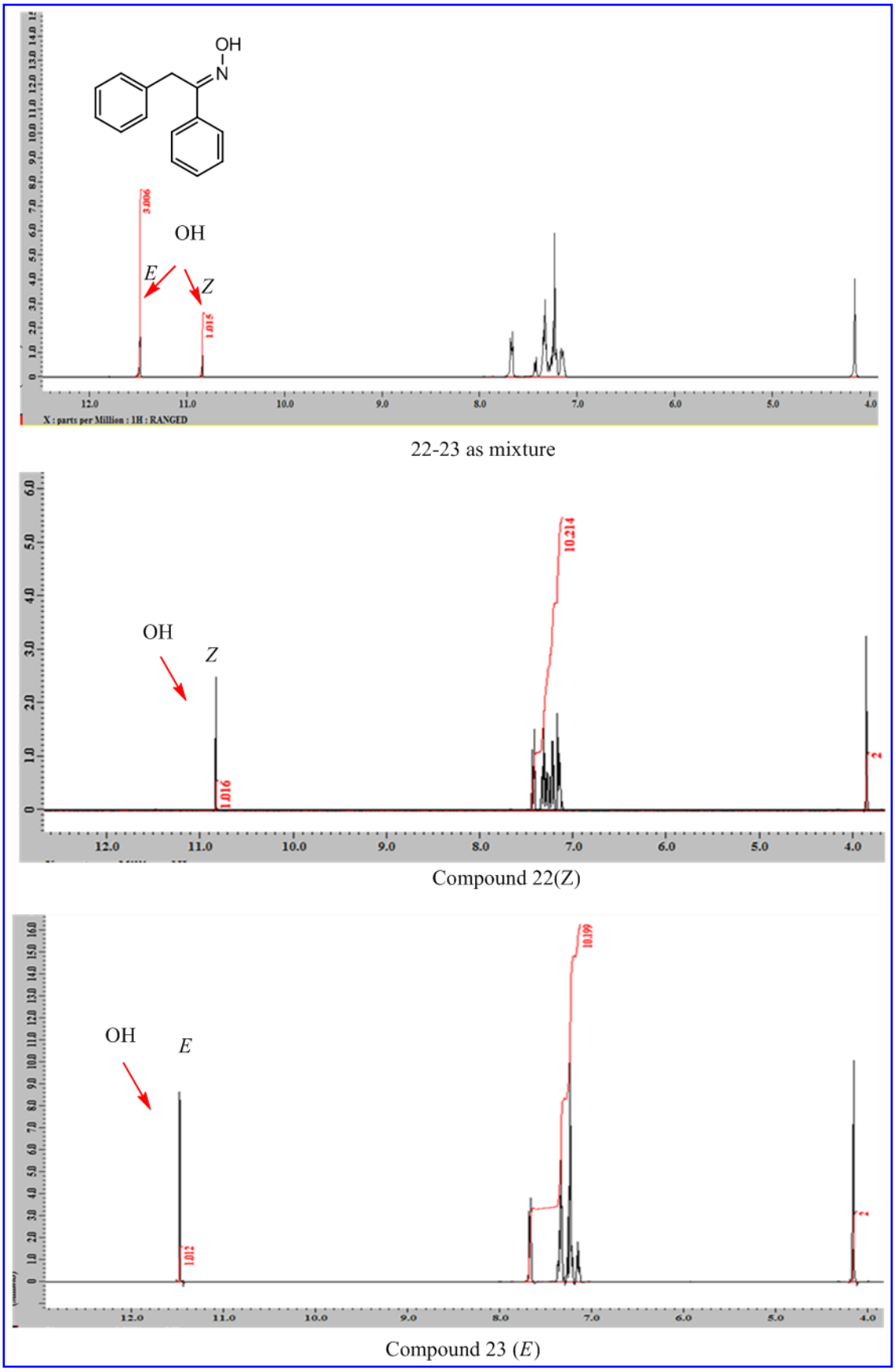

Figure 2.13: ^{1}HNMR spectrum shows separation of two isomers (22) and (23).

2.4.1 Separation of the two isomers

The two isomers were isolated by gravity column chromatography of the crude product using 1:9 diethyl ether; *n*-hexane system. The pure ***Z*** isomer was a white powder (21% yield) and the pure ***E*** isomer was white needle crystals (yield 56%). This separation was confirmed by proton NMR (Figure 2.13) where only one singlet was detected for the **OH** of the ***Z*** oxime at δ10.8 ppm and for the ***E*** oxime at 11.50 ppm. The carbon NMR spectrum supported these findings: all carbon atoms were duplicated in the crude mixture spectrum and showed only singlet peaks in the NMR spectrum of the pure isomer. All data from our proton and carbon NMR spectra were in agreement with the literature (Ooi *et al*., 2002).

2.4.2 Derivatization of compound 22.

Using the method described in strategy **1,** the **OH** of compound **22** was derivatized with a variety of chloroformates and acid chlorides to produce the library listed in Table 2.3. It should be noted that by removing a carbonyl group, the nomenclatures of the ***Z*** and ***E*** isomers are reversed; in this case, the ***E*** isomer is the required isomer.

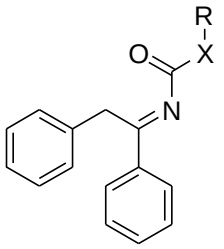

Table 2.3: The biological results for the third library.

Compound	X	R	Yield %	K_i µM*
24	CH_2		21	NA
25	CH_2		18	>30
26	O		64	NA
27	O		70	NA
28	O	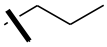	80	NA
29	O		64	NA
30	O		67	NA
LMC003B**	O		50	6.2

*K_i values are the average of two readings.

******Compound synthesised by a co-worker.

2.4.3 Docking and biological results

Our docking studies show that the absence of a carbonyl group should reduce hydrogen bonding interaction with key residues in the binding pocket. All compounds without a carbonyl group were inactive against DPP-IV (Table 2.3). Examining the docking pose of compounds **24** and **26** shows the possible reasons for the inactivity of these compounds (Figures 2.14 and 2.15).

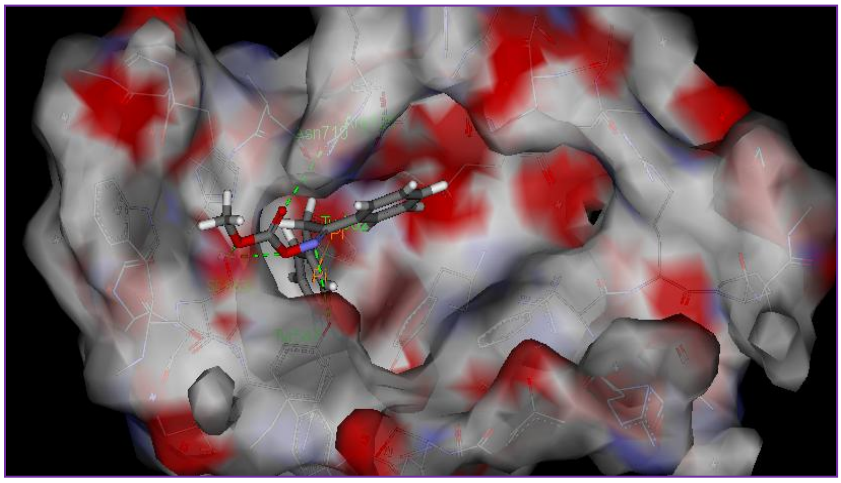

Figure 2.14: docked compound 26 in the active site of DPP-IV.

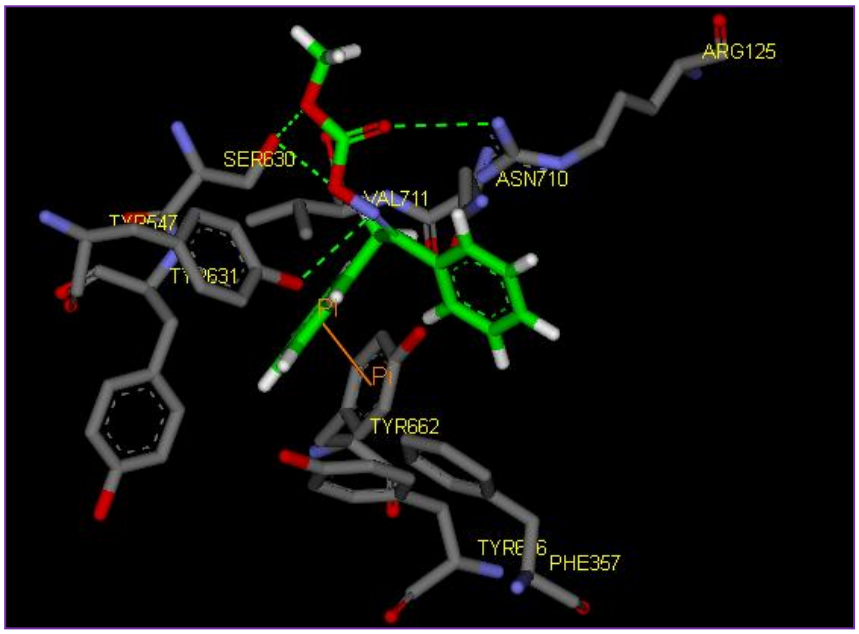

Figure 2.15: predicted binding interactions between compound 26 and DPP-IV.

Compound **26** (Figure 2.14) shows that the absence of a carbonyl group resulted in a loss of hydrogen bonds with Ser 630, Arg 125, and Tyr 662, but that the molecule was still orientated at the active site similar to AM11. Unlike AM11, both the oxime oxygen and nitrogen formed hydrogen bonds with residues Tyr 547 and Ser 630, respectively. π-Interactions were observed between the aromatic region of compound **26** and residue Tyr 662 of the DPP-IV as seen with sitagliptin, although the aromatic ring preferred to occupy the S_1 hydrophobic pocket and the oxygen of the formate side chain hydrogen bonded with Ser 630 (Figure 2.15). The inactivity of compound **26** (Table 3.2) could therefore be due to the absence of the carbonyl group and subsequent loss of the crucial hydrogen bond with Ser 630, Arg 125, and Tyr 662.

The biological results show that the majority of compounds in this library are inactive against DPP-IV, supporting the modelling postulation that the carbonyl group is essential for activity. As seen in Table 2.3, the only notable exception in this library is compound **LMCOO3B** (K_i = 6.2 μM) which can be explained by examining its docking pose (Figure 2.16).

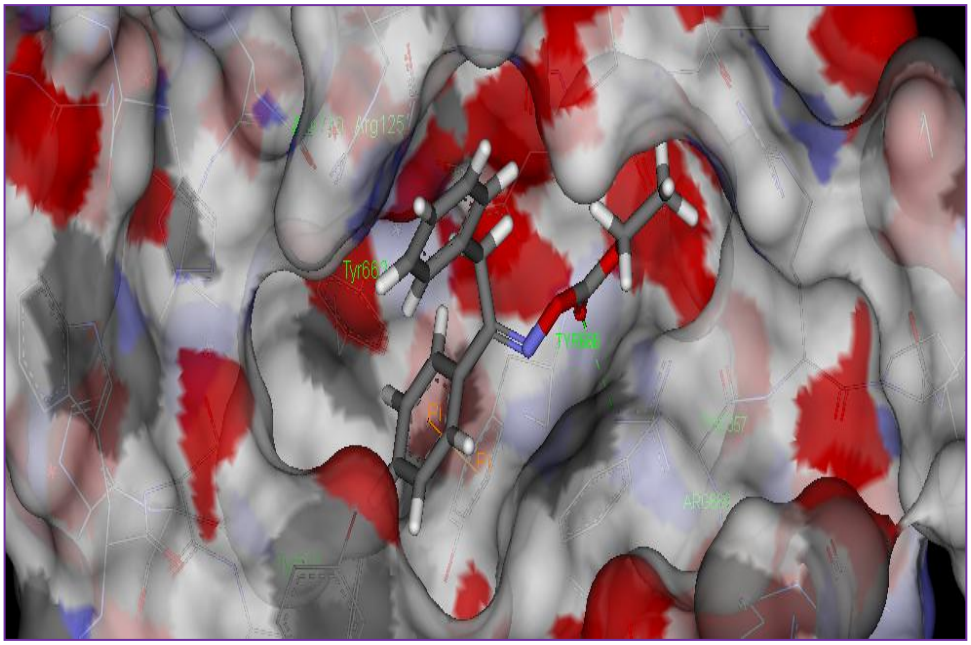

Figure 2.16: docked compound LMC003B) in the active site of DPP-IV.

The whole molecule was inverted inside the active site compared with other analogues from this library and the formate side chain occupied the S_2 pocket, with

the two aromatic rings pushed out of the S_1 pocket. The aromatic ring adjacent to the hydroxyimino group formed a π- π interaction with Tyr 666, which was not seen in the docked pose of AM11. Surprisingly, as shown in Figure 2.16, a new hydrogen bond was evident between Arg 669 and the oxygen of the oxime.

Overall, the biological results and docking studies for this library indicate that the role of the carbonyl groups of the oxime skeleton is to form a hydrogen bond that holds the molecule in a particular orientation, similar to that of AM11. The carbonyl group is also essential as the activity decreases from K_i = 0.5 μM for AM11 to K_i = 6.2 μM for **LMCOO3B**. It provides key interactions that are important for both the potency and orientation of the inhibitor within the active site of DPP-IV. Therefore, all compounds should contain a carbonyl group as an essential part of their structure. As seen in Table 2.3, both formate and acyl analogues with an ethyl side chain show promising activity against DPP-IV, which supports our previous finding that the ethyl group is optimal for inhibition of DPP-IV.

2.5 Library 4: Halogen substitutions onto the phenyl ring

To investigate the effect of halogens in the phenyl ring adjacent to the hydroxyimino group, ketoximes with fluoro or bromo substituents at the *para* and *meta* positions were synthesised and further functionalised to the formate derivatives (Scheme 2.5).

The first step was to prepare the appropriate benzoyl chloride from their benzoic acid derivatives using oxalyl chloride and dimethyl formamide (DMF) (scheme 2.6) followed by Freidel Crafts acylation to afford compounds **31, 39, 50,** and **LMC005B** in varying yields.

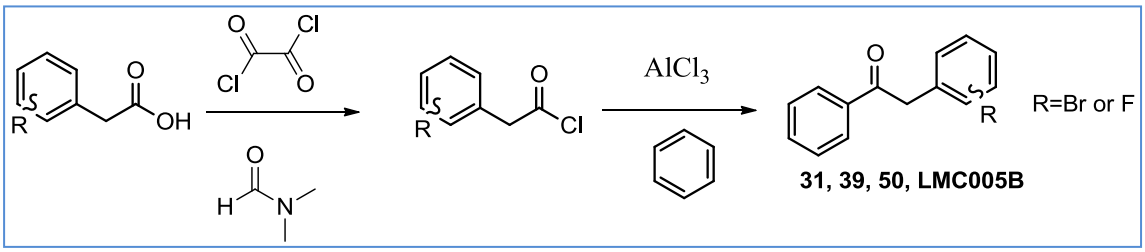

Scheme 2.5: Synthesis of ketones with fluoro or bromo substituents at the *para* and *meta* positions.

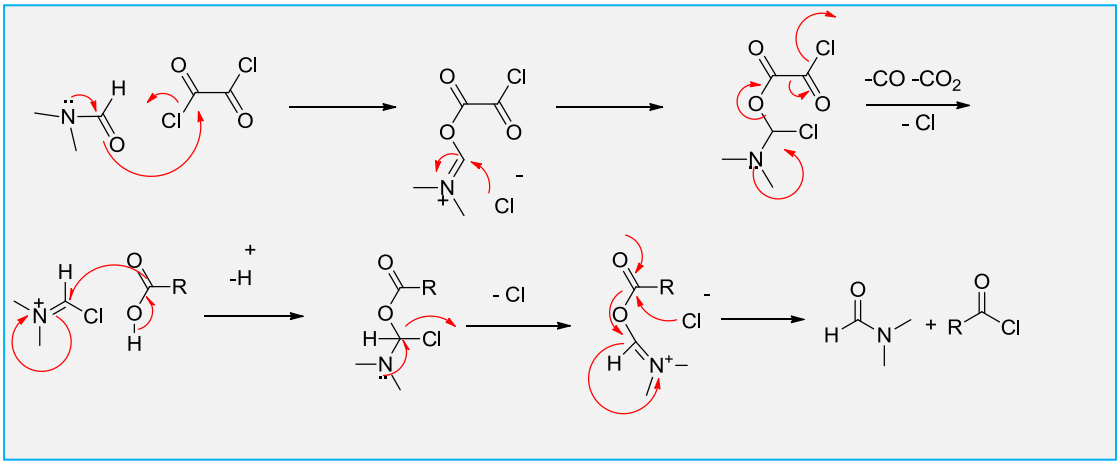

Scheme 2.6: General mechanism for formation of acid chlorides.

The mechanism for Freidel-Craft acylation is shown below (Kong *et al*., 2006). The first step includes the reaction of an acyl halide with a Lewis acid to form the more electrophilic acylium ion.

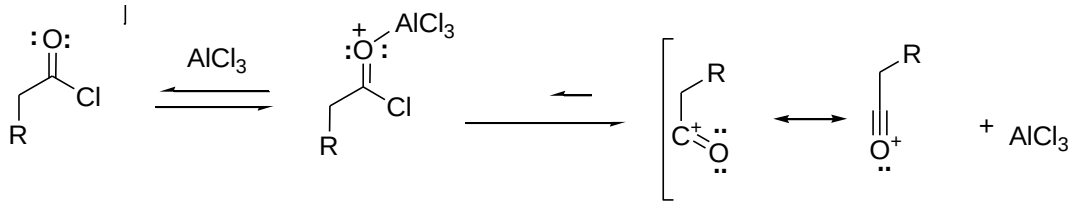

The second step involves the nucleophilic attack of the □ electrons of the aromatic C=C to the electrophilic C+. This step proceeds via the loss of aromaticity and the formation of a cyclohexadienyl cation as an intermediate.

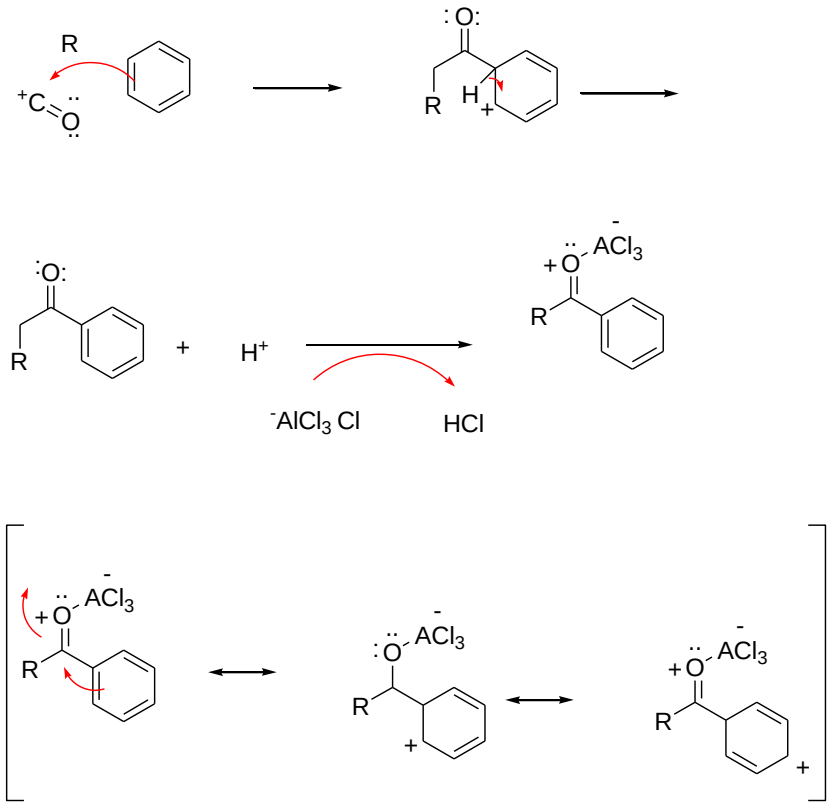

Re-aromatisation is via the removal of the proton from the sp^3 C bearing the acyl-group, and generation of HCl and the active catalyst.

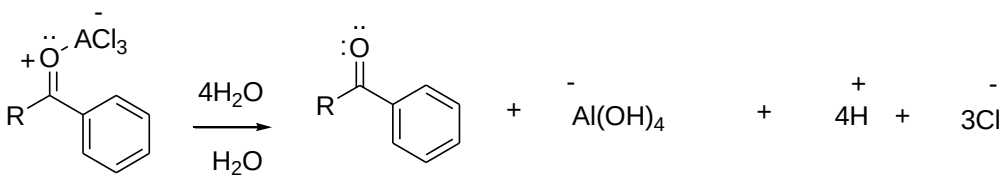

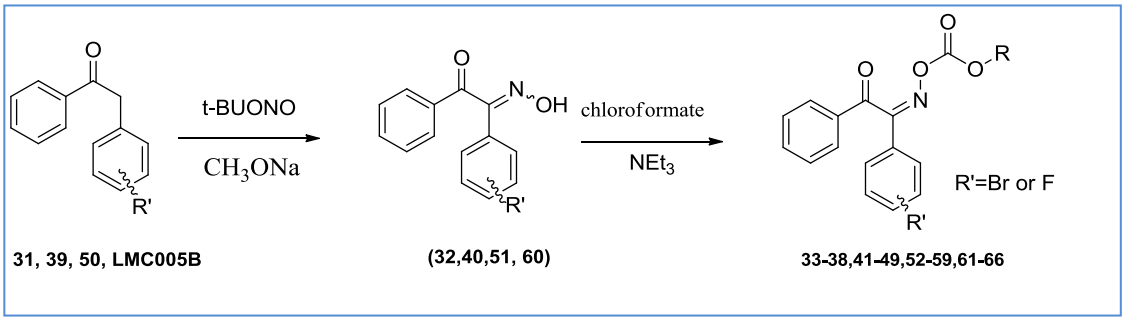

Scheme 2.7: Synthesis of ketoximes and formates with fluoro or bromo substituents at the *para* and *meta* positions.

The Freidel-Craft products were then converted to the corresponding oximes using the established procedure. Subsequently, compounds **32, 40, 51** and **60** were derivatized with a variety of chloroformates to produce the library listed in Table 2.4 and Table 2.6. The formate derivatives of compounds **32** and **40** (fluoro derivatives) were easily separated into the pure *Z* and *E* isomers by recrystallization from ethanol. Due to time constraints, compounds **51** and **60** were not separated and tested as a racemic mixture.

2.5.2 Docking and biological results

Based on our earlier findings that confirmed the carbonyl group and formate side chain as essential features for significant inhibition of DPP-IV, modifications were made to maintain the basic structure of AM11: halogens were introduced at different positions in the phenyl ring adjacent to the hydroxyimino group along with different formate side chains. The introduction of halogens was intended to explore the S_2 pocket of the active site for additional hydrophobic interactions and improve the activity.

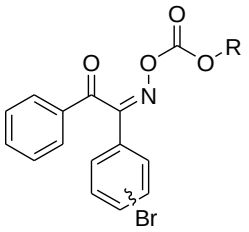

Table 2.4: The biological result for the bromine-containing analogues.

Compound	Position	R	Yield %	K_i (µM)*
52	*para*		48	NA
53	*para*	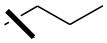	46	64.5
54	*para*		40	NA
55	*para*	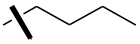	60	NA
56	*para*	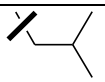	37	NA
57	*para*	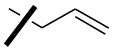	39	NA
58	*para*		46	NA
59	*para*	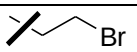	49	NA
61	*meta*		40	6.3
62	*meta*	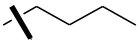	60	NA
63	*meta*		45.2	NA
64	*meta*	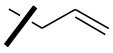	39.2	NA
65	*meta*	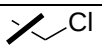	61.5	NA
66	*meta*	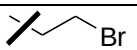	46.8	NA

*K_i values are the average of two readings.

Table2.5: Compounds synthesized by Laura McReady.

Compound	Position	R	Yield %	K_i (μM)
(LMC0015 B)	*meta*		70	6.3
(LMC014C)	*para*		37.8	NA
(LMC015A$_{1+2}$)	*meta*		12.9	NA
(LMC015C)	*meta*	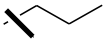	44.5	NA

*K_i values are the average of two readings.

2.5.3 Bromophenyl derivatives

Tables 2.4 and 2.5 show that the majority of the compounds that have bromine groups at the *meta* or *para* positions of the phenyl ring showed no activity against DPP-IV. The two notable exceptions were compound **61 (**K_i =6.3 μM) and compound **LMC0015B (**K_i =6.3 μM), which could be explained by examining the docking pose of compound **61**.

The compound was docked in the crystal structure of DPP-IV, as shown below (Figure 2.19). The orientation and interactions present are very similar to those seen in AM11, with hydrogen bonding taking place between the carbonyl and oxime functional groups of the inhibitor with residues Tyr 662 and Arg 125, respectively. Similarly, the aromatic ring still occupied the S_1 pocket with the formation of π - π interactions with Tyr 662 residue. However, bromophenyl groups sit in the S_2 pocket without the formation of any kind of interactions with key residues in the active site, suggesting that the activity of compound **61** (Table 2.4) could be due to similar interactions and orientation with AM11 within the active site.

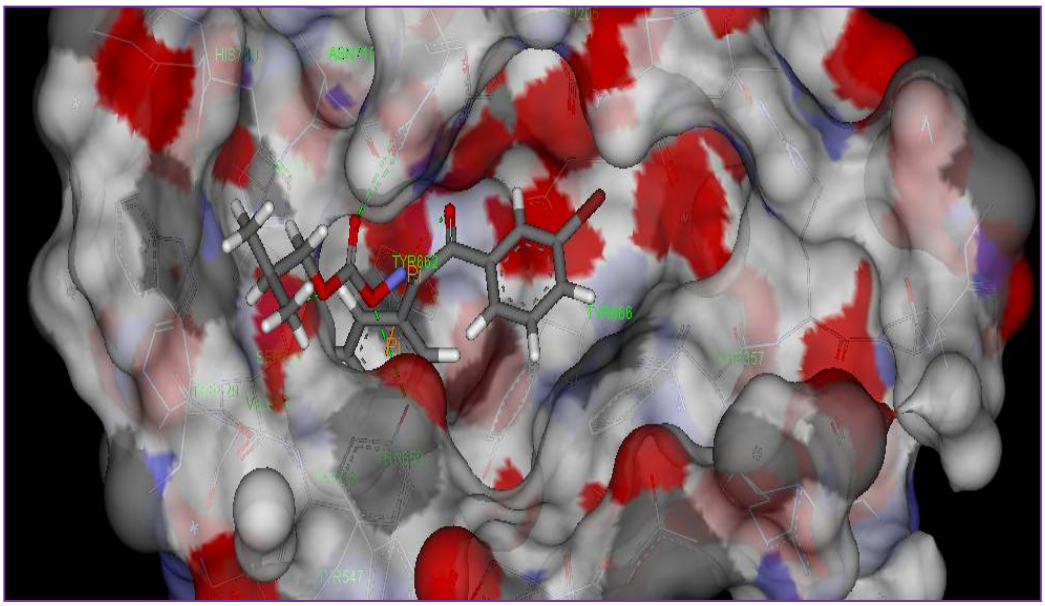

Figure 2.19: docked compound (61) in the DPP-IV active site.

Compound **53**, which has a propyl side chain, exhibited weak inhibition of DPP-IV, and suggests that no significant gain was made by introducing bromine substituents at any position on the phenyl ring.

2.5.4 Fluorophenyl derivatives

The rationale for the introduction of fluorine was based on the fact that the structure of the potent DPP-IV inhibitor sitagliptin contains a trifluoro-phenyl ring and that fluorine is a similar size to hydrogen.

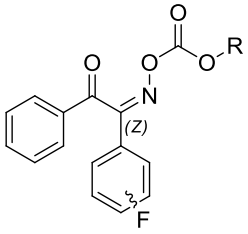

Table 2.6: The biological results for the fluorine-containing analogues.

Compound	Position	R	Yield %	K_i (μM)*
33	*para*		31	9
34	*para*		32.30	2.9
35	*para*	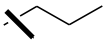	14.7	3.8
36	*para*		13	NA
37	*para*		35.4	4.6
38	*para*	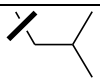	35.4	NA
41	*meta*		80.76	NA
42	*meta*		52	6.6
43	*meta*	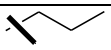	52	NA
44	*meta*		52	NA
45	*meta*	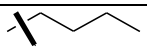	49.6	NA
46	*meta*	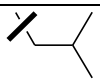	65.9	NA
47	*meta*	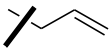	59.4	>100
48	*meta*	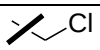	50.73	13.2
49	*meta*	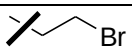	49.83	26.1

*K_i values are the average of two readings.

The biological results (Table 2.6) revealed that the mono *para*-fluoro group produced a 5.9-fold loss in inhibitory activity (2.9 μM) and the *meta*-fluoro group caused a 13.2-fold loss in inhibitory activity (6.6 μM) compared to the unsubstituted core scaffold (compound **AM11**).

Compound **34** (*para*) (Figure 2.20) and compound **42** (*meta*) (Figure 2.22) were docked in the DPP-IV active site.

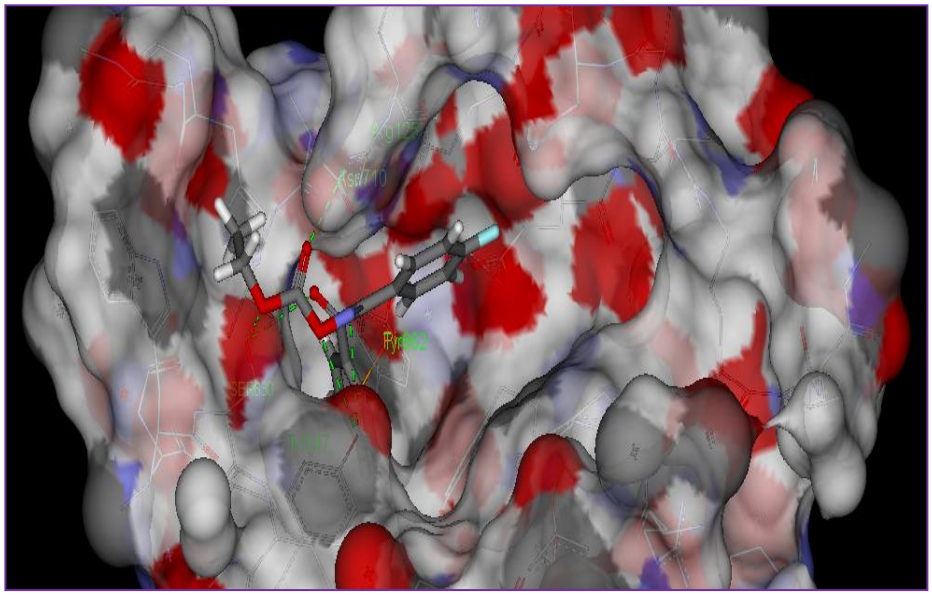

Figure 2.20: docked compound 34 in the DPP-IV active site.

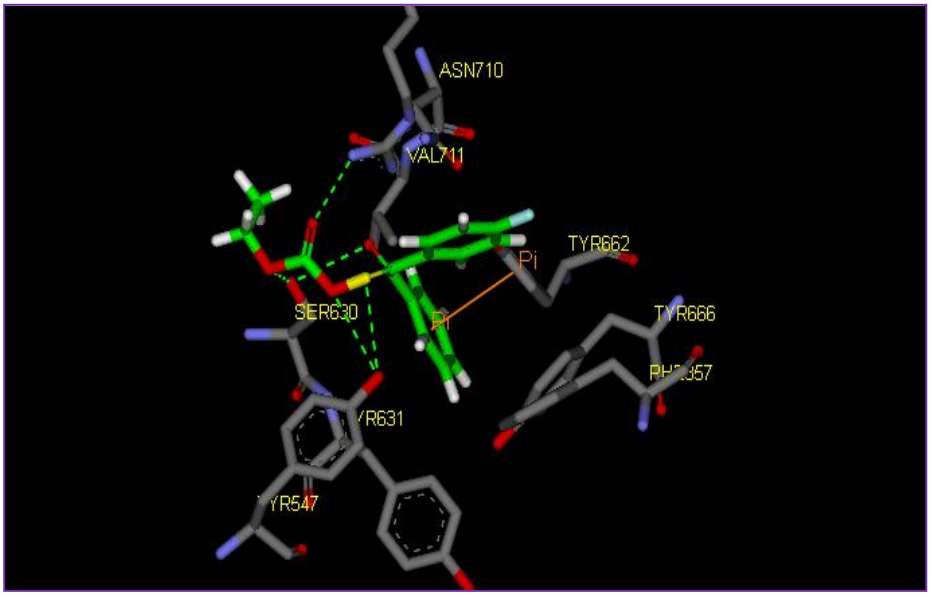

Figure 2.21: predicted binding interactions of compound 34 in the DPP-IV active site.

The orientation and interactions of compound **34** with the active site in comparison with those of compound **42** can be seen in more detail in the figures above. Both molecules showed very similar orientation in the DPP-IV active site. However, Table 2.6 revealed that there is decrease in the inhibitory activity, which could be due to the only notable differences in the interaction of both molecules with the active site. The carbonyl group of compound **34** shows only one hydrogen bond with Tyr 630, which is not seen in compound **42**, and the oxygen of the oxime of compound **42** forms only one hydrogen bond with Tyr 630 instead of two hydrogen bonds, which formed between the oxygen and the nitrogen of the oxime of compound **34** and Tyr 547. Both compounds showed fewer hydrogen bonds in comparison with AM11, which could be possible explanation for increasing in the K_i value from 0.5 μM for AM11 to 2.9 μM for compound **34** and 6.6 μM for compound **42.**

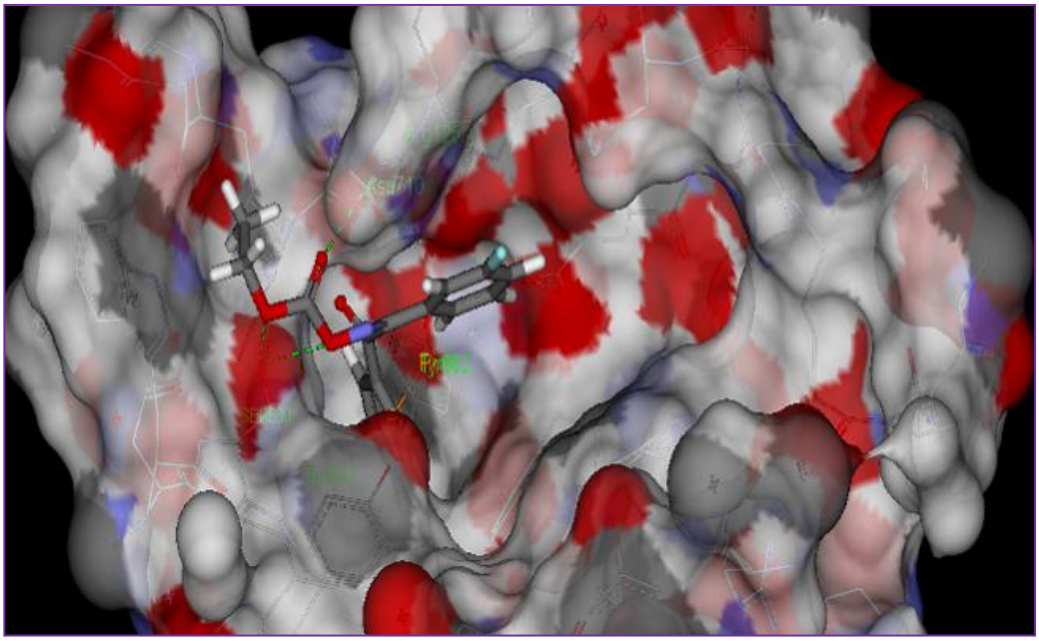

Figure 2.22: docked compound 42in the DPP-IV active site.

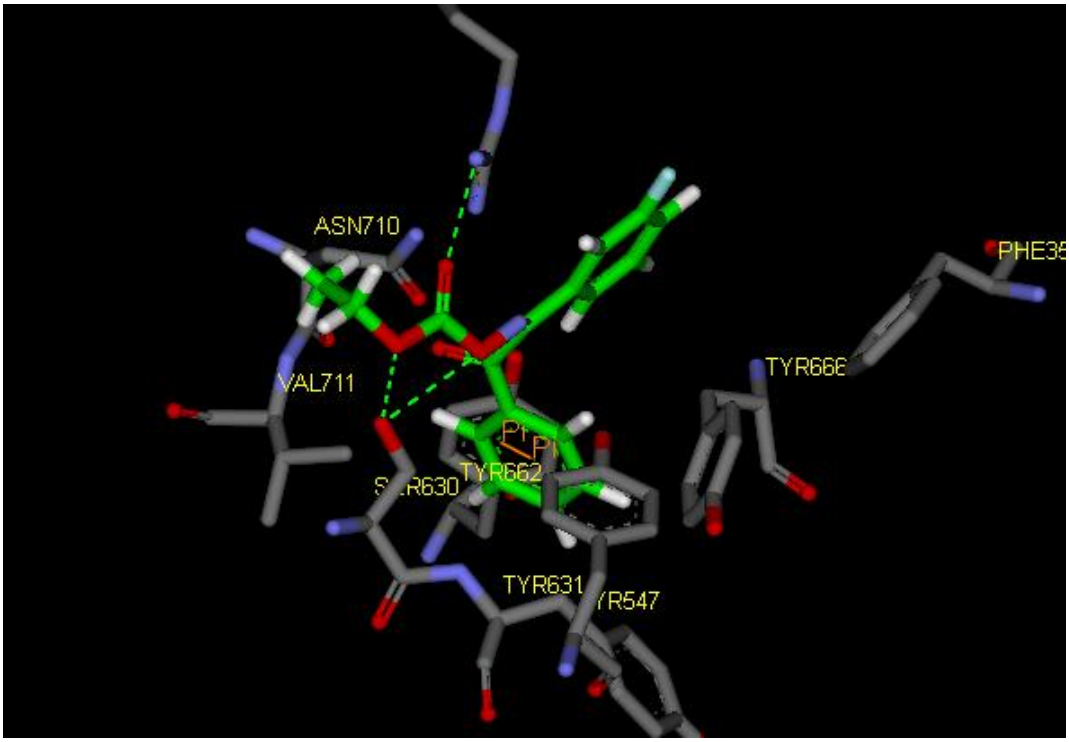

Figure 2.23: key interactions of compound 42in the DPP-IV active site.

As can be seen in Table 2.6, the majority of molecules with a fluorine atom at the *meta* position of the phenyl ring showed a range of activities against DPP-IV, which could be explained by the diversity in the formate side chains. Compound **34** (Figure 2.21), with an ethyl formate side chain showed the greatest inhibition, whilst compound **36** showed no activity, which could be due to of the steric effect of the bulky isopropyl group.

All compounds with a fluorine atom at the *para* position of the phenyl ring along with a bulky formate side chain (compounds **43**, **44**, **45**, and **46**) are inactive (Table 2.6), which could be down to negative steric effect inside the active site of DPP-IV (Figure 2.23).

Overall, the presence of the fluorine atom has less effect on molecular orientation in the active site compared with a bromine atom. The fluorine atom, which is a similar size to hydrogen, enables similar interactions to that of AM11.

2.6 Library 5: Halogenations in different benzoyl group sites

This library of compounds was synthesised to determine the effect of substituting halogens into the aromatic ring adjacent to the carbonyl group (the benzoyl group) in order to increase the hydrophobicity of the aromatic ring that occupies the S_1 pocket.

The first two compounds of this library (**76 –77**) were synthesised using the following steps:

- Synthesis of the Weinreb amide followed by the addition of benzylmagnesium bromide compounds **70 –72**. The mechanism for the reaction is detailed in Scheme 2.8 (Luca *et al*., 2001);
- Synthesis of ketoxime compounds **73 –75** (Scheme 2.9); and
- Derivatization of the ketoximes with ethylchloroformate to generate compounds **76 –77** (Table 2.9).

For compounds **79 – 81** (Table 2.9), the ketones were commercially obtained from Sigma Aldrich, and formation of a ketoxime using the previous method of derivatization with ethylchloroformate produced the two desired compounds (Scheme 2.9).

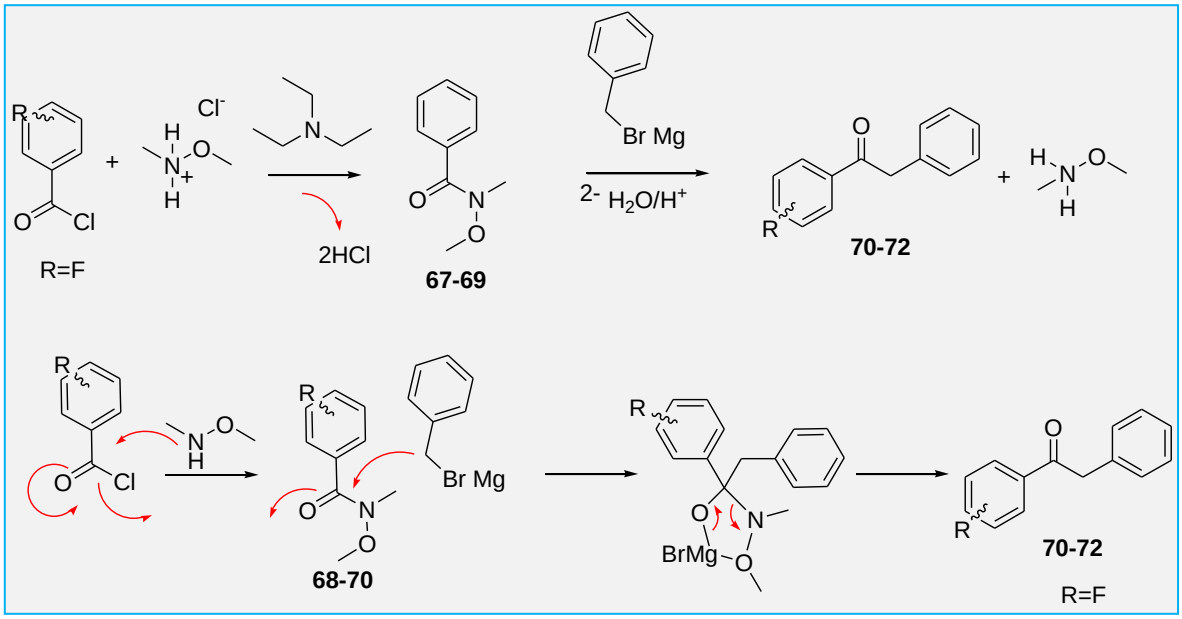

Scheme 2.8: Mechanism of Weinreb Ketone Synthesis.

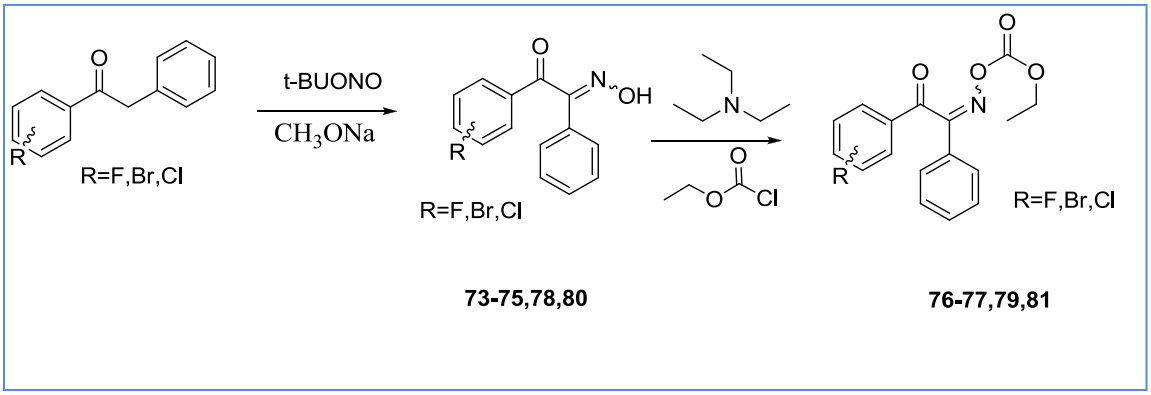

Scheme 2.9: Synthesis of compounds 76-77, 79, 81.

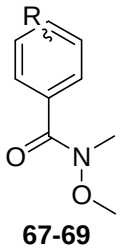

67-69

Table 2.7: Library (67-69).

Compound	R	Position	Yield %
67	F	*ortho*	30
68	F	*meta*	15
69	F	*para*	15

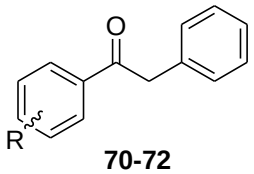

70-72

Table 2.8: Library (70-72).

Compound	R	Position	Yield %
70	F	*ortho*	59
71	F	*meta*	59
72	F	*para*	59

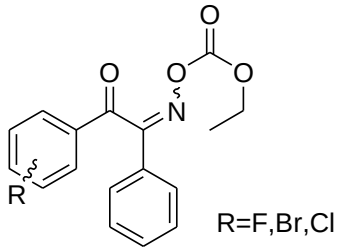

76-77,79,81

Table 2.9: The biological result for the fifth Library.

Compound	R	Position	Yield %	K_i(µM)*
76	F	*ortho*	38	NA
77	F	*meta*	38	7.1
79	Br	*para*	66	5.4
81	Cl	*para*	67	3.2

*K_i values are the average of two readings.

2.6.1 Docking and biological results

The idea for this modification was based on the fact that the S_1 pocket is highly hydrophobic and the presence of halogens on the phenyl ring would enhance the hydrophobic interactions. We docked three compounds with fluoro substituents at different positions on the benzoyl ring.

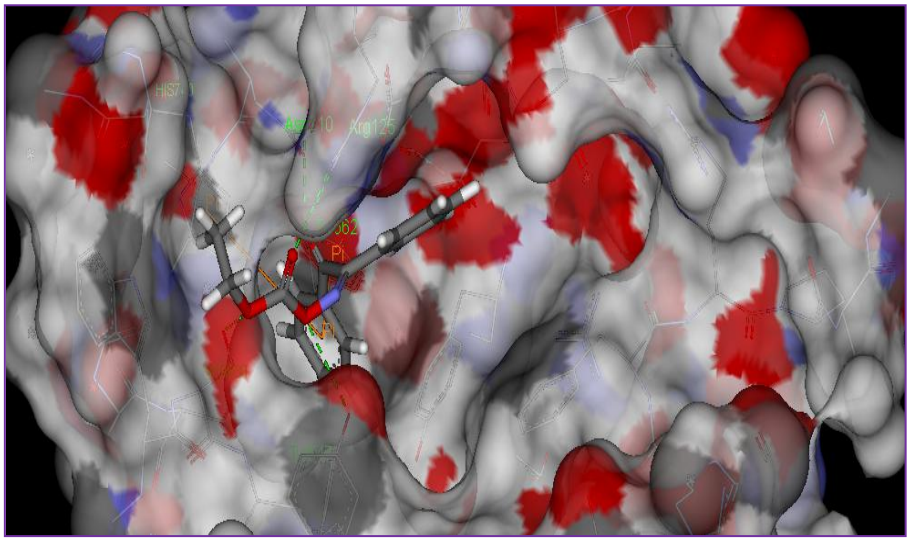

Figure 2.24: docked 4-fluoro-compound in the DPP-IV active site.

From the docked pose produced above, it is obvious that the presence of a fluorine group has a significant influence on both of the binding interactions of this molecule at the active site. Similar to AM11, the aromatic ring still prefers to be situated within the S_1 hydrophobic pocket; however, unlike AM11, the presence of a fluorine atom in the aromatic ring allows it to probe deeply inside the S_1 pocket, providing more hydrophobic interactions. Furthermore, π-interactions are observed between the aromatic region and Tyr 662 of DPP-IV, and a unique π-interaction is observed between the fluorinated aromatic ring and His 740. The molecules still form hydrogen bonding interactions between the formate carbonyl group and Arg 125 and Asn 710, as seen with compound AM11 (Figure 2.24).

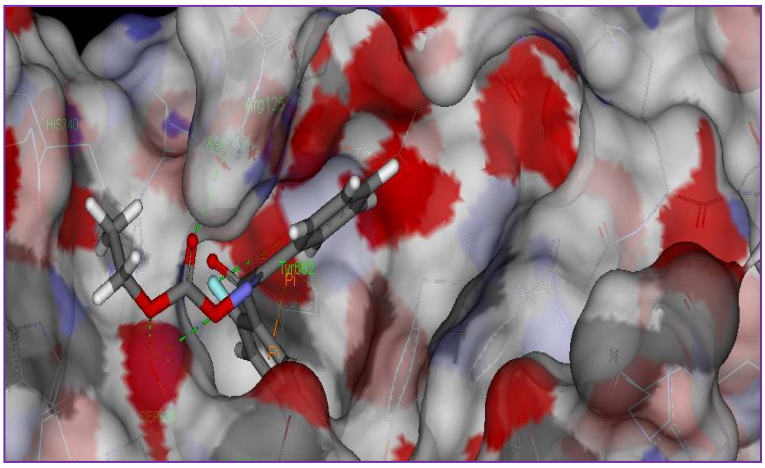

Figure 2.25: docked 76 compound in the DPP-IV active site.

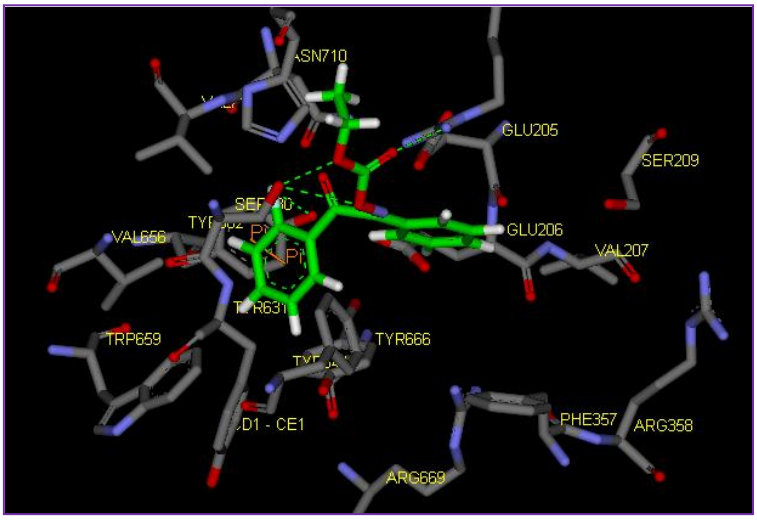

Figure 2.26: key interactions of compound76 in the DPP-IV active site.

Changing the fluorine atom on the aromatic ring to the *ortho* position affords compound **76**. Docking this compound into DPP-IV suggested that a new hydrogen bond formed between the fluorine atom and the hydroxyl of the Tyr 662 residue in the S_1 pocket, and the aromatic ring forms a π-π interaction with the same residue. However, the carbonyl group faces down, decreasing the its ability to form hydrogen bonds with any amino acid residues at the active site (Figures 2.25 and 2.26). Compound **77**, with a *meta*-fluoro substituent, had an additional hydrogen bond between the carbonyl group and Ser 630, and similar to compound **76**, the oxime forms two hydrogen bonds with Tyr 745. The aromatic ring still prefers to sit in the S_1 pocket forming a π-π interaction with Tyr 662 and the fluorine atom forms a

hydrogen bond with Tyr 666 (Figures 2.27 and 2.28). Interestingly, compound **77** had a K_i against DPP-IV (7.1 μM) (Table 2.9) whereas compound **76** was inactive, which could be due to loss of hydrogen bonds formed by the carbonyl and oxime groups.

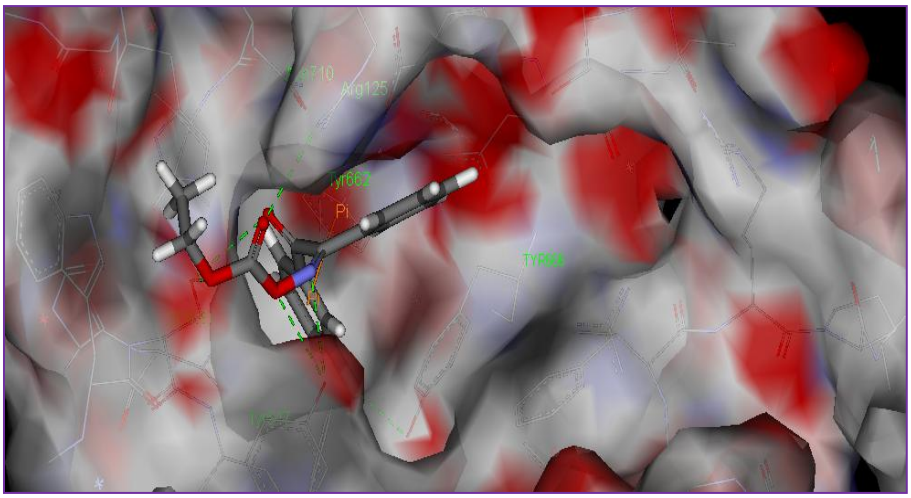

Figure 2.27: docked compound 77 in the DPP-IV active site.

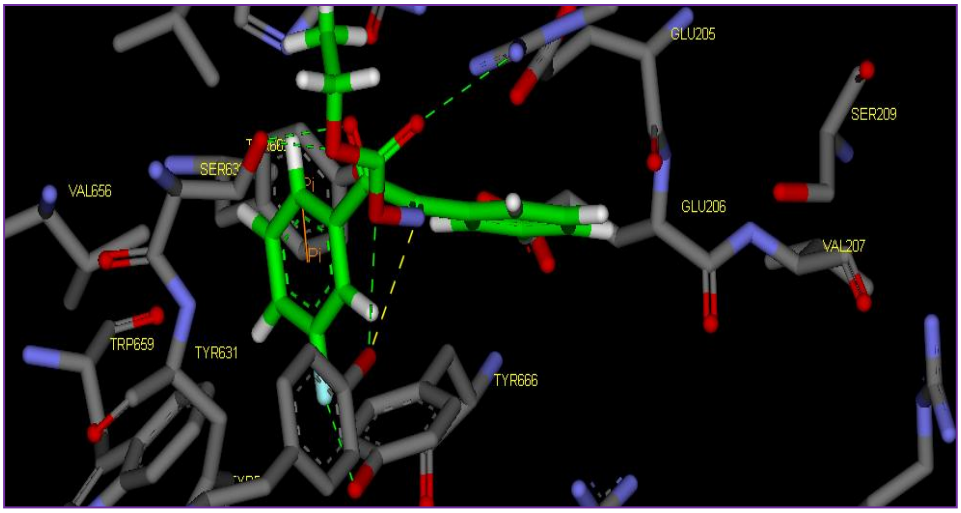

Figure 2.28: key interactions of compound 77 in the DPP-IV active site.

Compound **81**(Figure 2.29) restored the orientation and the majority of hydrogen bonds that were seen with AM11. The aromatic ring forms a π-π interaction with His 740. Compound **79** (Figure 2.30) appears to orientate similarly to compound **81**. However, the decrease in the inhibitory activity of this compound (K_i= 5.4 μM)

could be due to the only notable difference in the interaction with DPP-IV which is the absence of a π-π interaction with His 740.

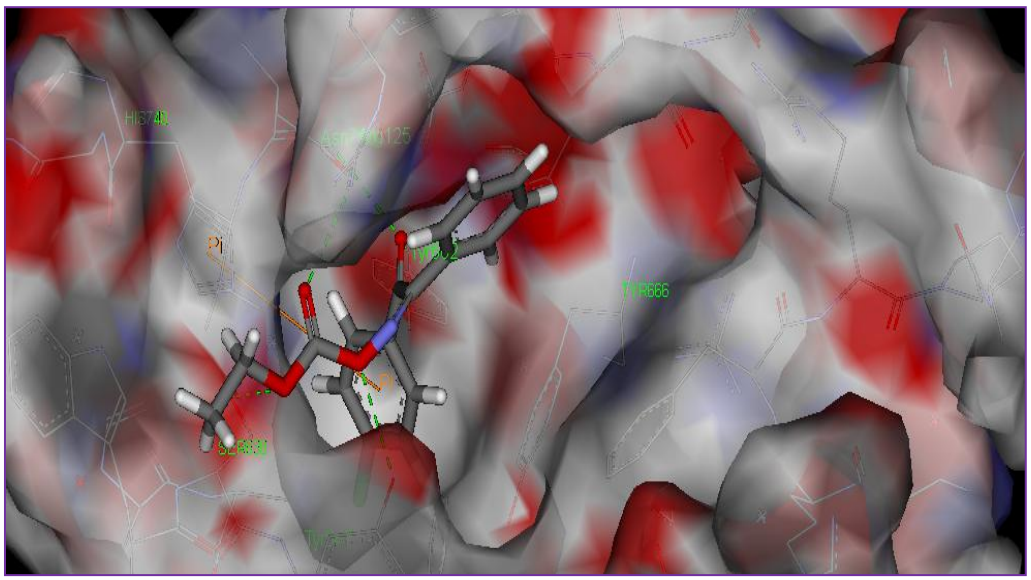

Figure 2.29: docked 81 compound in the DPP-IV active sit.

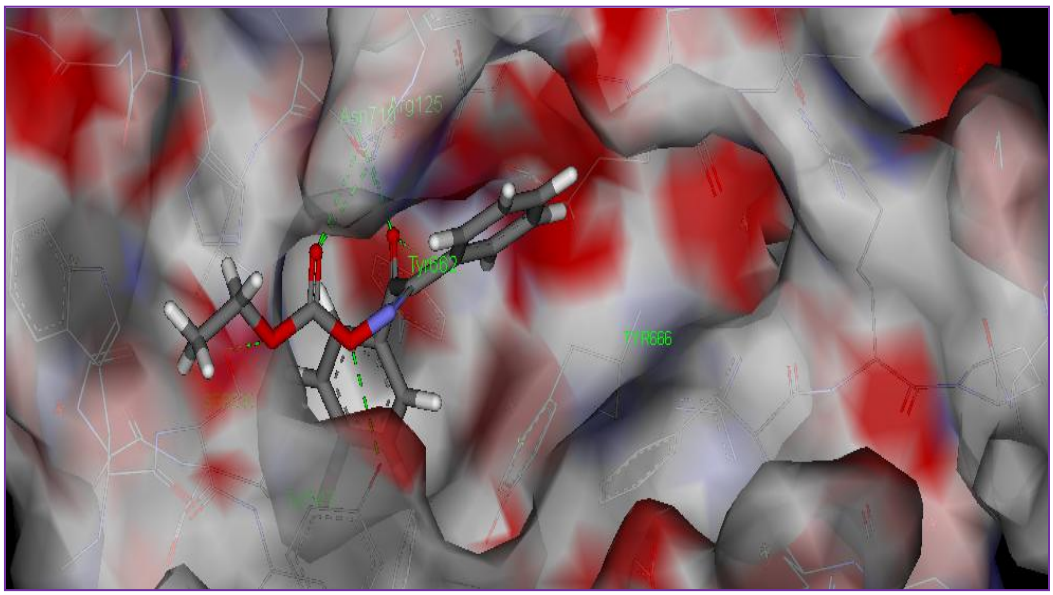

Figure 2.30: docked 79 compound in the DPP-IV active site.

Overall, Table 2.9 revealed that the *para*-chloro substituent produced a 6.4-fold (3.2 μM) loss in inhibitory activity, the *para*-bromo substituent caused a 10.8-fold (5.4

μM) loss in inhibitory activity, while the *meta*- fluoro group caused almost a 14 –fold (7.1 μM) loss in activity compared to AM11. One possible explanation for this decrease in the activity is that all of these compounds showed fewer hydrogen bonds in comparison with AM11.

2.7 Library 6: Modifications of two rings.

Our final approach was to determine the effect of substituting a methoxy group onto the two aromatic rings of AM11.

Compound **82** was synthesized using the general procedure as described before using the commercially available ketone, followed by derivatization of compound **82** with ethylchloroformate to afford compound **83** as a racemic mixture (1*E*:10*Z*) (scheme 2.10).

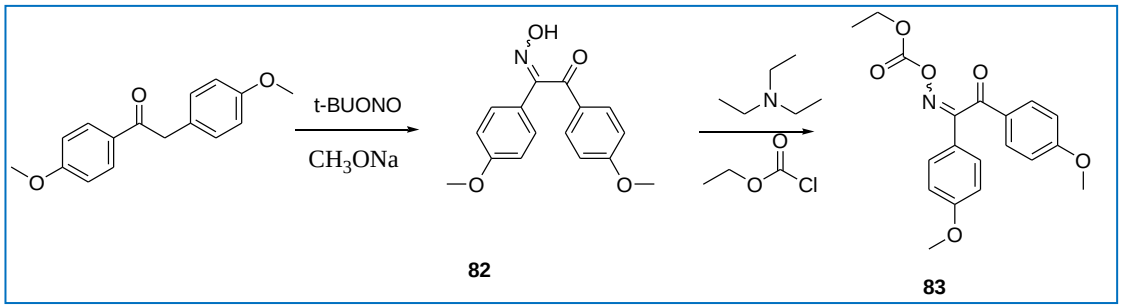

Scheme 2.10: Synthesis of compound 83.

Compound **83** showed the best inhibition for DPP-IV (K_i =0.4 μM) in the whole series, and the docking pose seen below (Figures 2.31 & 2.32), possible reasons for this 1.25-fold improvement in inhibitory activity against DPP-IV compared to AM11 are:

The methoxy groups enable the molecule to occupy the majority of DPP-IV pocket, and a new hydrogen bond is formed between the methoxy group and the aromatic ring and Tyr 631.Its orientation also allows π-interactions with residue Phe 357 and adopts a pose similar to sitagliptin.

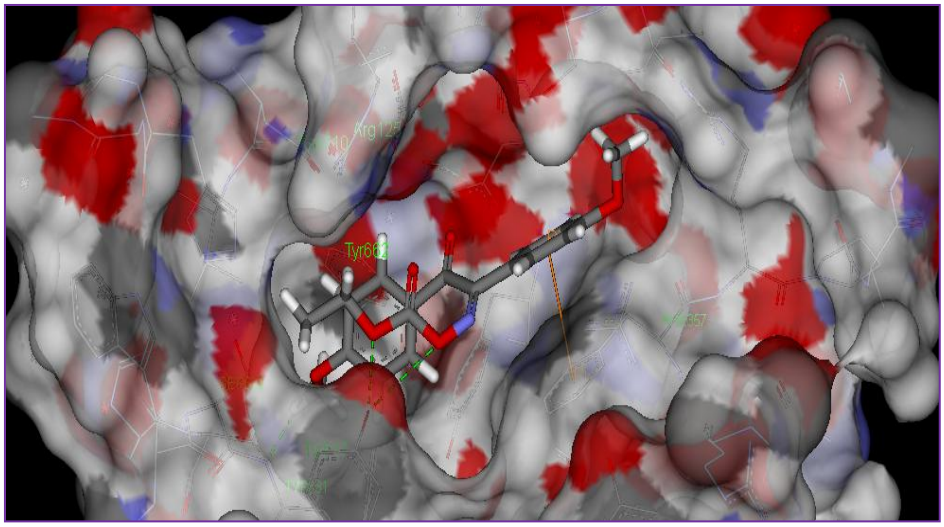

Figure 2.31: docked 83 compound in the DPP-IV active site.

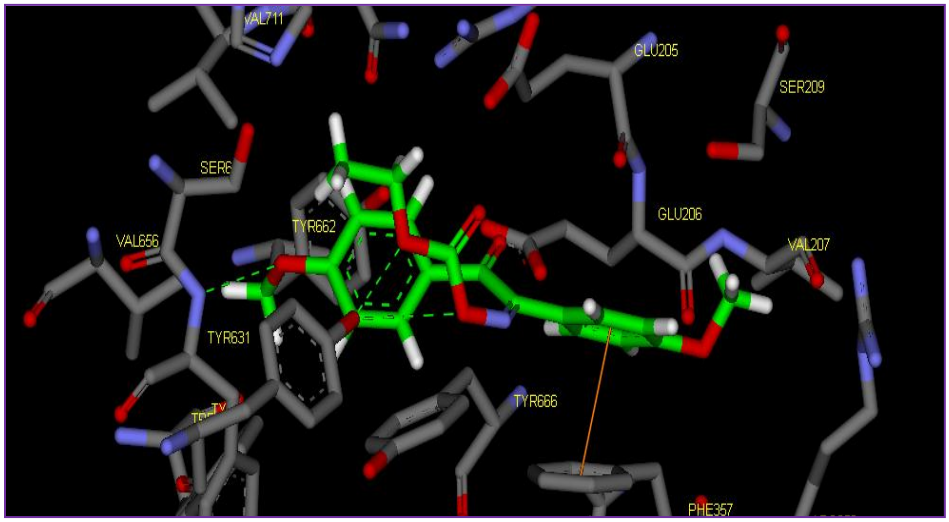

Figure 2.32: predicted binding interactions of compound 83 with DPP-IV active site.

2.8 Conclusions and future work:

Docking and biological results showed that the majority of compounds with an ethyl group in the formate side chain were good inhibitors of DPP-IV.

In Library (**1**), the only active compound was compound **15** with a chloromethyl formate side chain, which is a similar size as an ethyl group.

Compound **18** is the only active of Library (**2**), which has a propionyl side chain that is equivalent to an ethyl formate. In Library (**3**), compound **LMC003B** is the only active compound and has an ethyl formate side chain.

All compounds with a bromophenyl group in Library (**4)** were inactive with the exception of compound **LMC0015B** which also had an ethyl formate side chain.

All *meta*-fluoro analogues within Library (**4**) were inactive with the exception of compound **42**, which had good activity (K_i = 6.6μM). The majority of the *para*-fluoro derivatives were active, and the most active was compound **34** (K_i = 2.9 μM), which has an ethyl formate side chain.

All of these findings confirm the importance of an ethyl group in the alkyl formate side chain. Branching or substituting the alkyl side chain markedly decreased activity possibly through negative steric influences in the active site.

Replacement of the formate by an acyl side chain afforded inactive compounds against DPP-IV.

Comparing the biological and docking poses of **AM11** and **LMC003B** revealed that although the absence of a carbonyl group was expected to inactivate the molecules, **LMC003B** showed some activity (K_i = 6.2 μM). The carbonyl group appears to be important to orientate the molecules in the DPP-IV active site and optimising the hydrogen bond network.

Halogen substituents which were incorporated to increase hydrophobic interaction inside the S_1 pocket reduced the inhibitory activity against DPP-IV compared to AM11.

Addition of the bromine atom to *meta* or *para* positions of the phenyl ring significantly affects the orientation of the inhibitors in the DPP-IV pocket. Despite introducing new binding interactions with key residues in the active site such as □-π interactions, the bromine markedly decreases the activity. A fluorine atom at the *para* position of the phenyl ring appears to be preferred over the *meta* position.

In contrast to halogens in the phenyl ring, halogens in the benzoyl moiety markedly enhanced the hydrophobic interactions in the S_1 pocket. The docked pose of compound **81** had π-π interactions with Tyr 662 and with His 740.

The most effective inhibition of DPP-IV was achieved with compound **83** where the presence of two methoxy groups enables occupation of the full DPP-IV active site with additional hydrogen bonding.

Future work will involve the following:

- Contrary to porcine DPP-IV which has smaller S_1 pocket, preliminary molecular modeling studies have indentified in human DPP-IV a deeper S_1 pocket where the methoxy group of compound **83** can occupy and hydrogen bond with Glu 206. Other oxygenated substituents should be assessed.
- Replacement the carbonyl group with a sulphonyl group to provide two hydrogen bond acceptors.
- Preliminary modeling studies have shown that addition of a substituent such as an amino group on the phenyl ring (Figure 2.33) would provide further interactions with hydrogen bond acceptors in this region of the protein. Also, an indole moiety would make the compound more planar and more like other DPP-IV inhibitors.

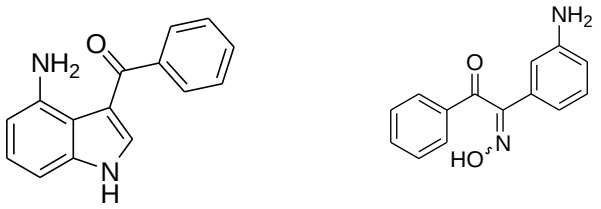

Figure 2.33: Suggested derivatives of AM11.

Chapter 3: Materials and methods

3.1 General experimental details

3.1.1 Melting point determination: Melting points (Mpt) were determined on Stuart Scientific Melting Point apparatus SMP1 and are in degrees Celsius (°C) and are uncorrected.

3.1.2 Elemental analysis: Elemental analysis was performed on Perkin Elmer 2400 Analyser Series II elemental analyser. Standard methods of measuring the thermal conductivity for the combustion product were used to determine C, H, and N simultaneously and halogens and sulphur separately by titration with carium percholate solution.

3.1.3 Infrared spectroscopy: Infra red spectra for liquid samples were run on Jasco FTIR-4200 ATR (Attenuated Total Reflection Mode) and solid samples compressed with KBr into disks and recorded with Mattson Genesis Series FT-IR spectrometers. Wavenumbers, νmax (cm-1) are quoted for appropriate functional groups.

3.1.4 Nuclear Magnetic Resonance (NMR) spectroscopy: Proton (^{1}H NMR) and carbon (^{13}C NMR) nuclear magnetic resonance spectra were run either on a JEOL Lambda Delta 400 (400 MHz) or Bruker AMX-400 (400 MHz) spectrometer. The deuterated solvent used for each of the compound is specified in the text. Chemical shifts are stated in parts per million (ppm) and multiplicity indicated as singlet (s), doublet (d), doublet of doublet (dd), triplet (t), quartet (q), pentet, sextet and multiplet (m). Coupling constants (*J*) are quoted in hertz (Hz).

3.1.5 Mass Spectroscopy: High-resolution mass spectroscopy (HRMS) was obtained using electron impact ionisation (ESI, 70 eV), in a Fourier transform analyser by Exactive® Thermo Scientific. Mass to charge ratio (*m/z*) molecular ion radical is given as [M+].

3.1.6 Reagents and solvents: All commercially available reagents and solvents used were obtained (and used without further purification) from Sigma-Aldrich, Alfa-Aesar or Fisher Scientific unless otherwise stated.

3.1.7 Purification of products: All compounds were purified by recrystallisation or by either gravity column chromatography or flash chromatography using a Biotage SP4 Automated Chromatography system. All chromatography was carried out on SiO_2 60A 6μm-35 μm (Fisher-Scientific). Thin-Layer Chromatography (TLC) was carried out on aluminium-backed SiO_2 plates (Merck) and spots visualised using ultra-violet light (254 nm). The stationary and mobile phases used are detailed in the text.

3.2 Biological evaluation against human dipeptidyl peptidase-IV (DPP-IV)

Human dipeptidyl peptidase-IV (DPP-IV, Enzo Life Sciences, ALX-201-128) was assayed in 100 mM Tris-HCl (pH 8, Sigma Aldrich, T5941) containing 0.1 mg/mL of Bovine Serum Albumin (BSA, Sigma Aldrich, A2153) in a total volume of 100 μL for 30 min at 37 °C, and read using a Wallac Victor plate reader (Perkin-Elmer, UK). The standard 3*N*-[(*2S, 3S*)-2-amino-3-methyl-pentanoyl]-1, 3-thiazolidine) hemifumarate (P32/98, Tocris, 2136) and substrate Gly-Pro-7-amido-4-methylcoumarin hydrobromide (Gly-Pro-AMC, Sigma Aldrich, G2761) were obtained from commercial sources. The excitation/emission wavelengths for the fluorogenic substrate are 360/460nm (umbelliferone, Sigma Aldrich, H24003). 1 mg of each test compound was submitted and diluted appropriately prior to assay. The assay protocol is as follows:

(1) Add 25 μL (120 μg/ mL) of P32/36 (standard) or test compound is added to each well.

(2) Add 50 μL (0.6 nM) of DPP-IV to all wells. Incubate for 30 minutes at 37^{o}C.

(3) Add 25 μL (120 μM) of the Gly-Pro-AMC (substrate) into all wells. Incubate for 30 minutes at 37 ^{o}C.

(4) Measure change in fluorescence using umbelliferone (355 nm / 460 nm) after 30 minutes using Wallac Victor plate reader.

All inhibitors tested were competitive reversible inhibitors and K_i values (μM) were calculated using the Michaelis–Menten equation for competitive inhibition:

$IC_{50} = K_i / (1 + [S] / K_m)$ (Michaelis–Menten equation) Equation 1

Where: IC_{50} = functional strength of the inhibitor (half maximal inhibitory concentration)

K_i = the binding affinity of the inhibitor.

[S] = substrate concentration.

Km = affinity of the substrate for the enzyme. For DPP- IV [Subs] is 30µM and Km is 22µM.

3.3 General synthetic procedures

3.3.1 General Procedure A (formation of ketoximes)

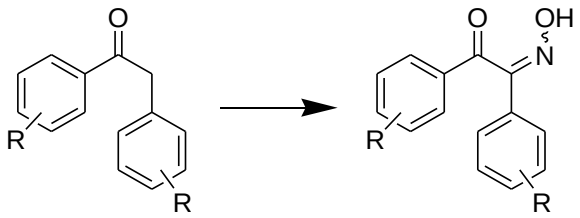

To a stirred solution of the ketone (1 eq) in anhydrous methanol (100 mL) at (0 °C) was added *tert*-butylnitrite (1.5 eq) dropwise followed by a solution of sodium methoxide (1.25 eq) in anhydrous methanol (50 mL). The mixture was stirred for 24 hours and then concentrated to give thick red orange oil. The oil was redissolved in water (50 mL) and extracted with diethyl ether (3 x 25 mL) (Extract A). The aqueous layer was then acidified with 1M HCl (85 mL) and extracted with dichloromethane (3 x 25 mL) (Extract B). The two separated organic extracts were concentrated at reduced pressure to give the crude crystalline products. Recrystallisation of Extract A with toluene gave the *Z* isomer (Z-monoxime). Extract B was boiled in toluene, filtered and to give the *E* isomer (*E*-monoxime) (SanMartín *et al.,* 1995).

3.3.2 General Procedure B (formation of choroformates and/or esters)

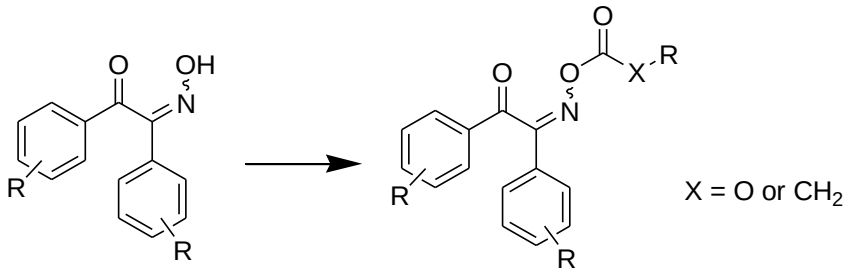

To a solution of monoxime (1 eq) and NEt_3 (1.1 eq) in chloroform (5 mL) at 0 °C was added the required acid chloride or chloroformate derivative (1.1 eq). The reaction mixture was heated to 50 ^{o}C and then stirred for 48 hours. The reaction was cooled and water (20 mL) added. The organic layer was washed with water (2 x 20 mL), dried over anhydrous $MgSO_4$ and concentrated to give a crude product which was further purified by either recrystallization or chromatography (Green and Dorhety, 1979).

3.3.3 General Procedure C (preparation of Weinreb amides)

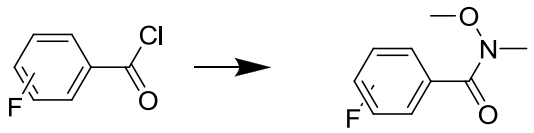

The required fluorobenzoyl chloride (1 eq) was added dropwise over 5 minutes to a cooled (0 ^{o}C) solution of *N*-methoxymethanamine hydrochloride (1.15 eq) and NEt_3 (2.5 eq) in anhydrous dichloromethane (20 mL). After stirring for 1 hour, the reaction mixture was warmed to room temperature and stirred for a further 24 hours. The mixture was quenched with water (10 mL) followed by aqueous hydrochloric acid (0.5 M, 25 mL) and then extracted with dichloromethane (3 x 25 mL). The combined organic extracts were dried over $MgSO_4$, concentrated and purified by flash chromatography (SiO_2; 0 – 50% EtOAc in *n*-hexane) to afford the desired Weinreb amide derivative (Hirashima *et al.*, 2006).

2-Fluoro-*N*-methoxy-*N*-methylbenzamide (67)

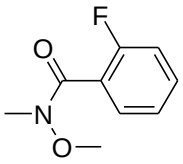

The reaction was carried out according to general procedure C using 2-fluorobenzoyl chloride (2 g, 12.60 mmol, 1 eq). The crude product was purified by flash chromatography (Biotage SP4, SiO_2; 0–50% EtOAc in *n*-hexane) to afford compound **67** (0.8 g, 30 %) as a colourless oil. ^{1}H NMR (400 MHz, $CDCl_3$) δ 7.28-7.46 (m, 4H, Ar-**H**), 3.55 (s, 3H, -OC**H**$_3$), 3.26 (s, 3H, -N-C**H**$_3$). ^{13}C NMR (400 MHz, $CDCl_3$): δ 165.1 (1C, C=O), 159.9 (1C, Ar), 133.8 (1C, Ar), 128.9 (1C, Ar), 124.9 (1C, Ar), 124.2 (1C, Ar), 115.2 (1C, Ar), 61.9 (1C, -O**C**H$_3$), 31.2 (1C, -N-**C**H$_3$). IR: νmax (ATR)/cm^{-1}: 1717 (C=O), 1651 (C=N), 1229 (C-O) and 983 (N-O). HRMS (ESI+, 70 eV) calculated for $C_9H_{11}FNO_2$ (M+H+): 184.0768, Found: 184.0768. Found C, 50.91; H, 4.57; N, 6.20 (Required for $C_9H_{10}FNO_2$: C, 59.01; H, 5.50; N, 7.65.

3-Fluoro-*N*-methoxy-*N*-methylbenzamide (68)

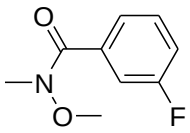

The reaction was carried out according to general procedure C using 3-fluorobenzoyl chloride (2.0 g, 12.6 mmol, 1 eq). The crude product was purified by flash chromatography (Biotage SP4, SiO_2; 0-50% EtOAc in *n*-hexane) to afford compound **68** (0.34 g, 15 %) as a colourless oil. ^{1}H NMR (400 MHz, $CDCl_3$) δ 8.12-7.06 (m, 4H, Ar-**H**), 3.56 (s, 3H, -OC**H**$_3$), 3.35 (s, 3H, -N-C**H**$_3$). ^{13}C NMR (400 MHz, $CDCl_3$): δ 169.1 (1C, C=O), 160.8 (1C, Ar), 135.8 (1C, Ar), 130.9 (1C, Ar), 123.9 (1C, Ar), 118.2 (1C, Ar), 112.2 (1C, Ar), 60.9 (1C, -O**C**H$_3$), 33.2 (1C, -N-**C**H$_3$). IR: νmax (ATR)/cm^{-1} : 1635 (C=O), 1603 (C-N), 1223 (O-C) and 978 (N-O). HRMS (ESI+, 70 eV) calculated for $C_9H_{11}FNO_2$ (M+H+): 184.0768, Found: 184.0767.

4-Fluoro-*N*-methoxy-*N*-methylbenzamide (69)

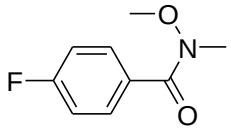

The reaction was carried out according to general procedure C using 4-fluorobenzoyl chloride (2 g, 12.60 mmol, 1 eq). The crude product was purified by flash chromatography (Biotage SP4, SiO_2; 0–50% EtOAc in *n*-hexane) to afford compound **69** (0.34 g, 15 %) as a colourless oil. ^{1}H NMR (400 MHz, $CDCl_3$): δ 8.12-7.05 (m, 4H, Ar-**H**), 3.7 (s, 3H, -OC**H**$_3$), 3.16 (s, 3H, -N-C**H**$_3$). ^{13}C NMR (400 MHz, $CDCl_3$): δ 168.8 (1C, C=O), 165.1 (1C, Ar), 129.8 (1C, Ar), 129.1 (2C, Ar), 115.2 (2C, Ar), 61.9 (1C, -O**C**H$_3$), 33.6 (1C, -N-**C**H$_3$). IR: νmax (ATR)/cm^{-1}: 1753 (C=O), 1633 (C-N), 1223 (O-C), 977 (N-O). HRMS (ESI+, 70 eV) calculated for $C_9H_{11}FNO_2$ (M+H+): 184.0768, Found: 184.0768.

3.3.4 General Procedure D (synthesis of ketone *via* reaction of Weinreb amides with Grignard reagents)

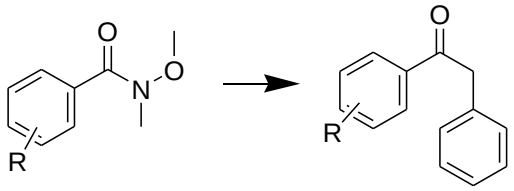

Benzylmagnesium bromide (2.0 M in THF, 2 eq) was added over 10 minutes to a cooled (0 ^{o}C) solution of the required fluoro-*N*-methoxy-*N*-methylbenzamide derivative (1 eq) in THF (12.4 mL) and stirred for 2 hours. The reaction mixture was warmed to room temperature, stirred for a further 2 hours and then quenched with saturated aqueous ammonium chloride solution (20 mL). The reaction mixture was extracted with EtOAc (3 x 25 mL) and the organics washed with water (75 mL), brine (75 mL) and dried over $MgSO_4$. The combined organic fractions were concentrated and the crude product was used in the subsequent steps without further purification (Hirashima *et al.*, 2006).

3.3.5 General Procedure E (synthesis of ketone *via* Friedal-Crafts acylation)

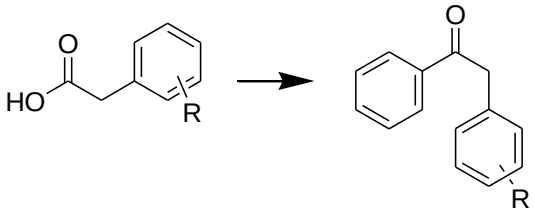

Phenylacetic acid (1 eq) was dissolved in anhydrous dichloromethane (100 mL) and then treated with oxalyl chloride (2 eq) and dimethylformamide (1 drop). The reaction mixture was stirred at room temperature under a N_2 atmosphere for 2.5 hours. The mixture was cooled to 0 ^{o}C and aluminum chloride (1 eq) and benzene (1 eq) added over 5 minutes. After addition the mixture quenched with concentrated hydrochloric acid (10 mL) and then extracted with chloroform (3 x 50 mL). The combined extracts were washed with saturated sodium carbonate (40 mL), dried over $MgSO_4$ and the crude product purified by either recrystallization or flash chromatography (Ramajayama *et al*, 2008).

3.4 Synthesis of target compounds

3.4.1 Synthesis of monoximes

2-(Hydroximino)-1,2-diphenylethanone (10-11)

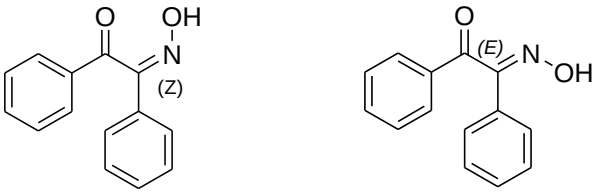

The reaction was carried out according to general procedure A using benzylphenyl ketone (4.25 g, 21.7 mmol). Recrystallisation gave the title compounds **10** as a white solid (0.5 g, 21 %) and **11** as an off-white solid (1.3 g, 56 %). *Z*-monoxime, **10:** MR. 100 – 102 °C. ^{1}H NMR (400 MHz, DMSO-d6): δ 11.76 (s, 1H, O**H**), 7.78-7.34 (m, 10H, Ar-**H**). ^{13}C NMR (400 MHz, $CDCl_3$): δ 192.0 (1C, -CO-Ar), 154.2 (1C,C=N), 137.1 (1C, Ar), 134.4 (1C, Ar), 133.2 (1C, Ar), 131.3 (1C, Ar), 129.7

(2C, Ar), 129.3 (2C, Ar), 129.2 (2C, Ar), 128.1 (2C, Ar). IR: νmax (KBr disc, cm^{-1}): 3394 (O-H),1776 (C=O), 1645(C=N) and932(N-O). HRMS (ESI+, 70 eV) calculated for $C_{14}H_{12}$ N O_2 (M+H+): 226.0863, Found: 226.0858. *E*-monoxime, **11**: MR. 130 – 132 °C. ^{1}H NMR (400 MHz, DMSO-d6:) δ 12.47 (s, 1H, O**H**), 7.92-7.41 (m, 10H, Ar-**H**). ^{13}C NMR (400 MHz, $CDCl_3$): δ 192.1 (1C, CO-Ar), 154.2 (1C, C=N), 137.2 (1C.Ar), 134.5 (1C, Ar), 133.1 (1C, Ar), 131.2 (1C, Ar), 129. 9 (2C, Ar), 129.4 (2C, Ar), 129.3 (2C, Ar), 128.3 (2C, Ar). IR: νmax (KBr disc, cm^{-1}): 3394 (O-H), 1776 (C=O), 1645 (C=N) and 932(N-O). HRMS (ESI+, 70 eV) calculated for $C_{14}H_{12}NO_2$ (M+H+): 226.0863, Found: 226.0858.

***N*-Hydroxy-1,2-diphenylethanimine (22-23)**

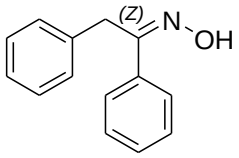

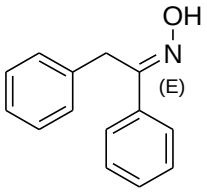

To solution of 1,2-benzylphenylketone (2.33 g, 11.92 mmol, 1 eq) and hydroxylamine hydrochloride (1.24 g, 17.84 mmol, 1.5 eq) in methanol (20 mL) was added aqueous potassium hydroxide solution (4 mL, 1.07 eq). The reaction mixture was stirred at room temperature for 24 hours, quenched with cold water (20 mL) and extracted with diethyl ether (1 x 20 mL and 3 x 40 mL). The combined organic extracts were washed with brine (40 mL), dried over anhydrous $MgSO_4$ and concentrated to give the crude *N*-hydroxy-1,2-diphenylethanimine (*E:Z*,3:1) mixture. Purification by gravity column chromatography [SiO_2; 10% diethyl ether in *n*-hexane] gave *E*-ketoxime (**23**, 1.30 g, 56 %) as white needles and *Z*-ketoxime (**22**, 0.5 g, 21 %) as a white powder (Ooi *et al.*, 2002). *E*-ketoxime, **23**: MR. 91-92 ^{o}C. ^{1}H NMR (400 MHz, DMSO-d6): δ 11.5 (s, 1H, O**H**), 7.68-7.22 (m, 10H, Ar-**H**), 3.34 (s, 2H, C$\mathbf{H}_2$). ^{13}C NMR (400 MHz, $CDCl_3$): δ 164.3 (1C=N), 137.6 (1C, Ar) 134.2 (1C, Ar), 131.3(1C, Ar), 129.2 (2C, Ar), 129.3 (2C, Ar), 129.0 (2C, Ar), 128.9 (2C, Ar), 125.9 (1C, Ar), 35.7 (1C, **C**H_2). IR: νmax (KBr disc, cm^{-1}): 3200 (O-H), 1600 (C=N) and 1000 (N-O). HRMS (ESI+, 70 eV) calculated for C_{14} H_{14}NO (M+H+): 212.1069, Found: 212.1069. *Z*-ketoxime, **22**: MR. 70-72 ^{o}C. ^{1}H NMR (400 MHz, DMSO-d6): δ 10.8 (s, 1H, O**H**), 7.68-7. 22 (m, 10 H, Ar- **H**), 3.33 (s, 2H, C$\mathbf{H}_2$). ^{13}C NMR (400 MHz, $CDCl_3$): δ 164.2 (1C=N), 137.5 (1C.Ar) 134.1 (1C, Ar), 131.2 (1C,

Ar), 129. 1 (2C, Ar), 129.2 (2C, Ar), 128.9 (2C, Ar), 128.8 (2C, Ar), 125.8 (1C, Ar), 35.6 (1C, **C**H_2). IR: νmax (KBr disc, cm^{-1}): 3300 (O-H), 1642 (C=N) and 969 (N-O). HRMS (ESI+, 70 eV) calculated for $C_{14}H_{14}NO$ (M+H+): 212.1069, Found: 212.1069.

2-(4-Fluorophenyl)-1-phenylethanone (31)

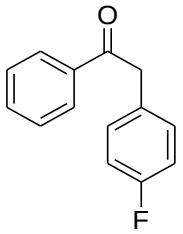

The reaction was carried out according to general procedure E using 4-fluorobenzylacetic acid (5.0 g, 32.43 mmol. 1 eq). Recrystallisation of the crude product from toluene gave compound **31** (4.92 g, 98 %) as a yellow solid. MR. 82-84 ^{o}C. ^{1}H NMR (400 MHz, $CDCl_3$): δ 8.00-7.07 (m, 9H, Ar-**H**), 4.33 (s, 2H, -C**H**$_2$). ^{13}C-NMR (400 MHz, $CDCl_3$): δ 196.9 (1C, C=O), 161.2 (1C, Ar) 137.1 (1C, Ar), 133.2 (1C, Ar), 132.3 (1C, Ar), 129.5 (2C, Ar), 129.0 (2C, Ar), 128.5 (2C, Ar), 115.5 (2C, Ar), 44.9 (1C, Ar-**C**H_2-CO). IR: νmax (KBr disc, cm^{-1}): 1721 (C=O) and1380 (C-F). HRMS (ESI+, 70 eV) calculated for $C_{14}H_{11}FO$ 214.0827, Found: 214.0826.

2-(4- Fluorophenyl)-2-(hydroxyimino)-1-phenylethanone (32)

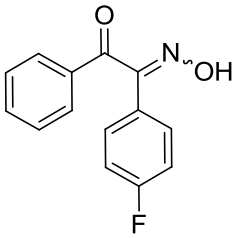

The reaction was carried out according to general procedure A using 2-(4-fluorophenyl)-1-phenylethanone (4.92 g, 20.57 mmol, 1 eq). The product was not separated as in general procdure A. Compound **32** obtained as a white solid as a racemic mixture (*E* /*Z* 1:3) (2.36 g, 47.2 %). *Z*-monoxime, ^{1}H NMR (400 MHz, DMSO-d6): δ 11.69 (s, 1H, O**H**), 7.91-7.21 (m, 9H, Ar-**H**). ^{13}C NMR (400 MHz, $CDCl_3$) : δ 192.2 (1C, CO-Ar), 165.2 (1C, Ar), 155.0 (1C, N= C), 137.8 (1C, Ar),

134.6 (1C, Ar), 130.8 (2C, Ar), 129.9 8(2C, Ar), 129.4 (2C, Ar), 128.7 (1C, Ar), 116.1(2C, Ar). *E*-monoxime, ^{1}H NMR (400 MHz, DMSO-d6): δ 12.65 (s, 1H, O**H**), 8.01-7.21 (m, 9H, Ar-**H**). ^{13}C NMR (400 MHz, $CDCl_3$): δ 192.3 (1C, CO-Ar), 165. 3(1C, Ar), 155.1(1C, N= C), 137.9 (1C, Ar), 134 7 (1C, Ar), 130.9 (2C, Ar), 129.9 (2C, Ar), 129.3 (2C, Ar), 128.8 (1C, Ar), 116.0 (2C, Ar). IR: νmax (KBr disc, cm^{-1}): 3385 (O-H), 1688 (C=O), 1662 (C=N), 1160 (C-F) and 949 (N-O). HRMS (ESI+, 70 eV) calculated for $C_{14}H_{10}FNO_2$ 243.06731, Found: 243.0670.

2-(3-Fluorophenyl)-1-phenylethanone (39)

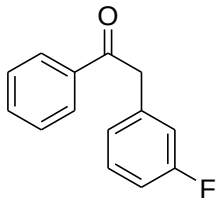

The reaction was carried out according to general procedure E using 3-fluorobenzylacetic acid (5.0 g, 32.4 mmol. 1 eq). Recrystallisation of the crude product from toluene gave compound **39** (4.82 g, 97 %) as a yellow solid. MR. 80-82 ^{o}C. ^{1}H NMR (400 MHz, $CDCl_3$): δ 8.01-6.99 (m, 9H, Ar-**H**), 4.26 (s, 2H, -C**H**$_2$). ^{13}C NMR (400 MHz, $CDCl_3$): δ 189.2 (1C, C=O), 164.0 (1C, Ar), 137.1 (1C, Ar), 136.5 (1C, Ar), 130.5 (1C, Ar), 128.5 (2C, Ar), 128.0 (2C, Ar), 126.6 (1C, Ar), 124.2 (1C, Ar), 119.5 (1C, Ar), 115.5 (1C, Ar), 44.92 (1C, Ar-**C**H_2-CO). IR: νmax (KBr disc, cm^{-1}): 1778 (C=O) and 1384 (C-F). HRMS (ESI+, 70 eV) calculated for $C_{14}H_{12}FO$ (M+H+): 215.0864, Found: 215.0866.

2-(3- Fluorophenyl)-2-(hydroxyimino)-1-phenylethanone (40)

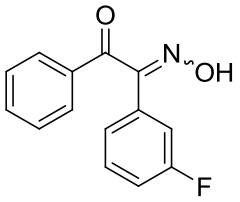

The reaction was carried out according to general procedure A using 2-(3-fluorophenyl)-1-phenylethanone (4.92 g, 20.57 mmol, 1 eq). The product was not separated into two isomers as in general procdure A the title compound **40** obtained as a white crystal (2.40 g, 48 %) as a racemic mixture of *E/Z* isomers (1:3). *Z*-monoxime, ^{1}H NMR (400 MHz, DMSO-d6): δ 11.69 (s, 1H, O**H**), 7.91-7.21 (m, 9H, Ar-**H**). ^{13}C NMR (400 MHz, $CDCl_3$): δ 190.2 (1C, CO-Ar), 164.3 (1C, C=N), 163.1 (1C, Ar), 137.0 (1C, Ar), 134.6 (1C, Ar), 134.3 (1C, Ar), 130.4 (1C, Ar), 129.9 (2C, Ar), 129.5 (2C, Ar), 124.1 (1C, Ar), 117.4 (1C, Ar), 115.4 (1C, Ar). *E*-monoxime, ^{1}H NMR (400 MHz, DMSO-d6): δ 12.70 (s, 1H, O**H**), 8.01-7.21 (m, 9H, Ar-**H**). ^{13}C NMR (400 MHz, $CDCl_3$): δ 190.3 (1C, CO-Ar), 164.3 (1C, C=N), 163.2 (1C, Ar), 137.1 (1C, Ar), 134.8 (1C, Ar), 134.4 (1C, Ar), 130.5 (1C, Ar), 130.0 (2C, Ar), 129.6 (2C, Ar), 124.2 (1C, Ar), 117.5 (1C, Ar), 115.5 (1C, Ar). IR: νmax (KBr disc, cm^{-1}): 3375 (O-H), 1781 (C=O), 1684 (C=N), 1384 (C-F) and 972 (N-O). HRMS (ESI+, 70 eV) calculated for $C_{14}H_{10}FNO_2$: 243.06731, Found: 243.0670.

2-(4-Bromophenyl)-1-phenylethanone (50)

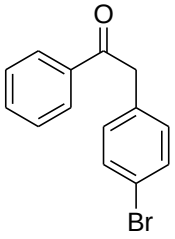

The reaction was carried out according to general procedure E using 4-bromobenzylacetic acid (5.0 g, 23.31 mmol. 1 eq). Recrystallisation of the crude from toluene afford compound **50** (3.66 g, 57 %) as a pale yellow solid. MR. 140-142 ^{o}C. ^{1}H-NMR (400 MHz, DMSO-d6): δ 8.00-7.18 (m, 9H, Ar-**H**), 4.25 (s, 2H, -C**H**$_2$). ^{13}C NMR (400 MHz, $CDCl_3$): δ 199.0 (1C, C=O), 136.0 (1C, Ar), 134.6 (1C, Ar), 133.2 (1C, Ar), 132.2 (2C, Ar), 131.9 (2C, Ar), 128.8 (2C, Ar), 128.3 (2C, Ar), 123.4 (1C, Ar), 44.50 (1C, Ar-**C**H$_2$-CO). IR: νmax (KBr disc, cm^{-1}): 2925 (C-H), 1683 (C=O) and 567 (C-Br). HRMS (ESI+, 70 eV) calculated for $C_{14}H_{12}BrO$ (M+H+): 275.0064, Found: 275.0066.

2-(4-Bromophenyl)-2-(hydroxyimino)-1-phenylethanone (51)

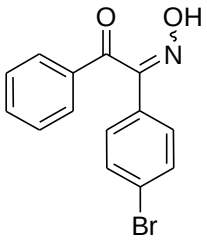

The reaction was carried out according to general procedure A using 2-(4-bromophenyl)-1-phenylethanone (2.34 g, 8.5 mmol, 1 eq). The diethyl ether organic extract were combined and concentrated under reduced pressure to afford compound **51** as a white solid (0.890 g, 34 %) as a racemic mixture of *E/Z* isomers (1:3). *Z*-monoxime, ^{1}H NMR (400 MHz, DMSO-d6): δ 11.93 (s, 1H, O**H**), 7.86-7.21 (m, 9H, Ar-**H**). ^{13}C NMR (400 MHz, $CDCl_3$): δ 190.0 (1C, CO-Ar), 164.0 (1C, C=N), 135.9 (1C, Ar), 134.1 (1C, Ar), 132.2 (1C, Ar), 131.8 (2C, Ar), 131.4 (2C, Ar), 129.8 (2C, Ar), 129.3 (2C, Ar), 125.4 (1C, Ar). *E*-monoxime, ^{1}H NMR (400 MHz, DMSO-d6): 12.68 (s, 1H, O**H**), 8.01-7.41 (m, 9H, Ar-**H**). ^{13}C NMR (400 MHz, $CDCl_3$): δ 190.1

(1C, C=O), 164.1 (1C, C=N), 136.0 (1C, Ar), 134.2 (1C, Ar), 132.3 (1C, Ar), 131.9 (2C, Ar), 131.5 (2C, Ar), 129.9 (2C, Ar), 129.4 (2C, Ar), 125.5 (1C, Ar). IR: νmax (KBr disc, cm^{-1}): (O-H) 3390, (C=O) 1702, (C=N) 1641, (C-Br) 655, (N-O) 972. HRMS (ESI+, 70 eV) calculated for $C_{14}H_{11}BrNO_2$ (M+H+): 303.9967, Found: 303.9968.

2-(3-Bromophenyl)-2-(hydroxyimino)-1-phenylethanone (60)

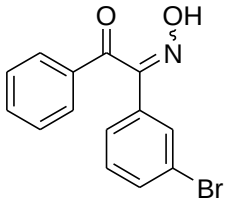

The reaction was carried out according to general procedure A using 2-(3-bromophenyl)-1-phenylethanone (3.6 g, 13.80 mmol, 1 eq). The diethyl ether organic extract was combined and concentrated under reduced pressure. The crude product was purified by column chromatography (SiO_2, 10% diethyl ether in *n*-hexane) to afford compound **60** as an off white solid (1.0 g, 25 %) as a racemic mixture of *E/ Z* isomers (1:2). *Z*-monoxime, ^{1}H NMR (400 MHz, DMSO-d6): δ 11.92 (s, 1H, O**H**), 7.93-7.51 (m, 9H, Ar-**H**). ^{13}C NMR (400 MHz, $CDCl_3$): δ 190.0 (1C, CO-Ar), 164.0 (1C, C=N), 137.1 (1C, Ar), 135.4 (1C, Ar), 134.6 (1C, Ar), 134.0 (1C, Ar), 132.7 (1C, Ar), 131.1 (1C, Ar), 129.8 (2C, Ar), 129.3 (2C, Ar), 128.2 (1C, Ar), 123.4 (1C, Ar). *E*-monoxime, ^{1}H NMR (400 MHz, DMSO-d6): δ 12.68 (s, 1H, O**H**), 8.01-7.51 (m, 9 H, Ar-**H**). ^{13}C NMR (400 MHz, $CDCl_3$): δ 190.1 (1C, CO-Ar), 164.1 (1C, C=N), 137.2 (1C, Ar), 135.5 (1C, Ar), 134.7 (1C, Ar), 134.1 (1C, Ar), 132.9 (1C, Ar), 131.3(1C, Ar), 129.9 (2C, Ar), 129.4 (2C, Ar), 128.3 (1C, Ar), 123.5 (1C, Ar). HRMS (ESI+, 70 eV) calculated for C_{14} $H_{11}BrNO_2$ (M+H+): 303.9967, Found: 303.9968.

1-(2-Fluorophenyl)-2-phenylethanone (70).

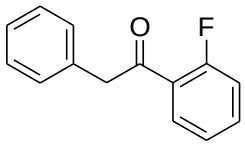

The reaction was carried out according to general procedure D using 2-fluoro-*N*-methoxy-*N*- methylbenzamide (0.34 g, 1.58 mmol, 1 eq) to afford compound **70** (0.2 g, 59 %) as a white solid which was used without further purification. MR. 77-80^{o}C. ^{1}H NMR (400 MHz, $CDCl_3$): δ 7.99 -7.06 (m, 9H, Ar-**H**), 4.29 (s, 2H, -C**H**$_2$). ^{13}C NMR (400 MHz, $CDCl_3$): δ 168.1 (1C, C=O), 163.5 (1C, Ar), 135.22 (1C, Ar), 134.9 (1C, Ar), 133.8 (1C, Ar), 130.8 (1C, Ar), 129.5 (2C, Ar), 129.4 (2C, Ar), 123.6 (1C, Ar), 119.2 (1C, Ar), 114.5 (1C, Ar), 61.0 (1C, - **C**H$_2$). IR: νmax (KBr disc, cm^{-1}): 1778 (C=O) and 1384 (C-F). HRMS (ESI+, 70 eV) calculated for $C_{14}H_{12}FO$ (M+H+): 215.0864, Found: 215.0866.

1-(3-Fluorophenyl)-2-phenylethanone (71).

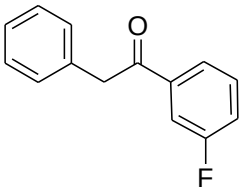

The reaction was carried out according to general procedure D using 3-fluoro-*N*-methoxy-*N*- methylbenzamide (0.34 g, 1.58 mmol, 1 eq) to afford compound **71** (0.2 g, 59 %) as a white solid which was used without further purification. MR. 81-83^{o}C. ^{1}H NMR (400 MHz, $CDCl_3$): δ 8.14–7.23.66 (m, 9H, Ar-**H**), 4.42 (s, 2H, -C**H**$_2$). ^{13}C NMR (400 MHz, $CDCl_3$): δ 190.2 (1C, C=O), 163.4 (1C, Ar), 141.4 (1C, Ar), 134.7 (1C, Ar), 133.8 (1C, Ar), 130.9 (1C, Ar), 129.7 (2C, Ar), 128.3 (2C, Ar), 124.5 (1C, Ar), 120.0 (1C, Ar), 114.6 (1C, Ar), 61.0 (1C, - **C**H$_2$). IR: νmax (KBr disc, cm^{-1}): 1778 (C=O) and 1384 (C-F). HRMS (ESI+, 70 eV) calculated for

$C_{14}H_{12}FO$ (M+H+): 215.0867, Found: 215.0867. Found C, 79.47; H, 5.69; (Required for $C_{14}H_{11}FO$: C, 78.49; H, 5.18).

1-(4-Fluorophenyl)-2-phenylethanone (72).

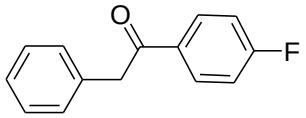

The reaction was carried out according to general procedure D using 4-fluoro-*N*-methoxy-*N*- methylbenzamide (0.34 g, 1.58 mmol, 1 eq) to afford comound **72** (0.2 g, 59 %) as a white solid which was used without further purification. MR. 82-84^{o}C. ^{1}H NMR (400 MHz, $CDCl_3$): δ 8.13 – 7.23 (m, 9H, Ar-**H**), 4.39 (s, 2H,-C**H**$_2$). ^{13}C NMR (400 MHz, $CDCl_3$): δ 190.2 (1C, C=O), 167.5 (1C, Ar), 134.1 (1C, Ar), 132.3 (1C, Ar), 130.8 (2C, Ar), 129.7(2C, Ar), 129.3 (2C, Ar), 127.7 (1C, Ar), 115.5 (2C, Ar), 44.5 (1C,- **C**H$_2$). IR: νmax (KBr disc, cm^{-1}): 1777 (C=O) and 1005 (C-F). HRMS (ESI+, 70 eV) calculated for C_{14} $H_{12}FO$(M+H+): 215.0865, Found: 215.0866.

1-(2-Fluorophenyl)-2-(hydroxyimino)-2-phenylethanone (73)

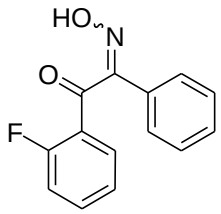

The reaction was carried out according to general procedure A using 1-(2-fluorophenyl)-2-phenylethanone (0.43 g, 2.17 mmol, 1 eq). The two isomers were not separated as in general procedure A. The diethyl ether organic extract were combined and concentrated under reduced pressure, then the crude was purified by flash chromatography (Biotage SP4, SiO_2, 10% diethyl ether in *n*-hexane)to afford compound **73** as a white solid (0.2 g, 37 %) as a racemic mixture of *E/ Z* isomers (1:2). *Z*-monoxime, ^{1}H NMR (400 MHz, DMSO-d6): 11.96 (s, 1H, O**H**), 7.93-7.33 (m, 9H, Ar-**H**). ^{13}C NMR (400 MHz, $CDCl_3$): δ 190.0 (1C, C=O),164.9 (1C, C=N), 164.4 (1C, Ar), 136.1 (1C, Ar), 134.9 (1C, Ar), 134.7 (1C, Ar), 131.7 (1C, Ar), 129.8

(2C, Ar), 129.5 (2C, Ar), 123.9 (1C, Ar), 119.1 (1C, Ar), 116.4 (1C, Ar). *E*-monoxime, ^{1}H NMR (400 MHz, DMSO-d6): 12.80 (s, 1H, O**H**), 8.01-7.51 (m, 9H, Ar-**H**). ^{13}C NMR (400 MHz, $CDCl_3$): δ 190.1 (1C, C=O), 165.0 (1C, C=N), 164.5 (1C, Ar), 136.2 (1C, Ar), 135.0 (1C, Ar), 134.8 (1C, Ar), 131.8 (1C, Ar), 129.9 (2C, Ar), 129.6 (2C, Ar), 124.0 (1C, Ar), 119.2 (1C, Ar), 116.5 (1C, Ar). IR: νmax (KBr disc, cm^{-1}): 3420 (O-H), 1738 (C=O), 1661 (C=N), 1224 (O-C), 1050 (C-F) and1002 (N-O). HRMS (ESI+, 70 eV) calculated for C_{14} $H_{11}FNO_2$ (M+H+): 244.0766, Found: 244.0768.

1-(3-Fluorophenyl)-2-(hydroxyimino)-2-phenylethanone (74)

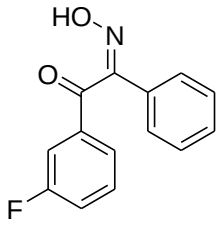

The reaction was carried out according to general procedure A using 1-(3-fluorophenyl)-2-phenylethanone (0.05 g, 0.23 mmol, 1 eq). The two isomers were not separated as in general procedure A. The diethyl ether organic extract were combined and concentrated under reduced pressure, then the crude was purified by flash chromatography (Biotage SP4) (SiO_2, 10% diethyl ether in *n*-hexane)to afford compound **74** as white solid (0.03 g, 52 %) as a racemic mixture of *E/Z* isomers (1:1). *Z*-monoxime, ^{1}H NMR (400 MHz, DMSO-d6): 11.91 (s, 1H, O**H**), 7.48-7.23 (m, 9H, Ar-**H**). ^{13}C NMR (400 MHz, $CDCl_3$): δ 190.0 (1C, C=O), 164.8 (1C, C=N), 163.3 (1C, Ar), 141.1 (1C, Ar), 134.6 (1C, Ar), 133.7 (1C, Ar), 130.0 (1C, Ar), 129.1 (2C, Ar), 128.1 (2C, Ar), 125.5 (1C, Ar), 120.0 (1C, Ar), 115.0 (1C, Ar). *E*-monoxime, ^{1}H NMR (400 MHz, DMSO-d6): δ 12.67 (s, 1H, O**H**), 8.01-7.23 (m, 9H, Ar-**H**). ^{13}C NMR (400 MHz, $CDCl_3$): δ 190.1 (1C, C=O), 164.9 (1C, C=N), 163.4 (1C, Ar), 141.2 (1C, Ar), 134.7 (1C, Ar), 133.8 (1C, Ar), 130.1 (1C, Ar), 129.2 (2C, Ar), 128.12 (2C, Ar), 125.6 (1C, Ar), 120.1 (1C, Ar), 115.1 (1C, Ar). IR: νmax (KBr disc, cm^{-1}): 3438 (O-H), 1688 (C=O), 1662 (C=N), 1224 (O-C), 1160 (C-F) and 949 (N-O). HRMS (ESI+, 70 eV) calculated for $C_{14}H_{11}FNO_2$ (M+H+): 244.0766, Found: 244.0768.

1-(4-Fluorophenyl)-2-(hydroxyimino)-2-phenylethanone (75)

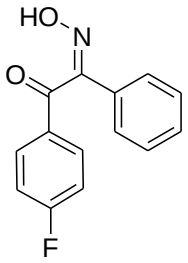

The reaction was carried out according to general procedure A using 1-(4-fluorophenyl)-2-phenylethanone (0.43 g, 2.17 mmol, 1 eq). The two isomers were not separated as in general procedure A due to time constrain. The diethyl ether organic extract were combined and concentrated under reduced pressure, then the crude was purified by flash chromatography (Biotage SP4, SiO_2, 10% diethylether in n-hexane)to afford compound **75** (0.23 g, 48 %) as a white solid as a racemic mixture of *E/Z* isomers (1:1). *Z*-monoxime, ^{1}H NMR (400 MHz, DMSO-d6): δ 11.96 (s, 1H, O**H**), 7.91-7.21 (m, 9H, Ar-**H**). ^{13}C NMR (400 MHz, $CDCl_3$): δ 190.2 (1C, C=O), 167.5 (1C, Ar), 164.8 (1C, C=N), 134.1 (1C, Ar), 132.3 (1C, Ar), 130.8 (1C, Ar), 130.5 (2C, Ar), 129.7(1C, Ar), 129.3 (2C, Ar), 127.7 (1C, Ar), 115.5 (2C, Ar), 44.5. *E*-monoxime, ^{1}H NMR (400 MHz, DMSO-d6): δ 12.65 (s, 1H, O**H**), 8.01-7.21 (m, 9H, Ar-**H**). ^{13}C NMR (400 MHz, $CDCl_3$): δ 190.3 (1C, C=O), 167.6 (1C, Ar), 164.9 (1C, C=N), 134.2 (1C, Ar), 132.4 (1C, Ar), 130.9 (1C, Ar), 130.6 (2C, Ar), 129.8 (1C, Ar), 129.4 (2C, Ar), 127.8 (1C, Ar), 115.6 (2C, Ar). IR: νmax (KBr disc, cm^{-1}): 3432 (O-H), 1788 (C=O), 1662 (C=N), 1235 (O-C), 1159 (C-F) and 945 (N-O). HRMS (ESI+, 70 eV) calculated for $C_{14}H_{11}FNO_2$ (M+H+): 244.0767, Found: 244.0768.

1-(4-Bromophenyl)-2-(hydroxyimino)-2-phenylethanone (78)

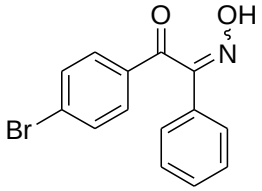

The reaction was carried out according to general procedure A using 2-(3-bromophenyl)-1-phenylethanone (0.47 g, 1.71 mmol, 1 eq). The diethyl ether organic extract were combined and concentrated under reduced pressure, then the crude was purified by flash chromatography (Biotage SP4, SiO_2, dichloromethane 100 %) to afford compound **78** as a white solid (0.25 g, 48 %) as a racemic mixture of *E/Z* isomers (1:5). *Z*-monoxime, ^{1}H NMR (400 MHz, DMSO-d6): δ 11.88 (s, 1H, O**H**), 7.92-7.44 (m, 9H, Ar-**H**). ^{13}C NMR (400 MHz, $CDCl_3$): δ 194.2 (1C, C=O), 154.2 (1C, C=N), 135.5 (1C, Ar), 133.2 (1C, Ar), 132.3 (2C, Ar), 132.2 (2C, Ar), 131.2 (1C, Ar), 129.3 (2C, Ar), 129.8 (2C, Ar), 127.2 (1C, Ar). *E*-monoxime, ^{1}H NMR (400 MHz, DMSO-d6): δ 12.65 (s, 1H, O**H**), 8.01-7.21 (m, 9H, Ar-**H**). ^{13}C NMR (400 MHz, $CDCl_3$): δ 194.3 (1C, C=O), 154.3 (1C, C=N), 135.6 (1C, Ar), 133.3 (1C, Ar), 132.3 (2C, Ar), 132.3 (2C, Ar), 131.3 (1C, Ar), 129.4 (2C, Ar), 129.9 (2C, Ar), 127.3 (1C, Ar). IR: νmax (KBr disc, cm^{-1}): 3438 (O-H), 1739 (C=O), 1661 (C=N),1235 (O-C) and 1004 (N-O). HRMS (ESI+, 70 eV) calculated for $C_{14}H_{11}BrNO_2$ (M+H+): 303.9967, Found: 303.9968.

1-(4-Chlorophenyl)-2-(hydroxyimino)-2-phenylethanone (80)

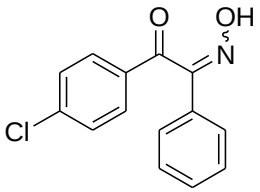

The reaction was carried out according to general procedure A using 4'–chloro-2-phenyl acetophenone (0.5 g, 2.17 mmol, 1 eq). The diethyl ether organic extract were combined and concentrated under reduced pressure, then the crude was purified

by flash chromatography (Biotage SP4, SiO_2; 0 – 50 % EtOAc in *n*-hexane) to afford compound **80** as a white solid (0.28 g, 49 %) as a racemic mixture of *E/Z* isomers (1:3). *Z*-monoxime, ^{1}H NMR (400 MHz, DMSO-d6): δ 11.88 (s, 1H, O**H**), 7.87 - 7.44 (m, 9H, Ar-**H**). ^{13}C NMR (400 MHz, $CDCl_3$): δ 194.1 (1C, C=O), 154.2 (1C, C=N), 139.6 (1C, Ar), 137.7 (1C, Ar), 133.2 (1C, Ar), 131.8 (1C, Ar),131.2 (2C, Ar), 129.8 (2C, Ar), 129.6 (2C, Ar), 125.6 (2C, Ar). *E*-monoxime, ^{1}H NMR (400 MHz, DMSO-d6): δ 12.55 (s, 1H, O**H**), 8.01-7.44 (m, 9H, Ar-**H**). ^{13}C NMR (400 MHz, $CDCl_3$): δ 194.2 (1C, C=O), 154.3 (1C, C=N), 139.7 (1C, Ar), 137.8 (1C, Ar), 133.3 (1C, Ar), 131.9 (1C, Ar),131.3 (2C, Ar), 129.9 (2C, Ar), 129.7 (2C, Ar), 125.7 (2C, Ar). IR: νmax (KBr disc, cm^{-1}): 3433 (O-H), 1730 (C=O), 1662 (C=N), 1235 (O-C) and 932 (N-O). HRMS (ESI+, 70 eV) calculated for $C_{14}H_{11}ClNO_2$ (M+H+) : 259, 0444, Found: 259, 0443.

2-(Hydroxyimino)-1, 2-*bis*-(4-methoxyphenyl) ethanone (82)

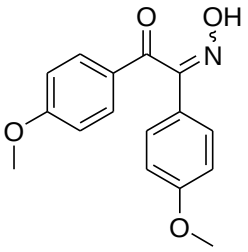

The reaction was carried out according to general procedure A using 1, 2-*bis*-(4-methoxyphenyl) ethanone (0.5 g, 1.90 mmol, 1 eq). The diethyl ether extract was combined and concentrated under reduced pressure and purified by flash chromatography (Biotage SP4, SiO_2; 0 – 50 % EtOAc in *n*-hexane) to afford compound **82** as a white solid (0.20 g, 36 %) as a racemic mixture of *E/Z* isomers (1:10). *Z*-monoxime, ^{1}H NMR (400 MHz, DMSO-d6): δ 11.41 (s, 1H, OH), 7.90 - 7.01 (m, 8H, Ar-H), 3.73 (s, *J* = 7.2 Hz, 6H, -OCH_3). ^{13}C NMR (400 MHz, $CDCl_3$) : δ 190.4 (1C, C=O), 154.4 (1C, C=N), 163.2 (1C, Ar), 160.3 (1C, Ar), 130.8(2C, Ar), 130.4 (2C, Ar), 130.1 (1C, Ar), 126.9 (1C, Ar), 114.0 (2C, Ar), 113.3 (2C, Ar), 54.7 (2C,-O**C**H_3). *E*-monoxime, ^{1}H NMR (400 MHz, DMSO-d6): δ 12.65 (s, 1H, O**H**), 8.01-7.44 (m, 8H, Ar-**H**), 3.74 (s, *J* = 7.2 Hz, 6H, -OC**H**$_3$). ^{13}C NMR (400 MHz, $CDCl_3$): δ 190.5 (1C, C=O), 154.5 (1C, C=N), 164.4 (1C, Ar), 160.0 (1C, Ar), 130.9 (2C, Ar), 130.5 (2C, Ar), 130.2 (1C, Ar), 127.0 (1C, Ar), 114.1 (2C, Ar),

113.4(2C, Ar), 54.9 (2C, -O**C**H_3). IR: νmax (KBr disc, cm^{-1}): 3070 (O-H), 1730 (C=O), 1664 (C=N), 1235 (O-C) and 949 (N-O). HRMS: (ESI+, 70 eV) calculated for $C_{16}H_{16}NO_4$ (M+H+): 286.1074, Found: 286.1074.

3.4.2 Synthesis of chloroformate derivatives

(2Z)-2-({[(Propan-2-yloxy)carbonyl]oxy}imino)-1,2-diphenylethanone (12)

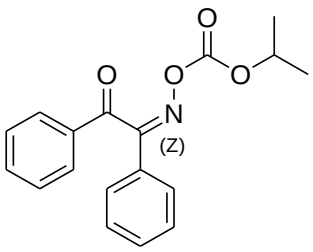

The reaction was carried out according to general procedure B using (2*Z*)-2-(hydroximino)-1,2-diphenylethanone (0.1 g, 0.44 mmol, 1 eq) and isopropylchloroformate (0.49 mL, 0.49 mmol, 1.1 eq). Recrystallisation of the crude from ethanol afford compound **12** (0.08 g, 57.2%) as a white solid. MR. 88 - 90 ^oC. ^1H NMR (400 MHz, $CDCl_3$): δ 8.00-7.26 (m, 10H, Ar-**H**), 4.95 (m, 1H, -O-C**H**-CH_3), 1.32 (d, *J* = 7.1 Hz, 6 H, O- CH-(C**H**$_3$)$_2$). ^{13}C NMR (400 MHz, $CDCl_3$): δ 192.1 (1C, CO-Ar), 162.2 (1C, C=N), 154.2 (1C, O-CO-O), 135.2 (1C, Ar) 134.1 (1C, Ar), 133.0 (1C, Ar), 131.1 (1C, Ar), 129.9 (2C, Ar), 129.2 (2C, Ar), 129.1 (2C, Ar), 128.2 (2C, Ar), 73.6 (1C, -O-**C**H-CH3), 21.6 (2C, O-CH –(**C**H3)$_2$). IR: νmax (KBr disc, cm^{-1}): 2963 (C-H), 1766 (C=O), 1679 (C=N), 1253 (O-C) and 951 (N-O). HRMS (ESI+, 70 eV) calculated for $C_{18}H_{21}N_2O_4$ (M+NH_4+): 329.1495, Found: 329.1495. Found C, 71.58; H, 6.11; N, 3.91 (Required for $C_{18}H_{17}NO_4$: C, 69.44; H, 5.50; N, 4.50).

(2*Z*)- 2-({[(Prop-2-en-1-yloxy)carbonyl]oxy}imino)-1,2-diphenylethanone (13)

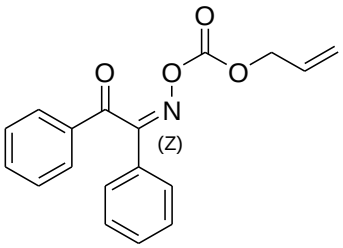

The reaction was carried out according to general procedure B (2*Z*)-2-(hydroximino)-1,2-diphenylethanone (0.2 g, 0.887 mmol, 1 eq) and allylchloroformate (0.103 mL, 0.9767 mmol 1.1 eq). Recrystallisation of the crude from ethanol afford compound **13** (0.08 g, 29.2 %) as a colorless crystalline solid. MR. 48 - 50 ^{o}C. ^{1}H NMR (400 MHz, $CDCl_3$): δ 7.94 -7.40 (m, 10H, Ar-**H**), 5.88 (dd, *J* = 17.3, 10.6, 9.6 Hz, 1H, O-CH_2-C**H** -CH_2), 5.28 (dd, *J* = 10.6, 1.2 Hz, 1H, O-CH_2-CH -C**H**$_2$), 5.24 (dd, *J* = 17.3, 1.2 Hz, 1H, O-CH_2-CH -C**H**$_2$), 4.66 (d, *J* = 9.6 Hz, 2 H, O-C**H**$_2$-CH -CH_2). ^{13}C NMR (400 MHz, $CDCl_3$): δ 192.2 (1C, CO-Ar), 162.1(1C, C=N), 150.0 (1C, O-CO-O), 137.9 (1C, Ar), 134.6 (1C, Ar), 133.0 (1C, Ar), 131.1 (1C, O-CH_2-**C**H -CH_2), 130.1 (1C, Ar), 129.8 (2C, Ar), 129.3 (2C, Ar), 129.2 (2C, Ar), 128.9 (2C, Ar), 120.9 (1C, O-CH_2-CH **=C**H_2), 68.1 (1C, O-**C**H_2-CH -CH_2). IR: νmax (KBr disc, cm^{-1}): 3061 (=CH), 2995 (C-H), 1778 (C=O), 1679 (C=N), 1235 (O-C) and 987 (N-O). HRMS: (ESI+, 70 eV) calculated for $C_{18}H_{15}NO_4$ 309.1065, Found: 309.1155.

(2Z)-2-({[(2-Bromoethoxy)carbonyl]oxy}imino)-1,2-diphenylethanone (14)

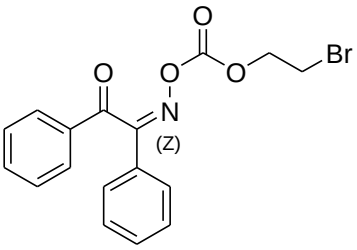

The reaction was carried out according to general procedure B using (2*Z*)-2-(hydroximino)-1,2-diphenylethanone (0.2 g, 0.89 mmol, 1 eq) and 2-bromoethylchloroformate (0.10 mL, 0.98 mmol, 1.1 eq). The crude product was chromatographed (SiO_2, dichloromethane 100%) to afford compound **14** (0.10 g,

29.9 %) as pure colorless crystals. MR. 60-62 ^{o}C. ^{1}H NMR (400 MHz, $CDCl_3$): δ 7.93-7.42 (m, 10H, Ar-**H**), 4.49 (t, *J* = 6.2 Hz, 2H, O-C**H**$_2$-CH_2 -Br), 3.47 (t, *J* = 6.2 Hz, 2H, O-CH_2-C**H**$_2$ –Br). ^{13}C NMR (400 MHz, $CDCl_3$): δ 191.1 (1C, CO-Ar), 162.1 (1C, C=N), 152.0 (1C, O-CO-O), 135.1 (1C, Ar) 134.3 (1C, Ar), 131.2 (1C, Ar), 130.5 (1C, Ar), 129.8 (2C, Ar), 129.4 (2C, Ar), 128.7 (2C, Ar), 127.8 (2C, Ar), 68.8 (1C, O-**C**H_2-CH_2 -Br), 27.8 (1C, O-CH_2-**C**H_2 -Br). IR: νmax (KBr disc, cm^{-1}): 2985 (C-H), 1778 (C=O), 1677 (C=N), 1246 (O-C) and 955 (N-O). HRMS (ESI+, 70 eV) calculated for $C_{17}H_{15}BrNO_4$ (M+H+): 376.999, Found: 376.997.

(2Z)-2-({[(Chloromethoxy)carbonyl]oxy}imino)-1,2-diphenylethanone (15)

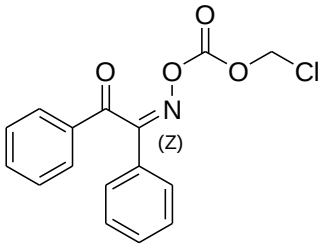

The reaction was carried out according to general procedure B using (2*Z*)-2-(hydroximino)-1,2-diphenylethanone (0.2 g, 0.89 mmol, 1 eq) and chloromethylchloroformate (0.07 mL, 0.97 mmol, 1.1 eq). The crude product was purified by flash chromatography (SiO_2, dichloromethane 100%) to afford compound **15** (0.04 g, 14.1 %) as a white solid. MR. 88 -90 ^{o}C. ^{1}H NMR (400 MHz, $CDCl_3$): δ 7.93-7.42 (m, 10H, Ar-**H**), 5.72 (s, 2H, O-C**H**$_2$-Cl). ^{13}C NMR (400 MHz, $CDCl_3$): δ 190.5 (1C, CO-Ar), 163.7 (1C, C=N), 151.4 (1C, O-CO-O), 134.9 (1C, Ar), 134.1 (1C, Ar), 131.0 (1C, Ar), 130.6 (1C, Ar), 129.7 (2C, Ar), 129.2 (2C, Ar), 128.8 (2C, Ar), 127.8(2C, Ar), 72.4 (1C, O-**C**H_2-Cl). IR: νmax (KBr disc, cm^{-1}): 2985 (C-H), 1778 (C=O), 1679 (C=N), 1235 (O-C), 946 (N-O) and 692 (C-Cl). HRMS (ESI+, 70 eV) calculated for $C_{16}H_{13}ClNO_4$ (M+H+): 318.7112, Found: 318.7114.

{[(Z)-(1,2-diphenylethylidene)amino]oxy}(methoxy)methanone (26)

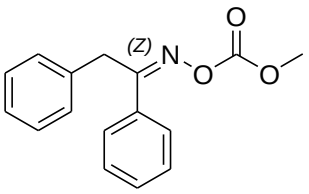

The reaction was carried out according to general procedure B using (1*Z*)-*N*-hydroxy-1,2-diphenylethanimine (0.10 g, 0.47 mmol, l.1 eq) and methylchloroformate (0.04 mL, 0.52 mmol, 1.1 eq). The crude product was purified by flash chromatography (SiO_2, dichloromethane 100%) to give compound **26** (0.09 g, 70 %) as white solid. MR. 58- 60 ^{o}C. ^{1}H NMR (400 MHz, $CDCl_3$): δ 7.68-7.16 (m, 10H, Ar-**H**), 4.25 (s, 2H, C**H**$_2$), 3.80 (s, 3H, O-C**H**$_3$). ^{13}C NMR (400 MHz, $CDCl_3$): δ 164.5 (1C, C=N), 157.8 (1C, O-CO-O), 136.0 (1C, Ar) 134.0 (1C, Ar), 131.1 (1C, Ar), 129.7 (2C, Ar), 129.5 (2C, Ar), 128.8 (2C,Ar), 128.7 (2C, Ar), 125.2 (1C, Ar), 55.6 (1C, O-**C**H$_3$), 31.5 (1C, N=C-**C**H$_2$-Ar). IR: νmax (KBr disc, cm^{-1}): 2959 (C-H), 1778 (C=O), 1623 (C=N), 1232 (O-C) and 964 (N-O). HRMS (ESI+, 70 eV) calculated for $C_{16}H_{15}NO_3$ 269.1011, Found: 269.1012. Found C,71.90; H,5.55; N, 5.28 (Required for $C_{16}H_{15}NO_3$; C, 71.36; H, 5.61; N, 5.20).

{[(*E*)-(1,2-Diphenylethylidene)amino]oxy}(methoxy)methanone (27)

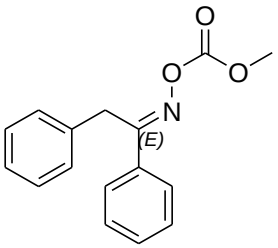

The reaction was carried out according to general procedure B using (1*E*)-*N*-hydroxy-1,2-diphenylethanimine (0.10 g, 0.47 mmol, 1 eq) and methylchloroformate (0.04 mL, 0.52 mmol, 1.1 eq). The crude product was purified by flash chromatography (SiO_2, dichloromethane 100%) to give compound **27** (0.082 g, 64 %) as white solid. MR. 48 -50 ^{o}C. ^{1}H NMR (400 MHz, $CDCl_3$): δ 7.69-7.17 (m, 10H, Ar-**H**), 4.26 (s, 2H, C**H**$_2$), 3.80 (s, 3H, O-C**H**$_3$). ^{13}C NMR (400 MHz, $CDCl_3$): δ

164.6 (1C, C=N), 157.9 (1C, O-CO-O), 136.1 (1C, Ar) 134.1 (1C, Ar), 131.2 (1C, Ar), 130.1 (1C, Ar), 129.8 (2C, Ar), 128.8 (2C, Ar), 126.8 (2C, Ar), 125.3 (2C, Ar), 55.7(1C, O-**C**H_3), 31.6 (1C, N=C-**C**H_2-Ar). IR: νmax (KBr disc, cm^{-1}): 2958 (C-H), 1776 (C=O), 1620 (C=N), 1230 (O-C) and 964 (N-O). HRMS (ESI+, 70 eV) calculated for $C_{16}H_{15}NO_3$ 269.1014, Found: 269.1016. Found C,71.90; H ,5.70; N, 5.28 (Required for $C_{16}H_{15}NO_3$; C,71.36; H, 5.61; N, 5.20).

{[(Z)-(1,2-Diphenylethylidene)amino]oxy}(propoxy)methanone (28)

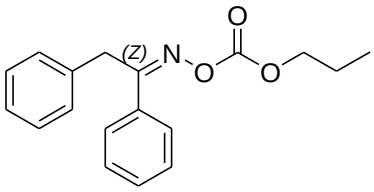

The reaction was carried out according to general procedure B using (1*Z*)-*N*-hydroxy-1,2-diphenylethanimine (0.2 g, 0.95 mmol, 1 eq) and propylchloroformate (0.11 mL, 1.04 mmol, 1.1 eq). Recrystallisation of the crude product from toluene afforded compound **28** (0.08 g, 80 %) as a white solid. MR. 36-38 ^oC ^1H NMR (400 MHz, $CDCl_3$): δ 7.72-7.13 (m, 10H, Ar-**H**), 4.23 (t,2 H, *J* = 7.3 Hz, O-C**H**$_2$-CH_2-CH_3), 4.22 (s, 2H, Ar-C**H**$_2$), 1 .75 (m, 2H, O-CH_2-C**H**$_2$-CH_3), 0.97 (t, *J* = 7.1 Hz, 3H, -O-CH_2-CH_2-C**H**$_3$). ^{13}C NMR (400 MHz, $CDCl_3$): δ 170.7 (1C, C=N), 162.7 (1C, O-CO-O), 137.5 (1C, Ar), 134.0 (1C, Ar), 131.1 (1C, Ar), 129.2 (2C, Ar), 129.1 (2C, Ar), 128.9 (2C, Ar), 128.7 (2C, Ar), 125.8 (1C, Ar), 71.3 (1C, O-**C**H_2-CH_2-CH_3), 31.5 (1C, N=C-**C**H_2-Ar), 22.0 (1C, O -CH_2-**C**H_2-CH_3), 9.9 (1C, O -CH_2-CH_2-**C**H_3). IR: νmax (KBr disc, cm^{-1}): 2974 (C-H), 1779 (C=O), 1685 (C=N), 1231 (O-C), 956 (N-O). HRMS (ESI+, 70 eV) calculated for $C_{18}H_{19}O_3NNa$ (M+Na+): 320.1260, Found: 320.1257. Found C, 72.76; H, 6.46; N, 4.75 (Required for $C_{18}H_{19}NO_3$; C, 72.71; H, 6.44; N, 4.71).

{[(*Z*)-(1,2-Diphenylethylidene)amino]oxy}(propan-2-yloxy)methanone (29)

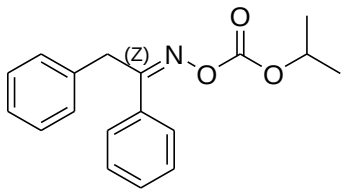

The reaction was carried out according to general procedure B using (1*Z*)-*N*-hydroxy-1,2-diphenylethanimin(0.2 g, 0.95 mmol, 1eq) and isopropylchloroformate (0.15 mL, 1.04 mmol, 1.1 eq). Recrystallisation of the crude product from toluene afforded compound **29** (0.20 g, 64 %) as a white solid. MR. 81-83 ^{o}C. ^{1}H NMR (400 MHz, $CDCl_3$): δ 7.72-7.26 (m, 10H, Ar-**H**), 5.04 (m, 1H, -O-C**H**-CH_3), 4.22 (s, 2H, Ar-C**H**$_2$), 1.35 (d, *J* = 7.1 Hz, 6 H, O- CH-(C**H**$_3$)$_2$). ^{13}C NMR (400 MHz, $CDCl_3$): δ 163.2(1C, C=N), 153.5 (1C, O-CO-O), 137.2 (1C, Ar), 134.0 (1C, Ar), 131.0 (1C, Ar), 129.5 (2C, Ar), 129.1 (2C, Ar), 128.8 (2C, Ar), 128.7 (2C, Ar), 125.8 (1C, Ar), 73.1 (1C, -O-**C**H-CH3),34.1(1C, N=C-**C**H$_2$-Ar), 21.8 (2C, O-CH –(**C**H3)$_2$). IR: νmax (KBr disc, cm^{-1}): 2977 (C-H), 1760 (C=O), 1611 (C=N), 1242 (O-C) and 929 (N-O). HRMS (ESI+,70eV) calculated for $C_{18}H_{23}N_2O_3$ (M+NH_4+): 315.1495, Found: 315.1495. Found C, 72.81; H, 6.35; N, 4.30 (Required for $C_{18}H_{19}N\ O_3$; C, 72.71; H, 6.44; N, 4.71).

{[(*Z*)-(1,2-Diphenylethylidene)amino]oxy}(2-methylpropoxy)methanone (30)

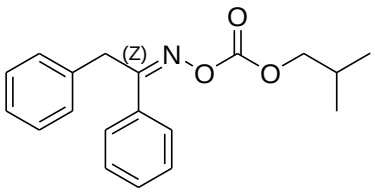

The reaction was carried out according to general procedure B using (1*Z*)-*N*-hydroxy-1,2-diphenylethanimine (0.2 g, 0.95 mmol, 1 eq) and isobutylchloroformate (0.14 mL, 1.04 mmol,1.1 eq). Recrystallisation of the crude product from toluene afforded compound **30** (0.20 g, 67 %) as colorless crystals. MR. 50-52^{o}C. ^{1}H NMR (400 MHz, $CDCl_3$): δ 7.72-7.20 (m, 10H, Ar-**H**), 4.29 (d, *J* = 6.6 Hz, 2H, O- C**H**$_2$ -

CH-$(CH_3)_2$), 4.09 (s, 2H, Ar-C**H**$_2$), 2.03 (m, 1H, O- CH_2 -C**H**-$(CH_3)_2$), 0.94 (d, *J* = 7.1 Hz, 6H, O- CH_2 -CH-(C**H**$_3)_2$). ^{13}C NMR (400 MHz, $CDCl_3$): δ 163.7 (1C, C=N), 154.1 (1C, O-CO-O), 137.2 (1C, Ar), 134.1 (1C, Ar), 131.2 (1C, Ar), 129.3 (2C, Ar), 129.2 (2C, Ar), 128.9 (2C, Ar), 128. 7 (2C, Ar), 126.8(1C, Ar), 76.8(1C, O-**C**H_2 -CH-$(CH_3)_2$), 34.2 (1C, N=C-**C**H_2-Ar), 27.8 (1C, O- CH_2 -**C**H-$(CH_3)_2$), 18.9 (2C, O- CH_2 -CH-(**C**$H_3)_2$). IR: νmax (KBr disc, cm-^{1}): 2961 (C-H), 1780 (C=O), 1643 (C=N),1239 (O-C) and 965 (N-O). HRMS (ESI+, 70 eV) calculated for $C_{19}H_{21}$Na NO_3 (M+Na+): 334.1410, Found: 334.1413. Found C, 73.29; H, 6.77.40; N, 4.26 (Required for $C_{19}H_{21}NO_3$; C, 73.29; H, 6.80; N, 4.50).

(2*Z*)-2-{[(Methoxycarbonyl)oxy]imino}-2-(4-fluorophenyl)-1-phenylethanone (33)

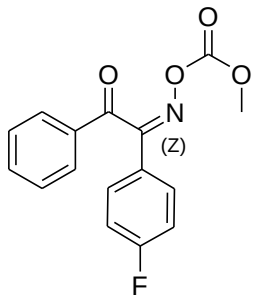

The reaction was carried out according to general procedure B using 2-(4-fluorophenyl)-2-(hydroximino)-1-phenylethanone (0.1g, 0.41 mmol, 1 eq) and methylchloroformate (0.04 mL, 0.45 mmol, 1.1 eq). The crude product was chromatographed (SiO_2, dichloromethane, 100 %) then recrystallised from ethanol to afford compound **33** (0.04 g, 31 %) as a white solid. MR. 106-108 ^{o}C. ^{1}H NMR (400 MHz, $CDCl_3$): δ 7.93-7.35 (m, 9H, Ar-**H**), 1.26 (s, 3H, O-C**H**$_3$). ^{13}C NMR (400 MHz, $CDCl_3$): δ 190.1 (1C, CO-Ar), 165.2 (1C, Ar), 164.1(1C, N= C), 155.0 (1C, O-CO-O), 135.9 (1C, Ar), 134.6 (1C, Ar), 130.7 (2C, Ar), 129.8 (2C, Ar), 129.1 (2C, Ar), 128.7 (1C, Ar), 115.0 (2C, Ar), 55.2 (1C, O-**C**H_3). IR: νmax (KBr disc, cm-^{1}): 2956 (C-H), 1787 (C=O), 1682 (C=N), 1236 (O-C) and 940 (N-O). HRMS (ESI+, 70 eV) calculated for $C_{16}H_{12}FNO_4$Na (M+Na+): 324.0642, Found: 324.0642.

(2*Z*)-2-{[(Ethoxycarbonyl)oxy]imino}-2-(4-fluorophenyl)-1-phenylethanone (34)

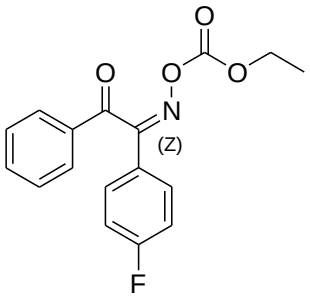

The reaction was carried out according to general procedure B using 2-(4-fluorophenyl)-2-(hydroximino)-1-phenylethanone (0.1g, 0.41 mmol, 1 eq) and ethylchloroformate (0.043 mL, 0.45 mmol, 1.1 eq). The crude product was chromatographed (SiO_2, dichloromethane, 100 %) then recrystallised from ethanol to afford compound **34** (0.042 g, 32.3 %) as a white solid. MR. 107-109 ^{o}C. ^{1}H NMR (400 MHz, $CDCl_3$): δ 7.93-7.09 (m, 9H, Ar-**H**), 2.42 (q, *J* = 7.1 Hz, 2 H, -O-C**H**$_2$-CH_3), 1.24 (t, *J* = 7.1 Hz, 3H, O-CH_2-C**H**$_3$). ^{13}C NMR (400 MHz, $CDCl_3$): δ 191.0 (1C, CO-Ar), 165.3 (1C, Ar), 165.1(1C, N= C), 155.5 (1C, O-CO-O), 136.1 (1C, Ar), 134.6 (1C, Ar), 130.7 (2C, Ar), 129.7 (2C, Ar), 129.2 (2C, Ar), 128.9 (1C, Ar), 115.3 (2C, Ar), 73.4 (1C, O-**C**H_2-CH_3), 35.5 (1C, - O-CH_2-**C**H_3). IR: νmax (KBr disc, cm^{-1}): 2925 (C-H), 1776 (C=O), 1683 (C=N), 1233 (O-C), 1180 (C-F) and 954 (N-O). HRMS: (ESI+, 70 eV) calculated for $C_{17}H_{14}FNO_4Na$ (M+Na+): 338.0794, Found: 338.07991. Found C, 64.70; H,4.48; N, 4.46 (Required for $C_{17}H_{14}FNO_4$: C, 64.76; H, 4.48; N, 4.44).

(2*Z*)-2-(4-Fluorophenyl)-1-phenyl-2-{[(propoxycarbonyl)oxy]imino}ethanone (35)

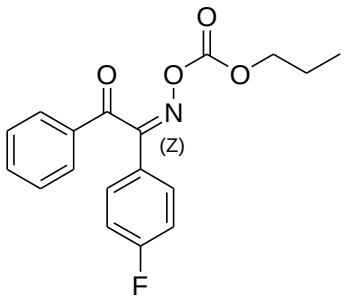

The reaction was carried out according to general procedure B using 2-(4-fluorophenyl)-2-(hydroximino)-1-phenylethanone (0.1g, 0.41 mmol, 1 eq) and propoylchloroformate (0.05 mL, 0.45 mmol, 1.1 eq). The crude product was chromatographed (SiO_2, dichloromethane, 100 %) then recrystallised from ethanol to afford compound **35** (0.02 g, 14.7%) as a white solid. MR. 108-110 ^{o}C. ^{1}H NMR (400 MHz, $CDCl_3$): δ 7.93-7.09 (m, 9H, Ar-**H**), 4.10 (t, 2 H, *J* = 7.11 Hz, O -C**H**$_2$-CH_2-CH_3), 1.60 (m, 2H, O-CH_2-C**H**$_2$-CH_3), 0.84 (t, *J* = 7.10 Hz, 3H, O-CH_2-CH_2-C**H**$_3$). ^{13}C NMR (400 MHz, $CDCl_3$): δ 191.3 (1C, CO-Ar), 165.1 (1C, Ar), 164.2 (1C, C=N), 156.5 (1C, O-CO-O), 137.1 (1C, Ar), 134.5 (1C, Ar), 130.6 (2C, Ar), 129.8 (2C, Ar), 129.5 (2C, Ar), 127.9 (1C, Ar), 116.3 (2C, Ar), 32.7 (1C, O -**C**H_2-CH_2-CH_3), 25.0 (1C, O -CH_2-**C**H_2-CH_3), 10.98 (1C, O -CH_2-CH_2-**C**H_3). IR: νmax (KBr disc, cm^{-1}): 2972 (C-H), 1773 (C=O), 1684 (C=N), 1231 (O-C), 1180 (C-F) and 959(N-O). HRMS (ESI+, 70 eV) calculated for $C_{18}H_{16}FNO_4Na$ (M+Na+): 352.0949, Found: 352.0955. Found C, 65.46; H, 4.46; N, 3.45 (Required for $C_{18}H_{16}FO_4$ N: C, 65.65; H, 4.90; N, 3.55).

(2*Z*)-2-(4-Fluorophenyl)-1-phenyl-2-({[(propan-2-yloxy)carbonyl]oxy}imino)ethanone (36)

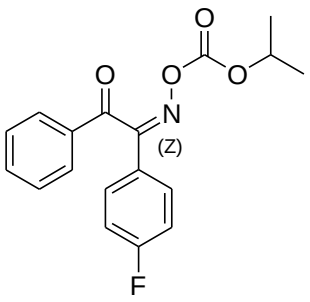

The reaction was carried out according to general procedure B using 2-(4-fluorophenyl)-2-(hydroximino)-1-phenylethanone (0.1g, 0.41 mmol, 1 eq) and isopropoylchloroformate (0.45 mL, 0.45 mmol, 1.1 eq). The crude product was chromatographed (SiO_2, dichloromethane, 100 %) then recrystallised from ethanol to afford compound **36** (0.02 g, 13 %) as a white solid. MR. 80-82 ^oC. ^1H NMR (400 MHz, $CDCl_3$): δ 7.93-7.09 (m, 9H, Ar-**H**), 4.91 (m, 1H, -O-C**H**-CH_3), 1.21 (d, *J* = 7.1 Hz, 6 H, O- CH-(C**H**$_3$)$_2$). ^{13}C NMR (400 MHz, $CDCl_3$): δ 192.2 (1C, CO-Ar), 164.7 (1C, Ar), 164.1(1C, C=N), 157.5 (1C, O-CO-O), 137.1 (1C, Ar), 135.1(1C, Ar), 131. 0 (2C, Ar), 129.9 (2C, Ar), 129.5(2C, Ar), 129.0 (1C, Ar), 116.3 (2C, Ar), 70.4 (1C, -O-**C**H-CH3), 20.5 (2C, O-CH –(**C**H3)$_2$). IR: νmax (KBr disc, cm^{-1}): 2988 (C-H), 1773 (C=O), 1678 (C=N), 1235 (O-C), 1179 (C-F) and 951 (N-O). HRMS (ESI+, 70 eV) calculated for C_{18} $H_{16}FNO_4Na$ (M+Na+): 352.0949, Found: 352.0964. Found C, 65.46; H, 4.46; N, 3.45 (Required for $C_{18}H_{16}FNO_4$: C, 65.30; H, 4.40; N, 3.45).

(2*Z*)-2-{[(Butoxycarbonyl)oxy]imino}-2-(4-fluorophenyl)-1-phenylethanone (37)

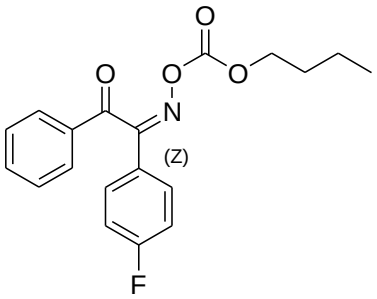

The reaction was carried out according to general procedure B using 2-(4-fluorophenyl)-2-(hydroximino)-1-phenylethanone (0.1g, 0.41 mmol, 1 eq) and butylchloroformate (0.06 mL, 0.45 mmol, 1.1 eq). The crude product was chromatographed (SiO_2, dichloromethane, 100%) then recrystallised from ethanol to afford compound **37** (0.05 g, 35.4 %) as colorless crystals. MR. 58-60 ^{o}C. ^{1}H NMR (400 MHz, $CDCl_3$): δ 7.93 -7.09(m, 9H, Ar-**H**), 2.22 (t, *J* = 6.6 Hz, 2H, C**H**$_2$-CH_2-CH_2-CH_3), 1.53 (m, 2H, CH_2-C**H**$_2$-CH_2-CH_3), 1.07 (m, 2H, CH_2-CH_2-C**H**$_2$-CH_3), 0 .82 (t, *J* = 7.1 Hz, 3H, CH_2-CH_2-CH_2-C**H**$_3$). ^{13}C NMR (400 MHz, $CDCl_3$): δ 189.0 (1C, CO-Ar), 165.5 (1C, Ar), 164.7 (1C, N= C), 155.6 (1C, O-CO-O), 136.3 (1C, Ar), 134.7 (1C, Ar), 130.9 (2C, Ar), 129.9 (2C, Ar), 1295 (2C, Ar), 128.8 (1C, Ar), 116.5 (2C, Ar), 34.1 (1C, O -**C**H_2-CH_2- CH_2CH_3), 28.6 (1C, O -CH_2-**C**H_2 CH_2-CH_3), 24.1 (1C, O -CH_2-CH_2 **C**H_2-CH_3), 15.1 (1C, O -CH_2-CH_2 CH_2-**C**H_3). IR: νmax (KBr disc, cm^{-1}): 2964 (C-H), 1776 (C=O), 1685 (C=N), 1226 (O-C), 1180 (C-F) and 939 (N-O). HRMS (ESI+, 70 eV) calculated for $C_{19}H_{22}FN_2O_4$ (M+NH_4+): 361.1556, Found: 361.1558. Found C, 66.30; H, 5.28; N, 4.11 (Required for $C_{19}H_{18}FNO_4$: C, 66.46; H, 5.28; N, 4.08).

(2Z)-2-(4-Fluorophenyl)-2-({[(2-methylpropoxy)carbonyl]oxy}imino)-1-phenylethanone (38)

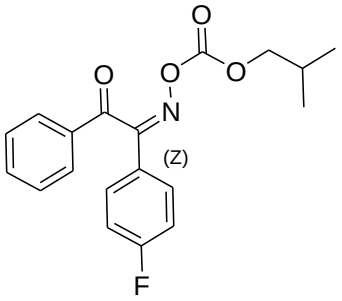

The reaction was carried out according to general procedure B using 2-(4-fluorophenyl)-2-(hydroximino)-1-phenylethanone (0.1g, 0.41 mmol, 1 eq) and isobutylchloroformate (0.06 mL, 0.45 mmol, 1.1 eq). The crude product was chromatographed (SiO_2, dichloromethane, 100%) then recrystallised from ethanol to afford compound **38** (0.05 g, 35.4 %) as colorless needles. MR. 80-82 ^oC. ^1H NMR (400 MHz, $CDCl_3$): δ 77.93-7.09 (m,9H,Ar-**H**), 3.83 (d, *J* = 6.5 Hz, 2H, O- C**H**$_2$ -CH-$(CH_3)_2$), 1.60 (m, 1H, O- CH_2 -C**H**-$(CH_3)_2$), 0.89 (d, *J* = 7.1 Hz, 6H, O- CH_2 -CH-(C**H$_3$)**$_2$). ^{13}C NMR (400 MHz, $CDCl_3$): δ 190.0 (1C, CO-Ar), 165.1 (1C, Ar), 164.5 (1C, N= C), 154.5 (1C, O-CO-O), 135.9 (1C, Ar), 134.1 (1C, Ar), 130.6 (2C, Ar), 129.5 (2C, Ar), 129.0(2C, Ar), 128.1 (1C, Ar), 115.1 (2C, Ar), 76.6 (1C, O-**C**H_2 -CH-$(CH_3)_2$), 27.8 (1C, O- CH_2 -**C**H-$(CH_3)_2$), 18.9 (2C, O- CH_2 -CH-(**C**$H_3)_2$). IR: νmax (KBr disc, cm^{-1}): 2968 (C-H), 1777 (C=O), 1685 (C=N), 1233 (O-C), 1180 (C-F) and 965 (N-O). HRMS (ESI+, 70 eV) calculated for $C_{19}H_{22}FN_2O_4$ ($M+NH_4+$): 361.1556, Found: 361.1557. Found C, 66.19; H, 5.20; N, 4.02 (Required for $C_{19}H_{18}FO_4N$: C, 66.46; H, 5.28; N, 4.08).

(2Z)-2-(3-Fluorophenyl)-2-{[(methoxycarbonyl)oxy]imino}-1-phenylethanone (41)

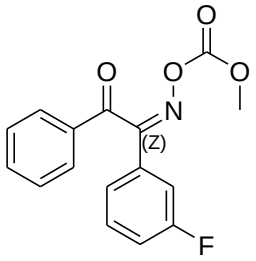

The reaction was carried out according to general procedure B using 2-(3-fluorophenyl)-2-(hydroximino)-1-phenylethanone (0.1g, 0.41 mmol, 1 eq) and methylchloroformate (0.04 mL, 0.45 mmol, 1.1 eq). The crude product was chromatographed (SiO_2, dichloromethane, 100%) then recrystallised from ethanol to afford compound **41** (0.10 g, 80.8 %) as white crystals. MR. 148-150 ^{o}C. ^{1}H NMR (400 MHz, $CDCl_3$): δ 7.93-7.35 (m, 9H, Ar-**H**), 1.26 (s 3H, O-C**H**$_3$). ^{13}C NMR (400 MHz, $CDCl_3$): δ 190.3 (1C, CO-Ar), 164. 4 (1C, C=N), 163.2 (1C, Ar), 157.2 (1C, O-CO-O), 137.1 (1C, Ar), 134.8 (1C, Ar), 134.4 (1C, Ar), 130.5 (1C, Ar), 129.8 (2C, Ar), 129.1 (2C, Ar), 124.1 (1C, Ar), 117.8 (1C, Ar), 114.5 (1C, Ar), 55.2 (1C, O-**C**H_3). IR: νmax (KBr disc, cm^{-1}): 2956 (C-H), 1787 (C=O), 1682 (C=N), 1236 (O-C) and 940 (N-O). HRMS (ESI+, 70eV) calculated for $C_{16}H_{12}FNO_4$ 324.0641, Found: 324.0641. Found C, 62.93; H, 3.91; N, 4.19 (Required for $C_{16}H_{12}FN\ O_4$: C, 63.79; H, 4.01; N, 4.65).

***(*2Z)-2-{[(Ethoxycarbonyl)oxy]imino}-2-(3-fluorophenyl)-1-phenylethanone (42)**

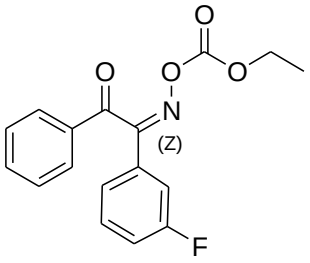

The reaction was carried out according to general procedure B using 2-(3-fluorophenyl)-2-(hydroximino)-1-phenylethanone (0.1g, 0.41 mmol, 1 eq) and ethylchloroformate (0.04 mL, 0.45 mmol, 1.1 eq). The crude product was chromatographed (SiO_2, dichloromethane, 100%) then recrystallised from ethanol to afford compound **42** (0. 07 g, 52%) as colorless crystals. MR.126-128 ^{o}C. ^{1}H NMR (400 MHz, $CDCl_3$): δ7.93-7.35 (m, 9H, Ar-**H**), 4.23 (q, *J* = 7.1 Hz, 2 H, -O-C**H**$_2$-CH_3), 1.25 (t, *J* = 7.1 Hz, 3H, O-CH_2-C**H**$_3$). ^{13}C NMR (400 MHz, $CDCl_3$): δ 190.2 (1C, CO-Ar), 164.5(1C, C=N), 163.1 (1C, Ar), 158.1 (1C, O-CO-O), 135.2 (1C, Ar), 133.8 (1C, Ar), 130.8 (1C, Ar), 130.7 (1C, Ar), 129.5 (2C, Ar), 129.4 (2C, Ar), 123.1 (1C, Ar), 119.1 (1C, Ar), 114.3 (1C, Ar), 65.3 (1C, O-**C**H_2-CH_3),14.8 (1C, -O-CH_2-**C**H_3). IR: νmax (KBr disc, cm^{-1}): 2995 (C-H), 1782 (C=O), 1682 (C=N), 1233 (O-C), 1189 (C-F) and 940 (N-O). HRMS: (ESI+, 70 eV) calculated for $C_{17}H_{14}FNO_4Na$ (M+Na+): 338.0797, Found: 338.0799. Found C, 64.60; H, 4.41; N, 4.12 (Required for $C_{17}H_{14}FNO_4$: C, 64.76; H, 4.48; N, 4.40).

(2Z)-2-(3-Fluorophenyl)-1-phenyl-2-{[(propoxycarbonyl)oxy]imino}ethanone (43)

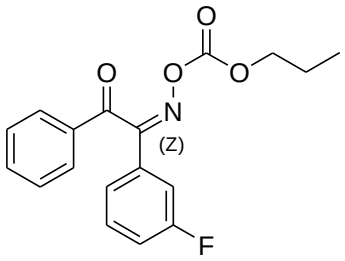

The reaction was carried out according to general procedure B using 2-(3-fluorophenyl)-2-(hydroximino)-1-phenylethanone (0.1g, 0.41 mmol, 1 eq) and propoylchloroformate (0.05 mL, 0.45 mmol, 1.1 eq). The crude product was chromatographed (SiO_2, dichloromethane, 100%) then recrystallised from ethanol to afford compound **43** (0.067 g, 52 %) as colorless crystals. MR. 116-118 ^{o}C. ^{1}H NMR (400 MHz, $CDCl_3$): δ 7.93-7.37 (m, 9H, Ar-**H**), 3.66 (t, 2H, *J* = 7.1 Hz, O -C**H**$_2$-CH_2-CH_3), 1.19 (m, 2H, O-CH_2-C**H**$_2$-CH_3), 0.85 (t, *J* = 7.1 Hz, 3H, O-CH_2-CH_2-C**H**$_3$). ^{13}C NMR (400 MHz, $CDCl_3$): δ 191.3 (1C, CO-Ar), 164.6 (1C, C=N), 163.3 (1C, Ar), 157.3 (1C, O-CO-O), 135.6 (1C, Ar), 134.8 (1C, Ar), 133.1(1C, Ar), 130.8 (1C, Ar), 129.6 (2C, Ar), 129.5 (2C, Ar), 124.1 (1C, Ar), 119.2 (1C, Ar), 115.3 (1C, Ar), 31.7 (1C, O -**C**H_2-CH_2-CH_3), 25.5 (1C, O -CH_2-**C**H_2-CH_3), 11.5 (1C, O -CH_2-CH_2-**C**H_3). IR: νmax (KBr disc, cm^{-1}): 2976 (C-H), 1775 (C=O), 1687 (C=N), 1238 (O-C), 1186, (C-F) and 940 (N-O). HRMS (ESI+, 70 eV) calculated for $C_{18}H_{16}FNO_4Na$ (M+Na+): 352.0955, Found: 352.0955. Found C, 65.46; H, 4.46; N, 3.45 (Required for $C_{18}H_{16}FNO_4$: C, 65.65; H, 4.90; N, 3.55).

(2Z)-2-(3-Fluorophenyl)-1-phenyl-2-({[(propan-2-yloxy)carbonyl]oxy}imino)ethanone (44)

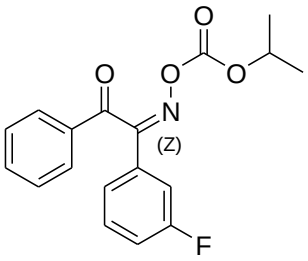

The reaction was carried out according to general procedure B using 2-(3-fluorophenyl)-2-(hydroximino)-1-phenylethanone (0.1g, 0.41 mmol, 1 eq) and isopropoylchloroformate (0.05 mL, 0.45 mmol, 1.1 eq). The crude product was chromatographed (SiO_2, dichloromethane, 100 %) then recrystallised from ethanol to afford compound **44** (0.067 g, 52%) as colorless crystals. MR. 134-136 ^{o}C. ^{1}H NMR (400 MHz, $CDCl_3$): δ 7.93-7.09 (m, 9H, Ar-**H**), 4.92 (m, 1H, -O-C**H**-CH_3), 1.24 (d, *J* = 7.1 Hz, 6 H, O-CH-(C**H**$_3$)$_2$). ^{13}C NMR (400 MHz, $CDCl_3$): δ 192.2 (1C, CO-Ar), 165. 4 (1C, C=N), 164.3 (1C, Ar), 156.9 (1C, O-CO-O), 136.6 (1C, Ar), 134.8 (1C, Ar), 134.7(1C, Ar), 130.2 (1C, Ar), 129.9 (2C, Ar), 129.4 (2C, Ar), 125.1 (1C, Ar), 119.2 (1C, Ar), 116.3 (1C, Ar), 69.3 (1C, -O-**C**H-CH_3), 19.5 (2C, O-CH-(**C**H_3)$_2$). IR: νmax (KBr disc, cm^{-1}): 2976 (C-H), 1777 (C=O), 1684 (C=N), 1239 (O-C), 1186 (C-F) and 944 (N-O). HRMS (ESI+, 70 eV) calculated for $C_{18}H_{16}FNO_4Na$ (M+Na+): 352.0955, Found: 352.0954. Found C, 66.54; H, 4.56; N, 3.50 (Required for $C_{18}H_{16}FNO_4$: C, 65.65; H, 4.90; N, 4.25).

(2Z)-2-{[(Butoxycarbonyl)oxy]imino}-2-(3-fluorophenyl)-1-phenylethanone (45)

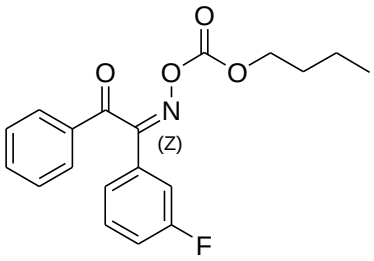

The reaction was carried out according to general procedure B using 2-(3-fluorophenyl)-2-(hydroximino)-1-phenylethanone (0.1g, 0.41 mmol, 1 eq) and butylchloroformate (0.06 mL, 0.45 mmol, 1.1 eq). The crude product was chromatographed (SiO_2, dichloromethane, 100 %) then recrystallised from ethanol to afford compound **45** (0.07 g, 49.6 %) as a white solid. MR. 82-84 ^{o}C. ^{1}H NMR (400 MHz, $CDCl_3$): δ 7.93 -7.41(m, 9H, Ar-**H**), 4.16 (t, *J* = 6.5 Hz, 2H, O-C**H**$_2$-CH_2-CH_2-CH_3), 1.54 (m, 2H, O-CH_2-C**H**$_2$-CH_2-CH_3), 1.29 (m, 2H, O-CH_2-CH_2-C**H**$_2$-CH_3), 0.85 (t, *J* = 7.1 Hz, 3H, CH_2-CH_2-CH_2-C**H**$_3$). ^{13}C NMR (400 MHz, $CDCl_3$): δ 189.2 (1C, CO-Ar), 163. 4(1C, C=N), 162.3 (1C, Ar), 156.1(1C, O-CO-O), 135.6 (1C, Ar),133.8 (1C, Ar), 130.7(1C, Ar), 130.8 (1C, Ar), 129.5 (2C, Ar), 129.4 (2C, Ar), 123.6 (1C, Ar), 118.2 (1C, Ar), 114.4 (1C, Ar), 34.1 (1C, O -**C**H_2-CH_2- CH_2CH_3), 28.6 (1C, O -CH_2-**C**H_2 CH_2-CH_3), 24.1 (1C, O -CH_2-CH_2 **C**H_2-CH_3), 15.1 (1C, O -CH_2-CH_2 CH_2-**C**H_3). IR: νmax (KBr disc, cm^{-1}): 2976 (C-H), 1775 (C=O), 1687(C=N), 1238 (O-C), 1187 (C-F) and 940 (N-O). HRMS (ESI+, 70 eV) calculated for $C_{19}H_{22}FN_2O_4$ (M+NH_4+): 361.1556, Found: 361.1561. Found C, 66.22; H, 5.25; N, 3.64 (Required for $C_{19}H_{18}FNO_4$: C, 66.46; H, 5.28; N, 4.08).

(2Z)-2-(3-Fluorophenyl)-2-({[(2-methylpropoxy)carbonyl]oxy}imino)-1-phenylethanone (46)

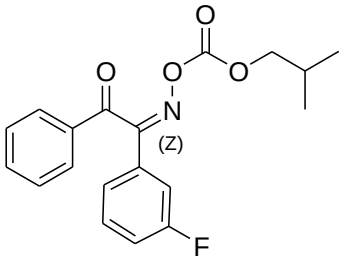

The reaction was carried out according to general procedure B using 2-(3-fluorophenyl)-2-(hydroximino)-1-phenylethanone (0.1g, 0.41 mmol, 1 eq) and isobutylchloroformate (0.06 mL, 0.45 mmol, 1.1 eq). The crude product was chromatographed (SiO_2, dichloromethane, 100 %) then recrystallised from ethanol to afford compound **46** (0.08 g, 65.9 %) as a white crytals. MR. 80-82 ^{o}C. ^{1}H NMR (400 MHz, $CDCl_3$): δ 77.93-7.37 (m,9H,Ar-**H**), 3.94 (d, *J* = 6.5 Hz, 2H, O- C**H**$_2$ -CH-$(CH_3)_2$), 1.90 (m, 1H, O- CH_2 -C**H**-$(CH_3)_2$), 0.84 (d, *J* = 7.1 Hz, 6H, O- CH_2 -CH-(C**H**$_3)_2$). ^{13}C NMR (400 MHz, $CDCl_3$): δ 190.2 (1C, CO-Ar), 164. 6 (1C, C=N), 163.5 (1C, Ar), 156.8 (1C, O-CO-O), 135.22 (1C, Ar), 134.9 (1C, Ar), 133.8 (1C, Ar), 130.8 (1C, Ar), 129.5 (2C, Ar), 129.4 (2C, Ar), 123.6 (1C, Ar), 119.2 (1C, Ar), 114.5 (1C, Ar),77.0 (1C, O- **C**H_2 -CH-$(CH_3)_2$), 27.8 (1C, O- CH_2 -**C**H-$(CH_3)_2$), 18.9 (2C, O-CH_2 -CH-(**C**$H_3)_2$). IR: νmax (KBr disc, cm^{-1}): 2959 (C-H), 1777 (C=O), 1684 (C=N), 1239 (O-C), 1186 (C-F) and 944 (N-O). HRMS (ESI+, 70 eV) calculated for $C_{19}H_{18}FNO_4Na$ (M+Na+): 366.1118, Found: 366.1112. Found C, 66.08; H, 5.23; N, 3.02 (Required for $C_{19}H_{18}FNO_4$: C, 66.46; H, 5.28; N, 4.08).

(2Z)-2-(3-Fluorophenyl)-1-phenyl-2-({[(prop-2-en-1-yloxy)carbonyl]oxy}imino)ethanone (47)

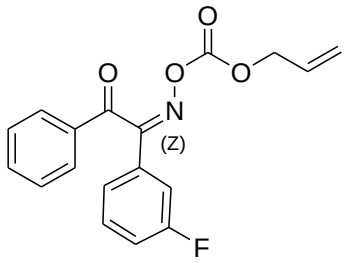

The reaction was carried out according to general procedure B using 2-(3-fluorophenyl)-2-(hydroximino)-1-phenylethanone (0.1g, 0.41 mmol, 1 eq) and allylchloroformate (0.05mL, 0.45 mmol, 1.1 eq). The crude product was chromatographed (SiO_2, dichloromethane, 100 %) then recrystallised from ethanol to afford compound **47** (0.08 g, 59.4 %) as white crytals. MR. 101-103 ^{o}C. ^{1}H NMR (400 MHz, $CDCl_3$): δ 7.91 -7.40 (m, 9H, Ar-**H**), 5.88 (ddt, *J* = 17.3, 10.6 9.6 Hz, 1H, O-CH_2-C**H** -CH_2), 5.28 (dd, *J* = 10.6 , 1.2 Hz, 1H, O-CH_2-CH -C$\mathbf{H}_2$), 5.24 (dd, *J*= 17.3 , 1.2 Hz, 1H, O-CH_2-CH -C$\mathbf{H}_2$), 4.66 (d, *J*= 9.6 Hz, 2 H, O-C$\mathbf{H}_2$-CH -CH_2). ^{13}C NMR (400 MHz, $CDCl_3$): δ 190.0 (1C, CO-Ar), 164.1(1C, C=N), 163.3 (1C, Ar), 155.5 (1C, O-CO-O), 135.1 (1C, Ar), 134.4(1C, Ar), 133.5 (1C, Ar), 130.4(1C, Ar), 131.1(1C, O-CH_2-**C**H═CH_2), 129.5 (2C, Ar), 129.2 (2C, Ar), 123.3 (1C, Ar), 119.9 (1C, O-CH_2-CH ═**C**H_2), 117.2 (1C, Ar), 114.0 (1C, Ar), 68.1 (1C, O-**C**H_2-CH =CH_2). IR: νmax (KBr disc, cm^{-1}): 3061 (=CH), 2995 (C-H), 1685 (C=O), 1679 (C=N), 1382(C-F), 1239 (O-C) and 944 (N-O). HRMS (ESI+, 70 eV) calculated for $C_{18}H_{14}FNO_4Na$ (M+Na+): 350.0798, Found: 350.0799. Found C, 66.25; H, 4.13; N, 3.69 (Required for $C_{18}H_{14}FNO_4$: C, 66.05; H, 4.31; N, 4.28).

(2*Z*)-2-({[(Chloromethoxy)carbonyl]oxy}imino)-2-(3-fluorophenyl)-1-phenylethanone (48)

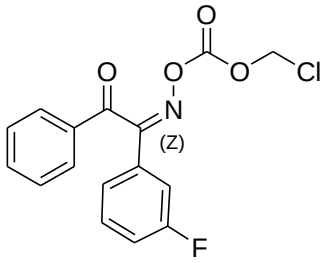

The reaction was carried out according to general procedure B using 2-(3-Fluorophenyl)-2-(hydroximino)-1-phenylethanone (0.1g, 0.41 mmol, 1 eq) and chloromethylchloroformate (0.04 mL, 0.45mmol, 1.1 eq). The crude product was chromatographed (SiO_2, dichloromethane, 100 %) then recrystallised from ethanol to afford compound **48** (0.07 g, 50.7 %) as a white crytals. MR. 118-120 ^{o}C. ^{1}H NMR (400 MHz, $CDCl_3$): δ 7.92-7.42 (m, 9H, Ar-**H**), 5.71 (s, 2 H, O-C**H**$_2$-Cl). ^{13}C NMR (400 MHz, $CDCl_3$): δ 191.0 (1C, CO-Ar), 165. 1(1C, C=N), 164.3 (1C, Ar),158.0 (1C, O-CO-O), 135.3 (1C, Ar), 134.8 (1C, Ar), 133.6 (1C, Ar), 130.5(1C, Ar), 129.6 (2C, Ar), 129.4 (2C, Ar), 123.3 (1C, Ar), 115.9 (1C, Ar), 114.5 (1C, Ar), 72.4 (1C,O-**C**H_2-Cl). IR: νmax (KBr disc, cm^{-1}): 2985 (C-H), 1777 (C=O), 1679 (C=N), 1221 (O-C), 1181 (C-F), 932 (N-O) and 702 (C-Cl). HRMS (ESI+, 70 eV) calculated for C_{16} $H_{11}FClNO_4$ 335.0411, Found: 335.0412.

(2*Z*)-2-({[(2-Bromoethoxy)carbonyl]oxy}imino)-2-(3-fluorophenyl)-1-phenylethanone (49)

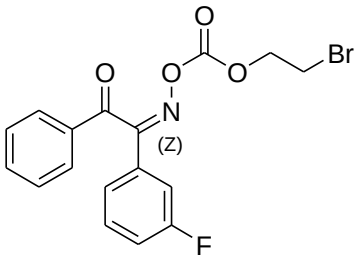

The reaction was carried out according to general procedure B using 2-(3-fluorophenyl)-2-(hydroximino)-1-phenylethanone (0.1g, 0.41 mmol, 1 eq) and 2-bromoethylchloroformate (0.05 mL, 0.45 mmol, 1.1 eq). The crude product was chromatographed (SiO_2, dichloromethane, 100 %) then recrystallised from ethanol to afford compound **49** (0.08 g, 49.4 %) as a white crytals. MR. 98-100 ^{o}C. ^{1}H NMR (400 MHz, $CDCl_3$): δ 7.91-7.37 (m, 9H, Ar-**H**), 4.44 (t, *J* = 6.2 Hz, 2 H, O-C**H**$_2$-CH_2 -Br), 3.45 (t, *J* = 6.2 Hz, 2 H, O-CH_2-C**H**$_2$ –Br). ^{13}C NMR (400 MHz, $CDCl_3$): δ191.1(1C, CO-Ar), 162.1(1C, C=N), 160.3(1C, Ar),152.0 (1C,O-CO-O), 135.1(1C, Ar), 134.3(1C, Ar), 131.2(1 C, Ar), 130.5 (1C, Ar), 129.8 (2 C,Ar), 128.7 (2 C, Ar), 127.8 (2C, Ar), 117.6 (1C, Ar), 68.9 (1C, O-**C**H_2-CH_2 -Br), 27.9 (1C, O-CH_2- **C**H_2 -Br). IR: νmax (KBr disc, cm^{-1}): 2985 (C-H), 1776 (C=O), 1685 (C=N), 1381 (C-F), 1227 (O-C) , 950 (N-O) and 641 (C-Br). HRMS: (ESI+, 70 eV) calculated for $C_{17}H_{13}BrFNO_4Na$ (M+Na+): 415.9902, Found: 415.9904.

2-(4-Bromophenyl)-2-{[(methoxycarbonyl)oxy]imino}-1-phenylethanone (52)

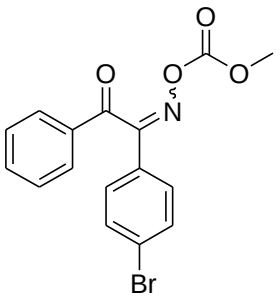

The reaction was carried out according to general procedure B using 2-(4-Bromophenyl)-2-(hydroximino)-1-phenylethanone (0.1 g, 0.33 mmol, 1 eq) and methylchloroformate (0.04 mL, 0.45 mmol, 1.1 eq). The crude product was purified by colum chromatography (SiO_2, 1:5, dichloromethane in *n*-hexane) to give compound **52** as an off white solid (0.06 g, 48 %) as a racemic mixture of *E/Z* isomers (1:3). *Z*-monoxime, ^{1}H NMR (400 MHz, $CDCl_3$): δ 7.93-7.49 (m, 9H, Ar-**H**), 3.80 (s, 3H, O-C**H**$_3$). ^{13}C NMR (400 MHz, $CDCl_3$): δ 189.1 (1C, CO-Ar), 163.9 (1C, C=N), 156.9 (1C, O-CO-O), 135.6 (1C, Ar), 134.5 (1C, Ar), 132.4 (1C, Ar), 131.8 (2C, Ar), 131.6 (2C, Ar), 129.7 (2C, Ar), 129.3 (2C, Ar), 124.5 (1C, Ar), 20.2 (1C, O-**C**H$_3$). *E*-monoxime, ^{1}H NMR (400 MHz, $CDCl_3$): δ 8.01-7.49 (m, 9H, Ar-**H**), 3.81 (s, 3H, O-C**H**$_3$). ^{13}C NMR (400 MHz, $CDCl_3$): δ 189.2 (1C, CO-Ar), 163.0 (1C, C=N), 157.0 (1 C, O-CO-O), 135.7 (1C, Ar), 134.6 (1C, Ar), 132.5 (1C, Ar), 131.9 (2C, Ar), 131.7 (2C, Ar), 129.8 (2C, Ar), 129.4 (2C, Ar), 124.6 (1C, Ar), 20.3 (1C, O-**C**H$_3$). IR: νmax (KBr disc, cm^{-1}): 2956, (C-H), 1787 (C=O), 1682, (C=N), 1236 (O-C) and 940 (N-O). HRMS (ESI+, 70 eV) calculated for $C_{16}H_{12}BrNO_4Na$ (M+Na+): 383.9840, Found: 383.9842.

2-(4-Bromophenyl)-1-phenyl-2-{[(propoxycarbonyl)oxy]imino}ethanone (53)

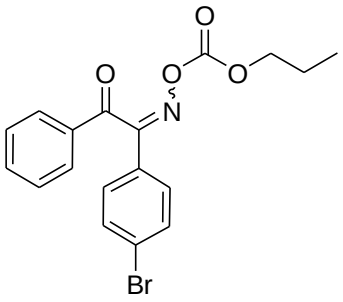

The reaction was carried out according to general procedure B using 2-(4-bromophenyl)-2-(hydroximino)-1-phenylethanone (0.1 g, 0.32 mmol, 1 eq) propylchloroformate (0.04 mL, 0.36 mmol, 1.1 eq). The crude product was purified by colum chromatography (SiO_2, 1:5, dichloromethane in *n*-hexane) to give compound **53** a white solid (0.06 g, 46 %) as a racemic mixture of *E/Z* isomers (1:3). *Z*-monoxime,^{1}H NMR (400 MHz, $CDCl_3$): δ 7.93-7.49 (m, 9H, Ar-**H**), 4.31 (t, 2H, *J* = 7.11 Hz, O -C**H**$_2$-CH_2-CH_3), 1.74 (m, 2H, O-CH_2-C**H**$_2$-CH_3), 0.97 (t, *J* = 7.10 Hz, 3H, O-CH_2-CH_2-C**H**$_3$). ^{13}C NMR (400 MHz, $CDCl_3$): δ 191.2 (1C, CO-Ar), 164.0 (1C, C=N), 158.5 (1C, O-CO-O), 136.0 (1C, Ar), 134.9 (1C, Ar), 132.6 (1C, Ar), 132.0 (2C, Ar), 131.8 (2C, Ar), 129.8 (2C, Ar), 129.5 (2C, Ar), 125.6 (1C, Ar), 30.6 (1C, O -**C**H_2-CH_2-CH_3), 26.0 (1C, O -CH_2-**C**H_2-CH_3), 11.9 (1C, O -CH_2-CH_2-**C**H_3). *E*-monoxime,^{1}H NMR (400 MHz, $CDCl_3$): δ 8.02-7.49 (m, 9H, Ar-**H**), 4.32 (t, 2H, *J* = 7.1Hz, O -C**H**$_2$-CH_2-CH_3), 1.76 (m, 2H, O-CH_2-C**H**$_2$-CH_3), 0.99 (t, *J* = 7.1 Hz, 3H, O-CH_2-CH_2-C**H**$_3$). ^{13}C NMR (400 MHz, $CDCl_3$): δ 191.3 (1C, CO-Ar), 164.1 (1C, C=N), 158.6 (1C, O-CO-O), 136.1 (1C, Ar), 135.0 (1C, Ar), 132.7 (1C, Ar), 132.1 (2C, Ar), 131.9 (2C, Ar), 129.9 (2C, Ar), 129.6 (2C, Ar), 125.7 (1C, Ar), 30.7 (1C, O -**C**H_2-CH_2-CH_3), 26.11 (1C, O -CH_2-**C**H_2-CH_3), 12.2 (1C, O -CH_2-CH_2-**C**H_3). IR: νmax (KBr disc, cm^{-1}): 2976 (C-H), 1782 (C=O), 1681 (C=N), 1229 (O-C), 917 (N-O) and 654 (C-Br). HRMS (ESI+, 70 eV) calculated for $C_{18}H_{16}BrNO_4Na$ (M+Na+): 412.0155, Found: 412.0156.

2-(4-Bromophenyl)-1-phenyl-2-({[(propan-2-yloxy)carbonyl]oxy}imino)ethanone (54)

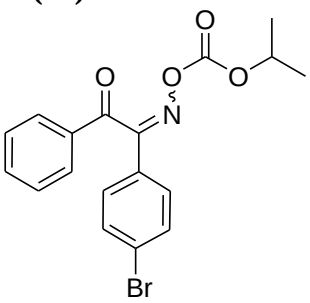

The reaction was carried out according to general procedure B using 2-(4-bromophenyl)-2-(hydroximino)-1-phenylethanone (0.1 g, 0.33 mmol, 1 eq) isopropyl chloroformate (0.36 mL, 0.36 mmol, 1.1 eq). The crude product was purified by colum chromatography (SiO_2, 1:5, dichloromethane in *n*-hexane) to give compound **54** (0.04 g, 40 %) as a white solid as a racemic mixture of *E/Z* isomers (1:3). *Z*-monoxime, ^{1}H NMR (400 MHz, $CDCl_3$): δ 7.92-7.49 (m, 9H, Ar-**H**), 4.91 (m, 1H, -O-C**H**-CH_3), 1.23(d, *J* = 7.1 Hz, 6H, O- CH-(C**H**$_3$)$_2$). ^{13}C NMR (400 MHz, $CDCl_3$): δ 190.2 (1C, CO-Ar), 164.1 (1C, C=N), 154.5 (1C, O-CO-O), 135.5 (1C, Ar), 134.3 (1C, Ar), 132.3 (1C, Ar), 131.6 (2C, Ar), 131.3 (2C, Ar), 129.5 (2C, Ar), 129.1 (2C, Ar), 124.1 (1C, Ar),70.3 (1C, -O-**C**H-CH_3), 20.1 (2C, O-CH–(**C**H_3)$_2$). *E*-monoxime, ^{1}H NMR (400 MHz, $CDCl_3$): δ 7.93-7.09 (m, 9H, Ar-**H**), 4.92(m, 1H, -O-C**H**-CH_3), 1.25 (d, 6 H, *J* = 7.1 Hz, O- CH-(C**H**$_3$)$_2$). ^{13}C NMR (400 MHz, $CDCl_3$): δ 190.3 (1C, CO-Ar), 164.2 (1C, C=N), 154.6 (1C, O-CO-O), 135.6 (1C, Ar), 134.4 (1C, Ar), 132.4 (1C, Ar), 131.7 (2C, Ar), 131.4 (2C, Ar), 129.6 (2C, Ar), 129.2 (2C, Ar), 124.2 (1C, Ar), 70.4 (1C, -O-**C**H-CH_3), 20.2 (2C, O-CH –(**C**H_3)$_2$). IR: νmax (KBr disc, cm^{-1}): 2975 (C-H), 1786 (C=O), 1679 (C=N), 1223 (O-C), 941 (N-O) and 652 (C-Br). HRMS (ESI+, 70 eV) calculated for $C_{18}H_{16}BrNO_4Na$ (M+Na+): 412.0155, Found: 412.0155.

2-(4-Bromophenyl)-2-{[(butoxycarbonyl)oxy]imino}-1-phenylethanone(55)

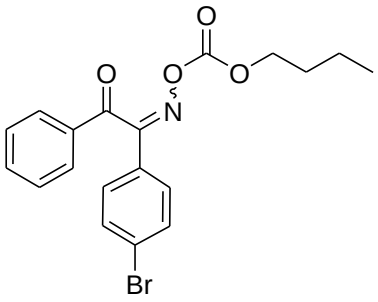

The reaction was carried out according to general procedure B using 2-(4-bromophenyl)-2-(hydroximino)-1-phenylethanone (0.1 g, 0.33 mmol, 1 eq) butylchloroformate (0.05 mL, 0.36 mmol, 1.1 eq). The crude product was purified by column chromatography (SiO_2, dichloromethane,100 %) to give compound **55** as a white solid (0.08 g, 60 %) as a racemic mixture of *E/Z* isomers (1:3). *Z*-monoxime, ^{1}H NMR (400 MHz, $CDCl_3$): δ 7.93 -7.41(m, 9H, Ar-**H**), 4.27 (t, *J* = 6.5 Hz, 2H, O-C**H**$_2$-CH_2-CH_2-CH_3), 1.58 (m, 2H, O-CH_2-C**H**$_2$-CH_2-CH_3), 1.41 (m, 2H, O-CH_2-CH_2-C**H**$_2$-CH_3), 0.93 (t, *J* = 7.1 Hz, 3H, CH_2-CH_2-CH_2-C**H**$_3$). ^{13}C NMR (400 MHz, $CDCl_3$): δ 188.5 (1C, CO-Ar), 159.1 (1C, C=N), 152.5 (1C, O-CO-O), 135.5 (1C, Ar), 134.3 (1C, Ar), 132.3 (1C, Ar), 131.6 (2C, Ar), 131.3 (2C, Ar), 129.5 (2C, Ar), 129.1 (2C, Ar), 124.1 (1C, Ar), 40.1 (1C, O -**C**H_2-CH_2- CH_2CH_3), 30.6 (1C, O -CH_2-**C**H_2 CH_2-CH_3), 20.1 (1C, O -CH_2-CH_2 **C**H_2-CH_3), 16.1 (1C, O -CH_2-CH_2 CH_2-**C**H_3). *E*-monoxime, ^{1}H NMR (400 MHz, $CDCl_3$): δ 7.93 -7.41(m, 9H, Ar-**H**), 4.29 (t, *J* = 6.5 Hz, 2H, O-C**H**$_2$-CH_2-CH_2-CH_3), 1.69 (m, 2H, O-CH_2-C**H**$_2$-CH_2-CH_3), 1.44 (m, 2H, O-CH_2-CH_2-C**H**$_2$-CH_3), 0 .96 (t, *J* = 7.1 Hz, 3H, CH_2-CH_2-CH_2-C**H**$_3$). ^{13}C NMR (400 MHz, $CDCl_3$): δ 188.6 (1C, CO-Ar), 159.2 (1C, C=N), 152.6 (1C, O-CO-O), 135.6 (1C, Ar), 134.4 (1C, Ar), 132.4 (1C, Ar), 131.7 (2C, Ar), 131.4 (2C, Ar), 129.6 (2C, Ar), 129.2 (2C, Ar), 124.2 (1C, Ar), 40.2 (1C, O -**C**H_2-CH_2- CH_2CH_3), 30.7 (1C, O -CH_2-**C**H_2 CH_2-CH_3), 20.2 (1C, O -CH_2-CH_2 **C**H_2-CH_3), 16.2 (1C, O -CH_2-CH_2 CH_2-**C**H_3). IR: νmax (KBr disc, cm^{-1}): 2980 (C-H), 1781 (C=O), 1678, (C=N), 1235 (O-C), 954 (N-O) and 642 (C-Br). HRMS (ESI+, 70 eV) calculated for $C_{19}H_{18}BrO_4NNa$ (M+Na+): 426.0308, Found: 426.0311.

2-(4-Bromophenyl)-2-({[(2-methylpropoxy)carbonyl]oxy}imino)-1-phenylethanone(56)

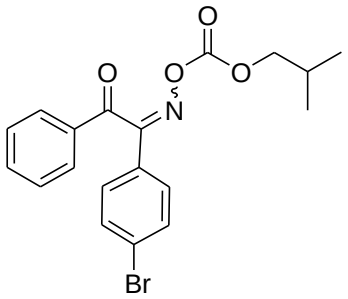

The reaction was carried out according to general procedure B using 2-(4-bromophenyl)-2-(hydroximino)-1-phenylethanone (0.1 g, 0.32 mmol, 1 eq) isobutylchloroformate (0.05 mL, 0.36 mmol, 1.1 eq). The crude product was purified by colum chromatography (SiO_2, dichloromethane, 100 %) to give compound **56** as a white solid (0.05 g, 37 %) a racemic mixture of *E/Z* isomers (1:3). *Z*-monoxime, ^{1}H NMR (400 MHz, $CDCl_3$): δ 7.92-7.42 (m,9H,Ar-**H**), 4.05 (d, *J* = 6.5 Hz, 2H, O- C**H**$_2$ -CH-(CH_3)$_2$), 1.99 (m, 1H, O- CH_2 -C**H**-(CH_3)$_2$), 0.94 (d, *J* = 7.1 Hz, 6H, O- CH_2 -CH-(C**H**$_3$)$_2$). ^{13}C NMR (400 MHz, $CDCl_3$): δ 189.6 (1C, CO-Ar), 160.0 (1C, C=N), 154.6 (1 C, O-CO-O), 135.9 (1C, Ar), 134.5 (1C, Ar), 132.6 (1C, Ar), 131.9 (2C, Ar), 131.8 (2C, Ar), 129.9 (2C, Ar), 129.5 (2C, Ar), 125.2 (1C, Ar), 76.0(1C, O- **C**H_2 -CH-(CH_3)$_2$), 28.8 (1C, O- CH_2 -**C**H-(CH_3)$_2$), 19.9 (2C, O- CH_2 -CH-(**C**H_3)$_2$). *E*-monoxime, ^{1}H NMR (400 MHz, $CDCl_3$): δ 7.93-7.42 (m, 9H, Ar-**H**), 4.06 (t, *J* = 6.5 Hz, 2H, O- C**H**$_2$ -CH-(CH_3)$_2$), 2.00 (m, 1H, O- CH_2 -C**H**-(CH_3)$_2$), 0.96 (d, *J* = 7.1 Hz, 6H, O- CH_2 -CH-(C**H**$_3$)$_2$). ^{13}C NMR (400 MHz, $CDCl_3$): δ 189.7 (1C, CO-Ar), 160.1 (1C, C=N), 154.7 (1C, O-CO-O), 136.0 (1C, Ar), 134.6 (1C, Ar), 132.7 (1C, Ar), 132.0 (2C, Ar), 131.9 (2C, Ar), 130.0 (2C, Ar), 129.6 (2C, Ar), 125.3 (1C, Ar), 76.1 (1C, O- **C**H_2 -CH-(CH_3)$_2$), 28.9 (1C, O- CH_2 -**C**H-(CH_3)$_2$), 20.0 (2C, O- CH_2 -CH-(**C**H_3)$_2$). IR: νmax (KBr disc, cm^{-1}): 2962 (C-H), 1782 (C=O), 1676 (C=N), 1218 (O-C), 928 (N-O) and 684 (C-Br). HRMS (ESI+, 70 eV) calculated for C_{19} $H_{18}BrNO_4Na$ (M+Na+): 426.0312, Found: 426.0311.

2-(4-Bromophenyl)-1-phenyl-2-({[(prop-2-en-1-yloxy)carbonyl]oxy}imino)ethanone (57)

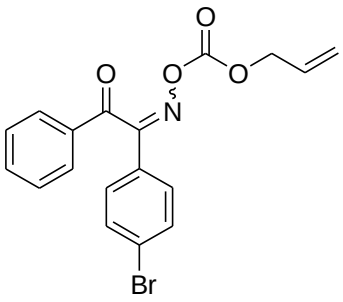

The reaction was carried out according to general procedure B using 2-(4-bromophenyl)-2-(hydroximino)-1-phenylethanone (0.1 g, 0.33 mmol, 1 eq) allylchloroformate (0.04 mL, 0.36 mmol, 1.1 eq). The crude product was purified by colum chromatography (SiO_2, dichloromethane, 100 %) to give compound **57** as a white solid (0.05 g, 39 %) as a racemic mixture of *E/Z* isomers (1:3). *Z*-monoxime, ^{1}H NMR (400 MHz, $CDCl_3$): δ 7.92 -7.46 (m, 9H, Ar-**H**), 6.00 (ddt, *J* = 15.9, 9.9, 9.3 Hz, 1H, O-CH_2-C**H** -CH_2), 5.38 (dd, *J* = 9.9 , 1.0 Hz, 1H, O-CH_2-CH -C**H**$_2$), 5.23 (dd, *J* = 15.9 , 1.0 Hz, 1H, O-CH_2-CH -C**H**$_2$), 4.79 (d, J = 9.3 Hz, 2 H, O-C**H**$_2$-CH -CH_2). ^{13}C NMR (400 MHz, $CDCl_3$): δ 189.9 (1C, CO-Ar), 160.1 (1C, C=N), 154.7 (C, O-CO-O), 136.0 (1C, Ar), 134.5 (1C, Ar), 132.9 (1C, Ar), 132.0 (2C, Ar), 131.9 (2C, Ar), 130.0 (2C, Ar), 129.6 (2C, Ar), 131.1(1C, O-CH_2-**C**H ═CH_2), 125.3 (1C, Ar), 119.9 (1C, O-CH_2-CH ═**C**H_2), 68.1(1C, O-**C**H_2-CH ═CH_2). *E*-monoxime, ^{1}H NMR (400 MHz, $CDCl_3$): δ 7.00 -7.49 (m, 9H, Ar-**H**), 6.01 (ddt, *J* = 15.9 , 9.9 , 9.3 Hz, 1H, O-CH_2-C**H** -CH_2), 5.39 (dd, *J* = 9.9 , 1.0 Hz, 1H, O-CH_2-CH -C**H**$_2$), 5.24 (dd, *J* = 15.9 ,1.0 Hz, 1H, O-CH_2-CH -C**H**$_2$), 4.80 (d, *J* = 9.3 Hz, 2 H, O-C**H**$_2$-CH -CH_2). ^{13}C NMR (400 MHz, $CDCl_3$): δ 190.0 (1C, CO-Ar), 160.2 (1C, C=N), 154.8 (1 C, O-CO-O), 136.1 (1C, Ar), 134.6 (1C, Ar), 133.0 (1C, Ar), 132.1 (2C, Ar), 132.0 (2C, Ar), 130.1 (2C, Ar), 129.7 (2C, Ar), 131.2 (1C, O-CH_2-**C**H ═CH_2), 125.4 (1C, Ar), 120.0 (1C, O-CH_2-CH ═**C**H_2), 68.2 (1C, O-**C**H_2-CH ═CH_2). IR: νmax (KBr disc, cm^{-1}) : 2951 (C-H), 1783 (C=O), 1676 (C=N), 1213 (O-C), 928 (N-O) and 685 (C-Br). HRMS: (ESI+, 70 eV) calculated for $C_{18}H_{14}BrNO_4Na$ (M+Na+): 409.9997, Found: 409.9998.

2-(4-Bromophenyl)-2-({[(chloromethoxy)carbonyl]oxy}imino)-1-phenylethanone (58)

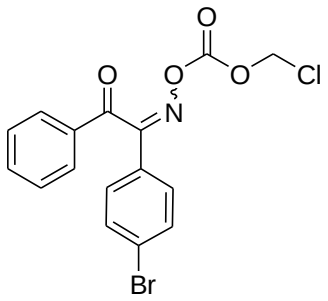

The reaction was carried out according to general procedure B using 2-(4-bromophenyl)-2-(hydroximino)-1-phenylethanone (0.1 g, 0.33 mmol, 1 eq) and choromethylchloroformate (0.03 mL, 0.36 mmol, 1.1 eq). The crude product was purified by column chromatography (SiO_2, dichloromethane, 100 %) to give compound **58** as a white solid (0.06 g, 46 %) as a racemic mixture of *E/Z* isomers (1:3). *Z*-monoxime, ^{1}H NMR (400 MHz, $CDCl_3$): δ 7.86 -7.51 (m, 9H, Ar-**H**), 5.70 (s, 2 H, O-C**H**$_2$-Cl). ^{13}C NMR (400 MHz, $CDCl_3$): δ 190.4 (1C, CO-Ar), 165.2 (1C, C=N), 155.6 (1C, O-CO-O), 136.6 (1C, Ar), 135.4 (1C, Ar), 133.4 (1C, Ar), 132.7 (2C, Ar), 132.4 (2C, Ar), 129.9 (2C, Ar), 129.3 (2C, Ar), 125.2 (1C, Ar), 70.4 (1C, O-**C**H_2-Cl). *E*-monoxime, ^{1}H NMR (400 MHz, $CDCl_3$): δ 8.00-7.51 (m, 9H, Ar-**H**), 5.80 (s, 2 H, O-C**H**$_2$-Cl). ^{13}C NMR (400 MHz, $CDCl_3$): δ 190.5 (1C, CO-Ar), 165.3 (1C, C=N), 155.7 (1 C, O-CO-O), 136.7 (1C, Ar), 135.5 (1C, Ar), 133.5 (1C, Ar), 132.8 (2C, Ar), 132.5 (2C, Ar), 130.0 (2C, Ar), 129.4 (2C, Ar), 125.3 (1C, Ar), 70.5 (1C, O-**C**H_2-Cl). IR: νmax (KBr disc, cm^{-1}): 2953 (C-H), 1796 (C=O), 1676 (C=N), 1230 (O-C), 928 (N-O) and 701 (C-Br). HRMS: (ESI+, 70 eV) calculated for $C_{16}H_{11}BrClNO_4Na$ (M+Na+): 417.9622, Found: 417.9623.

2-({[(2-Bromoethoxy)carbonyl]oxy}imino)-2-(4-bromophenyl)-1-phenylethanone (59)

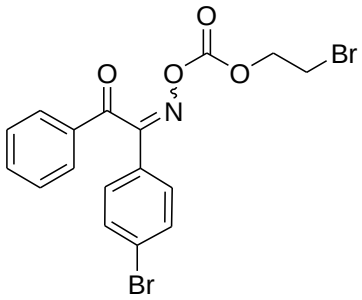

The reaction was carried out according to general procedure B using 2-(4-Bromophenyl)-2-(hydroximino)-1-phenylethanone (0.1 g, 0.33 mmol, 1 eq) and 2-bromoethylchloroformate (0.04 mL, 0.36 mmol, 1.1 eq). The crude product was purified by colum chromatography (SiO_2, dichloromethane, 100 %) to give compound **59** as a white solid (0.07 g, 49 %) as a racemic mixture of *E/Z* isomers (1:3). *Z*-monoxime, ^{1}H NMR (400 MHz, $CDCl_3$): δ 7.85-7.44 (m, 9H, Ar-**H**), 4.40 (t, *J* = 6.2 Hz, 2 H, O-C**H**$_2$- CH_2 -Br), 3.41 (t, *J* = 6.2 Hz, 2 H, O-CH_2-C**H**$_2$ –Br). ^{13}C NMR (400 MHz, $CDCl_3$): δ 191.2 (1C, CO-Ar), 164.0 (1C, C=N), 158.5(1C, O-CO-O), 136.0 (1C, Ar), 134.9 (1C, Ar), 132.6 (1C, Ar), 132.0 (2C, Ar), 131.8 (2C, Ar), 129.8 (2C, Ar), 129.5 (2C, Ar), 125.6 (1C, Ar) 69.9, (1C, O-**C**H_2-CH_2 -Br), 28.9 (1C, O-CH_2- **C**H_2 -Br). *E*-monoxime, ^{1}H NMR (400 MHz, $CDCl_3$): δ 7.00 -7.44 (m, 9H, Ar-**H**), 4.47 (t, *J* = 6.2 Hz, 2 H, O-C**H**$_2$- CH_2 -Br), 3.52 (t, *J* = 6.2 Hz, 2 H, O-CH_2-C**H**$_2$ –Br). ^{13}C NMR (400 MHz, $CDCl_3$): δ 191.3(1C, CO-Ar), 164.1 (1C, C=N), 158.6 (1C, O-CO-O), 136.1 (1C, Ar), 135.0 (1C, Ar), 132.7 (1C, Ar), 132.1 (2C, Ar), 131.9 (2C, Ar), 129.9 (2C, Ar), 129.6 (2C, Ar), 125.7 (1C, Ar), 70.0 (1C, O-**C**H_2-CH_2 -Br), 29.0 (1C, O-CH_2- **C**H_2 -Br). IR: νmax (KBr disc, cm^{-1}): 2960 (C-H), 1784 (C=O), 1682, (C=N), 1225, (O-C), 959 (N-O) and 656 (C-Br). HRMS (ESI+, 70 eV) for calculated $C_{17}H_{14}Br_2NO_4$ (M+H+): 453.9291, Found: 453.9284.

2-(3-Bromophenyl)-1-phenyl-2-({[(propan-2-yloxy)carbonyl]oxy}imino)ethanone (61)

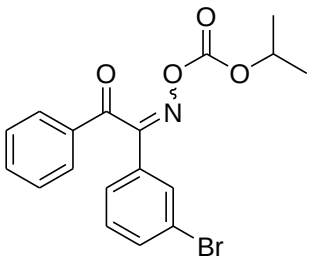

The reaction was carried out according to general procedure B using 2-(3-bromophenyl)-2-(hydroximino)-1-phenylethanone (0.1 g, 0.33 mmol, 1 eq) isopropylchloroformate (0.36 mL, 0.36 mmol, 1.1 eq). The crude product was purified by flash chromatography (Biotage SP4, SiO_2, 1:5, dichloromethane in *n*-hexane) to give compound **61** as a white solid (0.04 g, 40 %) a racemic mixture of *E/Z* isomers (1:2). *Z*-monoxime, ^{1}H NMR (400 MHz, $CDCl_3$): δ 7.93-7.51 (m, 9H, Ar-**H**), 4.93 (m, 1H, -O-C**H**-CH_3), 1.26 (d, *J* = 7.0 Hz, 6 H, O- CH-(C**H**$_3$)$_2$). ^{13}C NMR (400 MHz, $CDCl_3$): δ 190.1 (1C, CO-Ar), 159.9 (1C, C=N), 150.0 (1C,O-CO-O), 138.2 (1C, Ar), 135.6 (1C, Ar), 134.8 (1C, Ar), 134.2 (1C, Ar), 133.0(1C, Ar), 131.4(1C, Ar), 130.0 (2C, Ar), 129.5 (2C, Ar), 128.4 (1C, Ar), 123.6 (1C, Ar), 72.3 (1C, -O-**C**H-CH_3), 20.2 (2C, O-CH –(**C**H_3)$_2$). *E*-monoxime, ^{1}H NMR (400 MHz, $CDCl_3$): δ 8.11-7.51 (m, 9H, Ar-**H**), 5.00 (m, 1H, -O-C**H**-CH_3), 1.34 (d, *J* = 7.0 Hz, 6 H, O- CH-(C**H**$_3$)$_2$). ^{13}C NMR (400 MHz, $CDCl_3$): δ 190.2 (1C, CO-Ar), 160.0 (1C, C=N), 150.1 (1C,O-CO-O), 138.3 (1C, Ar), 135.7 (1C, Ar), 134.9 (1C, Ar), 134.3 (1C, Ar), 133.1(1C, Ar), 131.5 (1C, Ar), 130.1 (2C, Ar), 129.6 (2C, Ar), 128.5 (1C, Ar), 123.7 (1C, Ar), 73.3 (1C, -O-**C**H-CH_3), 21.2 (2C, O-CH –(**C**H_3)$_2$). IR: νmax (KBr disc, cm^{-1}): 2983(C-H), 1779 (C=O), 1687 (C=N), 1222 (O-C), 928 (N-O) and 684 (C-Br). HRMS (ESI+, 70 eV) for $C_{18}H_{16}BrNO_4Na$ (M+Na+): 412.0157, Found: 412.0155.

2-(3-Bromophenyl)-2-{[(butoxycarbonyl)oxy]imino}-1-phenylethanone (62)

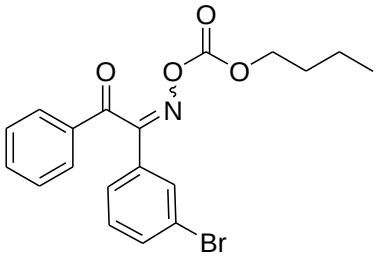

The reaction was carried out according to general procedure B using 2-(3-bromophenyl)-2-(hydroximino)-1-phenylethanone (0.1 g, 0.33 mmol, 1 eq) butylchloroformate (0.02 mL, 0.36 mmol, 1.1 eq). The crude product was purified by flash chromatography (Biotage SP4, SiO_2, 1:5, dichloromethane in *n*-hexane) to give compound **62** as a colorless oil (0.08 g, 60 %) as a racemic mixture of *E/Z* isomers (1:2). *Z*-monoxime, ^{1}H NMR (400 MHz, $CDCl_3$): δ 7.92 -7.33 (m, 9H, Ar-**H**), 4.28 (t, *J* = 6.5 Hz, 2H, O-C**H**$_2$-CH_2-CH_2-CH_3), 1.69 (m, 2H, O-CH_2-C**H**$_2$-CH_2-CH_3), 1.39 (m, 2H, O-CH_2-CH_2-C**H**$_2$-CH_3), 0 .96 (t, *J* = 7.1 Hz, 3H, CH_2-CH_2-CH_2-C**H**$_3$). ^{13}C NMR (400 MHz, $CDCl_3$): δ 190.0 (1C, CO-Ar), 159.8 (1C, C=N), 150.2 (1C,O-CO-O), 137.3 (1C, Ar), 135.2(1C, Ar), 134.5 (1C, Ar), 134.4 (1C, Ar), 133.2 (1C, Ar), 131.6 (1C, Ar), 130.0 (2C, Ar), 129.5 (2C, Ar), 128.0 (1C, Ar), 123.4 (1C, Ar), 40.3 (1C, O -**C**H_2-CH_2- CH_2CH_3), 31.6 (1C, O -CH_2-**C**H_2 CH_2-CH_3), 20.2 (1C, O -CH_2-CH_2 **C**H_2-CH_3), 17.1 (1C, O -CH_2-CH_2 CH_2-**C**H_3). *E*-monoxime, ^{1}H NMR (400 MHz, $CDCl_3$): δ 8.10 -7.33 (m, 9H, Ar-**H**), 4.18 (t, *J* = 6.5 Hz, 2H, O-C**H**$_2$-CH_2-CH_2-CH_3), 1.67 (m, 2H, O-CH_2-C**H**$_2$-CH_2-CH_3), 1.30 (m, 2H, O-CH_2-CH_2-C**H**$_2$-CH_3), 0.87 (t, *J* = 7.1 Hz, 3H, CH_2-CH_2-CH_2-C**H**$_3$). ^{13}C NMR (400 MHz, $CDCl_3$): δ 190.1 (1C, CO-Ar), 159.9 (1C, C=N), 150.3 (1C,O-CO-O), 137.4 (1C, Ar), 135.3 (1C, Ar), 134.6 (1C, Ar), 134.5 (1C, Ar), 133.3 (1C, Ar), 131.7 (1C, Ar), 130.1 (2C, Ar), 129.6 (2C, Ar), 128.1 (1C, Ar), 123.5 (1C, Ar), 41.4 (1C, O -**C**H_2-CH_2- CH_2CH_3), 32.7 (1C, O -CH_2-**C**H_2 CH_2-CH_3), 21.2 (1C, O -CH_2-CH_2 **C**H_2-CH_3), 18.2 (1C, O -CH_2-CH_2 CH_2-**C**H_3). IR: νmax (ATR)/cm^{-1} : 2980 (C-H), 1781 (C=O), 1678 (C=N), 1235 (O-C), 954 (N-O) and 642 (C-Br). HRMS (ESI+, 70 eV) calculated for $C_{19}H_{18}BrNO_4Na$ (M+Na+): 426.0411, Found: 426.0412.

2-(3-Bromophenyl)-2-({[(2-methylpropoxy)carbonyl]oxy}imino)-1-phenylethanone (63)

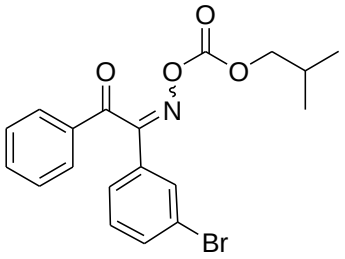

The reaction was carried out according to general procedure B using 2-(3-Bromophenyl)-2-(hydroximino)-1-phenylethanone (0.1 g, 0.33 mmol, 1 eq) isobutylchloroformate (0.05 mL, 0.36 mmol, 1.1 eq). The crude product was purified by flash chromatography (Biotage SP4, SiO_2, dichloromethane, 100 %) to give compound **63** as a pale yellow oil (0.06 g, 45.2 %) a racemic mixture of *E/Z* isomers (1:2). *Z*-monoxime, ^{1}H NMR (400 MHz, $CDCl_3$): δ 7.93-7.51 (m,9H,Ar-**H**), 4.05 (d, *J* = 6.5 Hz, 2H, O-C**H**$_2$ -CH-(CH_3)$_2$), 1.92 (m, 1H, O- CH_2 -C**H**-(CH_3)$_2$), 0.86 (d, *J* = 7.1 Hz, 6H, O-CH_2 -CH-(C**H**$_3$)$_2$). ^{13}C NMR (400 MHz, $CDCl_3$): δ 189.9 (1C, -CO-Ar), 159.9 (1C, C=N), 154.5 (1C, O-CO-O), 137.1 (1C, Ar), 135.4 (1C, Ar), 134.6 (1C, Ar), 134.0 (1C, Ar), 132.7 (1C, Ar), 131.1 (1C, Ar), 129.8 (2C, Ar), 129.3 (2C, Ar), 128.2 (1C, Ar), 123.4 (1C, Ar), 76.7 (1C, O- **C**H_2 -CH-(CH_3)$_2$), 27.7 (1C, O- CH_2 -**C**H-(CH_3)$_2$), 18.8 (2C, O- CH_2 -CH-(**C**H_3)$_2$). *E*-monoxime, ^{1}H NMR (400 MHz, $CDCl_3$): δ 77.93-7.42 (m,9H,Ar-**H**), 4.06 (t, *J* = 6.5 Hz, 2H, O-C**H**$_2$ -CH-(CH_3)$_2$), 2.00 (m, 1H, O- CH_2 -C**H**-(CH_3)$_2$), 0.96 (d, *J* = 7.1 Hz, 6H, O-CH_2 -CH-(C**H**$_3$)$_2$). ^{13}C NMR (400 MHz, $CDCl_3$): δ 190.0 (1C, CO-Ar), 160.0 (1C, C=N), 154.6 (1 C, O-CO-O), 137.2 (1C, Ar), 135.5 (1C, Ar), 134.7 (1C, Ar), 134.1 (1C, Ar), 132.8 (1C, Ar), 131.2 (1C, Ar), 129.9 (2C, Ar), 129.4 (2C, Ar), 128.3 (1C, Ar), 123.5 (1C, Ar), 77.7 (1C, O-**C**H_2 -CH-(CH_3)$_2$), 27.8 (1C, O-CH_2 -**C**H-(CH_3)$_2$), 18.9 (2C, O- CH_2 -CH-(**C**H_3)$_2$). IR: νmax (ATR)/cm^{-1}: 2962 (C-H), 1782 (C=O), 1676 (C=N), 1217 (O-C), 954 (N-O) and 684 (C-Br). HRMS (ESI+, 70eV) for $C_{19}H_{18}BrNO_4Na$ (M+Na+): 426.0312, Found: 426.0311.

2-(3-Bromophenyl)-1-phenyl-2-({[(prop-2-en-1-yloxy)carbonyl]oxy}imino)ethanone (64)

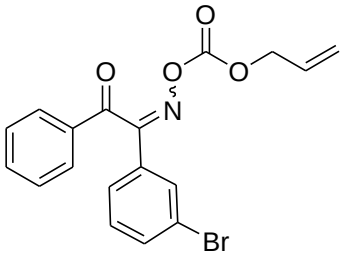

The reaction was carried out according to general procedure B using 2-(3-bromophenyl)-2-(hydroximino)-1-phenylethanone (0.1 g, 0.33 mmol, 1 eq) allylchloroformate (0.04 mL, 0.36 mmol, 1.1 eq). The crude product was purified by flash chromatography (Biotage SP4, SiO_2, dichloromethane, 100 %) to give compound **64** as a pale yellow oil (0.05 g, 39.2 %) a racemic mixture of *E/Z* isomers (1:2). *Z*-monoxime,^{1}H NMR (400 MHz, $CDCl_3$): δ 7.92 -7.46 (m, 9H, Ar-**H**), 5.91 (ddt, *J* = 17.3, 10.6 , 9.6 Hz, 1H, O-CH_2-C**H** -CH_2), 5.36 (dd, *J* = 10.6, 1.25 Hz, 1H, O-CH_2-CH -C**H**$_2$), 5.22 (dd, *J* = 17.3 , 1.2 Hz, 1H, O-CH_2-CH -C**H**$_2$), 4.75 (d, *J* = 9.6 Hz, 2 H, O-C**H**$_2$-CH -CH_2). ^{13}C NMR (400 MHz, $CDCl_3$): δ 190.0 (1C, CO-Ar), 160.0 (1C, C=N), 154.6 (1C, O-CO-O), 135.5 (1C, Ar), 135.0 (1C, Ar), 134.3 (1C, Ar), 134.0 (1C, Ar),132.2 (1C, Ar), 131.0 (1C, Ar), 130.0(1C, O-CH_2-**C**H ═CH_2), 129.1 (2C, Ar), 129.0 (2C, Ar), 128.1 (1C, Ar), 123.0 (1C, Ar), 119.9 (1C, O-CH_2-CH ═**C**H_2), 69.1 (1C, O-**C**H_2-CH ═CH_2). *E*-monoxime,^{1}H NMR (400 MHz, $CDCl_3$): δ 8.00 -7.49 (m, 9 H, Ar-**H**), 5.92 (ddt, *J* = 17.3, 10.6 ,9.6 Hz, 1H, O-CH_2-C**H** -CH_2), 5.37 (dd, *J* = 10.6, 1.25 Hz, 1H, O-CH_2-CH -C**H**$_2$), 5.23 (dd, *J* = 17.3, 1.2 Hz, 1H, O-CH_2-CH -C**H**$_2$), 4.76 (d, *J* = 9.6 Hz, 2 H, O-C**H**$_2$-CH -CH_2). ^{13}C NMR (400 MHz, $CDCl_3$): δ 190.1 (1C, CO-Ar), 160.1 (1C, C=N), 154.7 (1C, O-CO-O), 135.6 (1C, Ar), 135.1 (1C, Ar), 134.4 (1C, Ar), 134.1 (1C, Ar), 132.3 (1C, Ar), 131.1 (1C, Ar), 130.1(1C, O-CH_2-**C**H═CH_2), 129.2 (2C, Ar), 129.1 (2C, Ar), 128.2 (1C, Ar), 123.1 (1C, Ar), 120.0 (1C, O-CH_2-CH═**C**H_2), 69.2 (1C, O-**C**H_2-CH ═CH_2). IR: νmax (ATR)/cm^{-1} : 2953 (C-H), 1782 (C=O), 1677 (C=N), 1212 (O-C), 928 (N-O) and 685 (C-Br). HRMS: (ESI+, 70 eV) calculated for $C_{18}H_{14}BrNO_4Na$ (M+Na+): 409.9997, Found: 409.9998.

2-(3-Bromophenyl)-2-({[(chloromethoxy)carbonyl]oxy}imino)-1-phenylethanone (65)

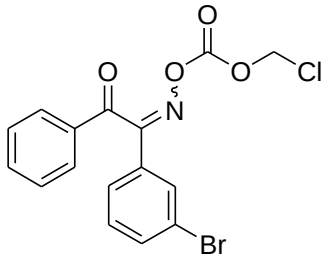

The reaction was carried out according to general procedure B using 2-(3-bromophenyl)-2-(hydroximino)-1-phenylethanone (0.1 g, 0.33 mmol, 1 eq) and choromethylchloroformate (0.04 mL, 0.36mmol, 1.1 eq). The crude product was purified by flash chromatography (Biotage SP4, SiO_2, dichloromethane, 100 %) to give compound **65** as a white solid (0.08 g, 61.5 %) a racemic mixture of *E/Z* isomers (1:2). *Z*-monoxime, ^{1}H NMR (400 MHz, $CDCl_3$): δ 7.92 -7.52 (m, 9H, Ar-**H**), 5.79 (s, 2 H, O-C**H**$_2$-Cl). ^{13}C NMR (400 MHz, $CDCl_3$): δ 188.3 (1C, CO-Ar), 159.9 (1C, C=N), 151.6 (1C, O-CO-O), 137.2(1C, Ar), 135.5 (1C, Ar), 134.5 (1C, Ar), 134.0 (1C, Ar), 132.6 (1C, Ar), 131.1 (1C, Ar), 129.5 (2C, Ar), 129.0 (2C, Ar), 128.0 (1C, Ar), 122.6 (1C, Ar), 72.5 (1C, O-**C**H$_2$-Cl). *E*-monoxime, ^{1}H NMR (400 MHz, $CDCl_3$): δ 8.00-7.51 (m, 9H, Ar-**H**), 5.80 (s, 2 H, O-C**H**$_2$-Cl). ^{13}C NMR (400 MHz, $CDCl_3$): δ 189.3 (1C, CO-Ar), 160.0 (1C, C=N), 151.7(1C, O-CO-O), 137.3 (1C, Ar), 135.6 (1C, Ar), 134.6 (1C, Ar), 134.1(1C, Ar), 132.7 (1C, Ar), 131.2 (1C, Ar), 129.6 (2C, Ar), 129.1 (2C, Ar), 128.1 (1C, Ar), 122.7 (1C, Ar), 72.6 (1C, O-**C**H$_2$-Cl). IR: νmax (KBr disc, cm^{-1}): 2988 (C-H), 1796 (C=O), 1681 (C=N), 1228 (O-C), 905 (N-O) and 682 (C-Br). HRMS: (ESI+, 70 eV) calculated for $C_{16}H_{11}BrClNO_4Na$ (M+Na+): 417.9622, Found: 417.9622.

2-({[(2-Bromoethoxy)carbonyl]oxy}imino)-2-(3-bromophenyl)-1-phenylethanone (66)

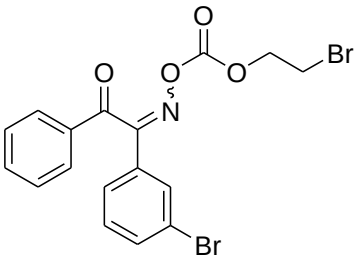

The reaction was carried out according to general procedure B using 2-(3-bromophenyl)-2-(hydroximino)-1-phenylethanone (0.1 g, 0.33 mmol, 1 eq) and 2-bromoethylchloroformate (0.04 mL, 0.36 mmol, 1.1 eq). The crude product was purified by flash chromatography (Biotage SP4) (SiO_2, dichloromethane, 100 %) to give compound **66** as a white solid (0.07 g, 46.8 %) a racemic mixture of *E/Z* isomers (1:2). *Z*-monoxime, ^{1}H NMR (400 MHz, $CDCl_3$): δ 7.85-7.44 (m, 9H, Ar-**H**), 4.90 (t, *J* = 6.2 Hz, 2 H, O-C**H**$_2$- CH_2 -Br), 3.48 (t, *J* = 6.2 Hz, 2 H, O-CH_2-C**H**$_2$ –Br). ^{13}C NMR (400 MHz, $CDCl_3$): δ 188.5 (1C, CO-Ar), 159.2 (1C, C=N), 151.7(1C, O-CO-O), 136.3(1C, Ar), 134.6 (1C, Ar), 134.3(1C, Ar), 134.1(1C, Ar), 131.7 (1C, Ar), 130.2 (1C, Ar), 129.6 (2C, Ar), 129.1 (2C, Ar), 128.1 (1C, Ar), 122.7 (1C, Ar), 68.9, (1C, O-**C**H_2-CH_2 -Br), 28.9(1C, O-CH_2- **C**H_2 -Br). *E*-monoxime, ^{1}H NMR (400 MHz, $CDCl_3$): δ 7.00 -7.44 (m, 9H, Ar-**H**), 4.47 (t, *J* = 6.2 Hz, 2 H, O-C**H**$_2$-CH_2 -Br), 3.52 (t, *J* = 6.2 Hz, 2 H, O-CH_2-C**H**$_2$ –Br). ^{13}C NMR (400 MHz, $CDCl_3$): δ 190.5 (1C, CO-Ar), 161.2 (1C, C=N), 152.7 (1C,O-CO-O), 136.4 (1C, Ar), 134.7 (1C, Ar), 134.4(1C, Ar), 134.2(1C, Ar), 131.8(1C, Ar), 130.3 (1C, Ar), 129.7 (2C, Ar), 129.2 (2C, Ar), 128.2 (1C, Ar), 122.8 (1C, Ar), 69.0 (1C, O-**C**H_2-CH_2 -Br), 27.0 (1C, O-CH_2-**C**H_2 -Br). IR: νmax (KBr disc, cm^{-1}): 2965 (C-H),1783 (C=O), 1677 (C=N),1210 (O-C), 928 (N-O) and 683 (C-Br). HRMS (ESI+, 70 eV) for calculated $C_{17}H_{13}Br_2NO_4Na$ (M+Na+): 475.9105, Found: 475.9104.

2-{[(Ethoxycarbonyl) oxy] imino}-1-(2-fluorophenyl)-2-phenylethanone (76)

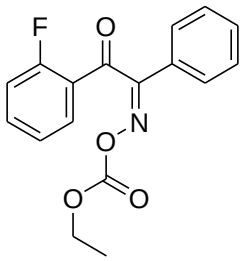

The reaction was carried out according to general procedure B using 1-(2-fluorophenyl)-2-(hydroxyimino)-2-phenylethanone (0.2g, 0.82 mmol, 1 eq) and ethylchloroformate (0.09 mL, 0.90 mmol, 1.1 eq). The crude was purified by flash chromatography (Biotage SP4, SiO_2, dichloromethane, 100 %) to afford compound **76** as a white solid (0.1 g, 38 %) as a racemic mixture of *E/Z* isomers (1:2). *Z*-monoxime, ^{1}H NMR (400 MHz, $CDCl_3$): δ 7.92-7.45 (m, 9H, Ar-**H**), 1.32 (q, *J* = 7.1 Hz, 2 H, -O-C**H**$_2$-CH$_3$), 4.27 (t, *J* = 7.1 Hz, 3H, O-CH$_2$-C**H**$_3$). ^{13}C NMR (400 MHz, $CDCl_3$): δ 190.0 (1C, CO-Ar), 164.9 (1C, C=N), 160.4 (1C, Ar), 157.1 (1C, O-CO-O), 136.2 (1C, Ar), 133.2 (1C, Ar), 131.5 (1C, Ar), 131.2 (1C, Ar), 129.5 (2C, Ar), 129.8 (2C, Ar), 124.9 (1C, Ar), 123.2 (1C, Ar), 116.1 (1C, Ar), 66.0 (1C, O-**C**H$_2$-CH$_3$), 31.1 (1C, - O-CH$_2$-**C**H$_3$). *E*-monoxime, ^{1}H NMR (400 MHz, $CDCl_3$): δ 8.01-7.45 (m, 9H, Ar-**H**), 1.33 (q, *J* = 7.10 Hz, 2 H, -O-C**H**$_2$-CH$_3$), 4.28 (t, *J* = 7.10 Hz, 3H, O-CH$_2$-C**H**$_3$). ^{13}C NMR (400 MHz, $CDCl_3$): δ 190.1 (1C, CO-Ar), 165.0 (1C, C=N), 160.5 (1C, Ar), 157.2 (1C, O-CO-O), 136.3 (1C, Ar), 133.3 (1C, Ar), 131.6 (1C, Ar), 131.3 (1C, Ar), 129.6 (2C, Ar), 129.9 (2C, Ar), 125.0 (1C, Ar), 123.3 (1C, Ar), 116.2 (1C, Ar), 66.1 (1C, O-**C**H$_2$-CH$_3$), 31.2 (1C, - O-CH$_2$-**C**H$_3$). IR: νmax (KBr disc, cm^{-1}): 2985 (C-H), 1783 (C=O), 1682 (C=N), 1220 (O-C), 115 (C-F)and 957 (N-O). HRMS: (ESI+, 70 eV) calculated for $C_{17}H_{14}NFO_4Na$ (M+Na+): 338.0798, Found: 338.0799.

2-{[(Ethoxycarbonyl)oxy]imino}-1-(3-fluorophenyl)-2-phenylethanone (77)

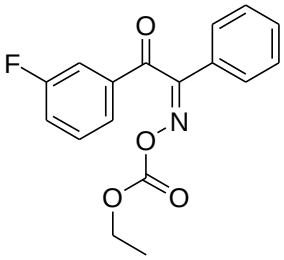

The reaction was carried out according to general procedure B using 1-(3-fluorophenyl)-2-(hydroxyimino)-2-phenylethanone (0. 02 g, 0.082 mmol, 1 eq) and ethylchloroformate (0.009 mL, 0.090 mmol, 1.1 eq). The crude product was purified by flash chromatography (Biotage SP4, SiO_2, dichloromethane, 100 %) to afford compound **77** as a white solid (0. 01 g, 38 %) as a racemic mixture of *E/ Z* isomers (1:1). *Z*-monoxime, ^{1}H NMR (400 MHz, $CDCl_3$): δ 7.93-7.35 (m, 9 H, Ar-**H**), 4.22 (q, *J* = 7.2 Hz, 2 H, O-C**H**$_2$-CH$_3$), 1.24 (t, *J* = 7.2 Hz, 3H, O-CH$_2$-C**H**$_3$). ^{13}C NMR (400 MHz, $CDCl_3$): δ 190.0 (1C, CO-Ar), 164.4 (1C, C=N), 163.4(1C, Ar), 157.2 (1C,O-CO-O), 139.5 (1C, Ar), 133.2 (1C, Ar), 131.1 (1C, Ar), 130.9 (1C, Ar), 128.6 (2C, Ar), 129.2 (2C, Ar), 125.0 (1C, Ar), 121.3 (1C, Ar), 114.8(1C, Ar), 70.1 (1C, O-**C**H$_2$-CH$_3$), 35.2 (1C, - O-CH$_2$-**C**H$_3$). *E*-monoxime, ^{1}H NMR (400 MHz, $CDCl_3$): δ 8.01-7.35 (m, 9H, Ar-**H**), 4.24 (q, *J* = 7.2 Hz, 2 H, -O-C**H**$_2$-CH$_3$), 1.26 (t, *J* = 7.2 Hz, 3H, O-CH$_2$-C**H**$_3$). ^{13}C NMR (400 MHz, $CDCl_3$): δ 190.1 (1C, CO-Ar), 164.5 (1C, C=N), 163.5 (1C, Ar), 157.3 (1C, O-CO-O), 139.6 (1C, Ar), 133.3 (1C, Ar), 131.2 (1C, Ar), 131.0 (1C, Ar), 128.7 (2C, Ar), 129.3 (2C, Ar), 125.1 (1C, Ar), 121.4 (1C, Ar), 114.9 (1C, Ar), 70.2 (1C, O-**C**H$_2$-CH$_3$), 35.3(1C - O-CH$_2$-**C**H$_3$). IR: νmax (KBr disc, cm^{-1}): 2995 (C-H), 1782 (C=O) 1682 (C=N), 1233 (O-C), 1189 (C-F) and 940 (N-O). HRMS: (ESI+, 70 eV) calculated for $C_{17}H_{14}N_2O_4F$ (N+NH$_4$+): 333.1243, Found: 333.1245.

1-(4-Bromophenyl)-2-{[(ethoxycarbonyl) oxy] imino}-2-phenylethanone (79)

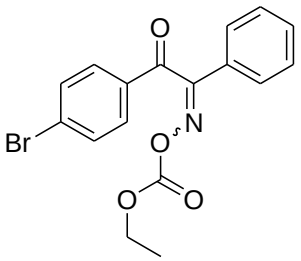

The reaction was carried out according to general procedure B using 2-(3-bromophenyl)-2-(hydroxyimino)-1-phenylethanone (0.25 g, 0.83 mmol, 1 eq) and ethylchloroformate (0.09 mL, 0.92 mmol, 1.1 eq). The crude product was purified by flash chromatography (Biotage SP4) (SiO_2, dichloromethane, 100 %) to afford compound **79** as pure a colorless oil (0.21 g, 66 %) a racemic mixture of *E/Z* isomers (1:25). *Z*-monoxime, ^{1}H NMR (400 MHz, $CDCl_3$): δ 7.92-7.40 (m, 9H, Ar-**H**), 4.24 (q, *J* = 7.0 Hz, 2 H, -O-C**H**$_2$-CH_3), 1.24 (t, *J* = 7.0 Hz, 3H, O-CH_2-C**H**$_3$). ^{13}C NMR (400 MHz, $CDCl_3$): δ 190.3 (1C, CO-Ar), 163.2 (1C, C=N), 157.3 (1C, O-CO-O), 136.1 (1C, Ar),133.2 (1C, Ar), 132.1 (2C, Ar), 132.0 (2C, Ar), 131.0 (1C, Ar), 129.8 (2C, Ar), 128.7 (2C, Ar), 128.2 (1C, Ar), 63.8 (1C, O-**C**H_2-CH_3), 16.3 (1C, - O-CH_2-**C**H_3). *Z*-monoxime, ^{1}H NMR (400 MHz, $CDCl_3$): δ 8.01-7.40 (m, 9H, Ar-**H**), 4.26 (q, *J* = 7.0 Hz, 2 H,-O-C**H**$_2$-CH_3), 1.27. (t, *J* = 7.0 Hz, 3H, O-CH_2-C**H**$_3$). ^{13}C NMR (400 MHz, $CDCl_3$): δ 190.4 (1C, CO-Ar), 163.3 (1C, C=N), 157.4 (1C,O-CO-O), 136.2 (1C, Ar), 133.3 (1C, Ar), 132.2 (2C, Ar), 132.1 (2C, Ar), 131.1 (1C, Ar), 129.9 (2C, Ar), 128.8 (2C, Ar), 128.3(1C, Ar), 63.9 (1C O-**C**H_2-CH_3), 16.4 (1C - O-CH_2-**C**H_3). IR: νmax (ATR)/cm^{-1} : 2983 (C-H),1780 (C=O), 1682 (C=N), 1215 (O-C), 959(N-O) and 699(C-Br). HRMS:(ESI+,70eV)calculated for $C_{17}H_{14}BrO_4NNa$ (M+Na+): 397.9997, Found: 397.9998.

1-(4-Chlorophenyl)-2-{[(ethoxycarbonyl)oxy]imino}-2-phenylethanone (81)

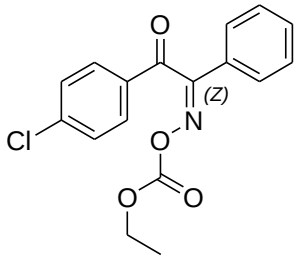

The reaction was carried out according to general procedure B using 1-(4-Chlorophenyl)-2-(hydroxyimino)-2-phenylethanone (0.1g, 0.38mmol, 1 eq) and ethylchloroformate (0.04 mL, 0.42 mmol, 1.1 eq). The crude product was chromatographed (SiO_2, dichloromethane, 100%) to afford compound **81** (0.067 g, 67 %) as off white solid. MR. 90-92 ^{o}C. ^{1}H NMR (400 MHz, $CDCl_3$): δ 7.92-7.40 (m, 9H, Ar-**H**), 4.24 (q, *J* = 7.1 Hz, 2 H, -O-C**H**$_2$-CH$_3$), 1.24 (t, *J* = 7.1 Hz, 3H, O-CH$_2$-C**H**$_3$). ^{13}C NMR (400 MHz, $CDCl_3$): δ 190.1 (1C, CO-Ar), 154.2 (1C, O-CO-O), 164.1 (1C, C=N), 141.9 (1C, Ar), 135.7 (1C, Ar), 132.2 (1C, Ar), 131.2 (2C, Ar), 130.8 (1C, Ar), 129.9 (2C, Ar), 129.3 (2C, Ar), 127.9 (2C, Ar), 65.4 (1C, O-**C**H$_2$-CH$_3$), 14.3 (1C, O-CH$_2$-**C**H$_3$). IR: νmax (KBr disc, cm^{-1}): 2995 (C-H), 1780 (C=O), 1683 (C=N), 1218 (O-C), 1174 (C-Cl) and 940 (N-O). HRMS: (ESI+, 70 eV) calculated for C$_{17}$H$_{14}$ClN O$_4$ Na (M+Na+): 354.0503, Found: 354.0504. Found C, 60.61; H, 4.19; N, 3.96; Cl, 13.23 (Required for C$_{17}$ H$_{14}$ClN O$_4$: C, 61.55; H, 4.25; N, 4.22; Cl, 10.69).

2-{[(Ethoxycarbonyl)oxy]imino}-1,2-*bis(*4-methoxyphenyl)ethanone (83)

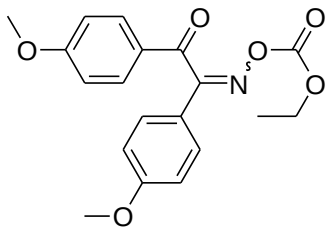

The reaction was carried out according to general procedure B using (2-(Hydroxyimino)-1, 2-*bis* (4-methoxyphenyl) ethanone (0.1 g, 0.30 mmol, 1 eq) and ethylchloroformate (0.03 mL, 0.33 mmol, 1.1 eq). The crude was purified by flash chromatography (Biotage SP4) (SiO_2, dichloromethane, 100 %) to afford to afford

compound **83** as a white solid (0.05 g, 53 %) a racemic mixture of *E/Z* isomers (1:10). *Z*-monoxime, ^{1}H NMR (400 MHz, $CDCl_3$): δ 7.98-7.85 (m, 8H, Ar-**H**), 4.24 (q, *J* = 7.2 Hz, 2 H, -O-C**H**$_2$-CH_3),), 3.77 (s, *J* = 7.2 Hz, 6H, -OC**H**$_3$), 1.24 (t, *J* = 7.2 Hz, 3H, O-CH_2-C**H**$_3$). ^{13}C NMR (400 MHz, $CDCl_3$): δ 189.9 (1C, CO-Ar), 165.1 (1C, Ar), 164.2 (1C, O-CO-O), 162.3 (1C, Ar), 154.5 (1C, C=N), 130.5 (2C, Ar), 130.4 (2C, Ar), 130.1 (1C, Ar), 127.5 (1C, Ar), 114.7 (2C,Ar), 114.2 (2C, Ar), 65.0 (1C, O-**C**H_2-CH_3), 55.5 (2C, -O**C**H_3), 13.2 (1C,-O-CH_2-**C**H_3). *E*-monoxime, ^{1}H NMR (400 MHz, $CDCl_3$): δ 8.01-7.40 (m, 8H, Ar-**H**), 4.26 (q, *J* = 7.2 Hz, 2 H, -O-C**H**$_2$-CH_3), 3.78 (s, 6H, -OC**H**$_3$), 1.27 (t, *J* = 7.2 Hz, 3H, O-CH_2-C**H**$_3$). ^{13}C NMR (400 MHz, $CDCl_3$): δ 190.0 (1C, CO-Ar),165.2 (1C, Ar), 154.1 (1C, O-CO-O), 162.4 (1C, Ar), ,154.6 (1C, C=N), 130.6 (2C, Ar), 130.5 (2C, Ar), 130.2 (1C, Ar), 127.6 (1C, Ar), 114.8 (2C, Ar), 114.3 (2C, Ar), 65.1 (1C, O-**C**H_2-CH_3), 55.6 (2C,-O**C**H_3), 13.3 (1C,-O-CH_2-**C**H_3). IR: νmax (KBr disc, cm^{-1}): 2983 (C-H), 1787 (C=O), 1664 (C=N), 1215 (O-C) and 949 (N-O). HRMS: (ESI+, 70 eV) calculated for $C_{19}H_{20}NO_6$ (M+H+): 358.1284, Found: 358.1285.

3.4.3 Synthesis of ester derivatives

(2*Z*)-2-[(Acetyloxy)imino]-1,2-diphenylethanone (16)

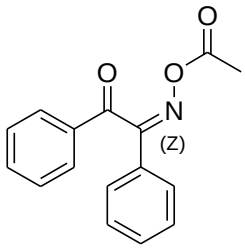

The reaction was carried out according to general procedure B using (2*Z*)-2-(Hydroximino)-1,2-diphenylethanone (0.2 g, 0.89 mmol, 1 eq) and ethanoyl chloride (0.07 mL, 0.98 mmol, 1.1 eq). The crude product was chromatographed (SiO_2, dichloromethane 100%) to afford compound **16** (0.12 g, 50.1 %) as colorless crystals. MR. 68-70 ^{o}C. ^{1}H NMR (400 MHz, $CDCl_3$): δ 8.01-7.26 (m, 10H, Ar-**H**), 1.98 (s, 3H, -C**H**$_3$). ^{13}C NMR (400 MHz, $CDCl_3$): δ 190.3 (1 C, CO-Ar), 168.9 (1C, O-CO-O), 160.6 (1C, C=N), 135.2 (1C, Ar), 134.6 (1C, Ar), 131.1 (1C, Ar), 130.5 (1C, Ar), 129.5 (2C, Ar), 129.2 (2C, Ar),128.7 (2C, Ar), 128.5 (2C, Ar), 19.4 (1C, -

CH_3). IR: νmax (KBr disc, cm^{-1}): 2961 (C-H), 1766 (C=O), 1681 (C=N), 1232 (O-C) and 964 (N-O). HRMS (ESI+, 70 eV) calculated for $C_{16}H_{13}NO_3Na$ (M+Na+): 290.0787, Found: 290.0787. Found C,60.65; H, 4.78; N, 3.02 (Required for $C_{16}H_{13}O_3N$: C, 60.48; H,4. 90; N, 5.24).

1-{[(*Z*)-(2-Oxo-1,2-diphenylethylidene)amino]oxy}propan-1-one (17)

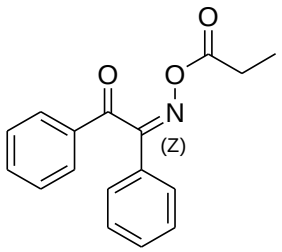

The reaction was carried out according to general procedure B using (2*Z*)-2-(hydroximino)-1, 2-diphenylethanone (0.2 g, 0.89 mmol, 1 eq) and propionylchloride (0.085 mL, 0.98 mmol, 1.1 eq). Recrystallisation of the crude from ethanol afford compound **17** (0.044 g, 45.6 %) as a white solid. MR. 78-80 ^oC. ^1H NMR (400 MHz, $CDCl_3$): δ 7.91-7.36 (m, 10H, Ar-H), 2.15 (q, *J* = 7.0 Hz, 2H, -C**H**$_2$-CH_3), 0.95 (t, *J* = 7.0 Hz, 3H, -CH_2-C**H**$_3$). ^{13}C NMR (400 MHz, $CDCl_3$): δ 190.5 (1C, CO-Ar), 163.7 (1C, O-CO-O), 151.4 (1C, C=N), 135.3 (1C, Ar) 134.5(1C, Ar), 131.1 (1C, Ar), 130.4 (1C, Ar), 129.9 (2C, Ar), 129.4 (2C, Ar), 128.7 (2C, Ar), 128.5 (2C, Ar), 72.4 (1C, -**C**H_2-CH_3), 31.0 (1C, -CH_2-**C**H_3). IR: νmax (KBr disc, cm^{-1}): 2988 (C-H), 1781 (C=O), 1681 (C=N), 1229 (O-C) and954 (N-O). HRMS (ESI+, 70 eV) calculated for $C_{17}H_{15}NO_3Na$ (M+Na+): 304.0945, Found: 304.0944. Found C, 72.09; H, 5.76; N, 4.91(Required for $C_{17}H_{15}NO_3$: C, 72.58; H,5. 73; N, 4.98).

1-{[(*Z*)-(2-Oxo-1,2-diphenylethylidene)amino]oxy}butan-1-one (18)

.

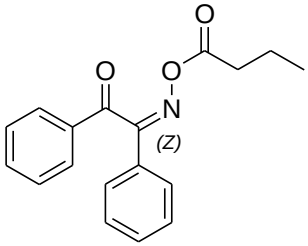

The reaction was carried out according to general procedure B using (2*Z*)-2-(hydroximino)-1,2-diphenylethanone (0.2 g, 0.89 mmol, 1 eq*)* and butryl chloride (0.10 mL, 0.98 mmol, 1.1 eq). Recrystallisation of the crude from ethanol afford compound **18** (0.119 g, 45.2%) as colourless crystals. MR. 40-42 ^{o}C. ^{1}H NMR (400 MHz, $CDCl_3$): δ 7.94-7.36 (m, 10H, Ar-**H**), 4.40 (t, 2H, *J* = 7.4 Hz -C**H**$_2$-CH_2-CH_3), 1 .57 (m, 2H, -CH_2-C**H**$_2$-CH_3), 0.94 (t, *J* = 6.7 Hz, 3H, -CH_2-CH_2-C**H**$_3$). ^{13}C NMR (400 MHz, $CDCl_3$): δ 191.8 (1C, CO-Ar), 170.8 (1C, O-CO-O), 162.7 (1C, C=N), 135.4 (1C, Ar), 134.4 (1C, Ar), 131.0 (1C, Ar), 130.0 (1C, Ar), 129.5 (2C, Ar), 129.1 (2C, Ar), 128.7 (2C, Ar), 128.2 (2C, Ar), 31.7 (1C, -**C**H_2-CH_2-CH_3), 22.0 (1C, -CH_2-**C**H_2-CH_3), 9.9 (1C, -CH_2-CH_2-**C**H_3). IR: νmax (KBr disc, cm^{-1}): 2966 (C-H), 1770 (C=O), 1677 (C=N), 1228 (O-C) and 962 (N-O). HRMS (ESI+, 70 eV) calculated for $C_{18}H_{17}NO_3Na$ (M+Na+): 318.1099, Found: 318.1101. Found C, 73.09; H, 5.76; N, 4.41(Required for $C_{18}H_{17}NO_3$: C, 73.20; H, 5.80; N, 4.74).

1-{[(*Z*)-(2-Oxo-1,2-diphenylethylidene)amino]oxy}pentan-1-one(19)

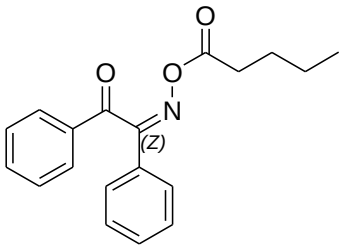

The reaction was carried out according to general procedure B using (2*Z*)-2-(hydroximino)-1,2-diphenylethanone (0.2 g, 0.89 mmol, 1 eq*)* and valeryl chloride (0.12 mL, 0.98 mmol, 1.1 eq). The crude product was chromatographed (SiO_2, dichloromethane 100%) to afford compound **19** (0.06 g, 21.8 %) as a colorless oil. ^{1}H NMR (400 MHz, $CDCl_3$): δ 7.94 -7.40 (m, 10H, Ar-**H**), 2.22 (t, *J* = 6.8 Hz, 2H, -

C**H**$_2$-CH_2-CH_2-CH_3), 1.31 (m, 2H, -CH_2-C**H**$_2$-CH_2-CH_3), 1.22 (m, 2H, -CH_2-CH_2-C**H**$_2$-CH_3), 0 .72 (t, J = 7.3 Hz, 3H, -CH_2-CH_2-CH_2-C**H**$_3$). ^{13}C NMR (400 MHz, $CDCl_3$): δ 191.8 (1C, CO-Ar), 170.1 (1C, O-CO-O), 162.7 (1C, C=N), 135.4 (1C, Ar), 134.9 (1C, Ar), 132.0 (1C, Ar), 130.0 (1C, Ar), 129.9 (2C, Ar), 129.3 (2C, Ar), 128.7 (2C, Ar), 128.3 (2C, Ar), 32.5 (1C, O -**C**H_2-CH_2- CH_2CH_3), 26.6 (1C, -CH_2-**C**H_2 CH_2-CH_3), 22.0 (1C, -CH_2-CH_2 **C**H_2-CH_3), 13.7 (1C, -CH_2-CH_2 CH_2-**C**H_3). IR: νmax (ATR)/cm^{-1} : 2966 (C-H), 1771 (C=O), 1681 (C=N), 1226 (O-C)and 937 (N-O). HRMS (ESI+, 70 eV) calculated for C_{19} $H_{19}NO_3Na$ (M+Na+): 332.1257, Found: 332.1258. Found C,73.70; H, 6.30; N, 4.46 (Required for $C_{19}H_{19}O_3N$: C, 73.77; H,6.19; N, 4.53).

3-Methyl-1-{[(*Z*)-(2-oxo-1,2-diphenylethylidene)amino]oxy}butan-1-one (20)

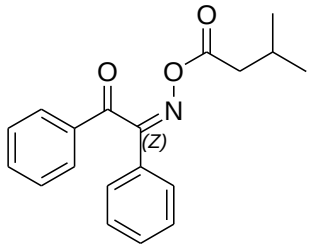

The reaction was carried out according to general procedure B using (2*Z*)-2-(Hydroximino)-1,2-diphenylethanone (0.2 g, 0.89 mmol, 1 eq) and isovaleryllchloride (0.12 mL, 0.98 mmol, 1.1 eq). The crude product was chromatographed (SiO_2, dichloromethane 100 %) to afford compound **20** (0.05 g, 22 %) as a white solid. Mpt. 36-38 ^{o}C. ^{1}H NMR (400 MHz, $CDCl_3$): δ 77.94-7.40 (m, 10H, Ar-**H**), 2.80 (d, J = 6.8 Hz, 2H, -C**H**$_2$ -CH-$(CH_3)_2$), 1.85 (m, 1H, -CH_2 -C**H**-$(CH_3)_2$) 0.79 (d, J = 6.8 Hz, 6H, - CH_2 -CH-(C**H**$_3)_2$). ^{13}C NMR (400 MHz, $CDCl_3$): δ 191.8 (1C, CO-Ar), 169.3 (1C, O-CO-O), 162.4 (1C, C=N), 135.3 (1C, Ar), 134.1 (1C, Ar), 132.0 (1C, Ar), 130.2 (1C, Ar), 129.9 (2C, Ar), 129.3 (2C, Ar), 128.7 (2C, Ar), 127.7 (2C, Ar), 41.7(1C, -**C**H_2 -CH-$(CH_3)_2$), 25.6 (1C, - CH_2 -**C**H-$(CH_3)_2$), 22.2 (2C, - CH_2 -CH-(**C**$H_3)_2$). IR: νmax (KBr disc, cm-^{1}): 2960 (C-H), 1773 (C=O), 1683 (C=N), 1228 (O-C) and 948 (N-O). HRMS (ESI+, 70 eV) calculated for $C_{19}H_{23}N_2O_3$ (M+NH_4+): 327.1702, Found: 327.1703. Found C, 73.75; H, 6.20; N, 4.53(Required for $C_{19}H_{19}NO_3$: C, 73.77; H, 6.19; N, 4.53).

2-Methyl-1-{[(*Z*)-(2-oxo-1,2-diphenylethylidene)amino]oxy}propan-1-one (21)

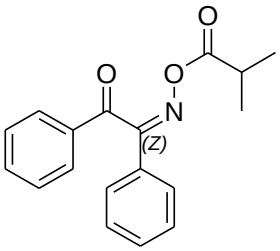

The reaction was carried out according to general procedure B using (2*Z*)-2-(hydroximino)-1,2-diphenylethanone (0.2 g, 0.89 mmol, 1 eq*)* and isobutrylchloride (0.1 mL, 0.98 mmol, 1.1 eq). Recrystallisation of the crude product from ethanol afforded compound **21** (0.119 g, 45.2 %) as colorless crystals. MR. 88-90 ^{o}C. ^{1}H NMR (400 MHz, $CDCl_3$): δ 8.01-7.26 (m, 10H, Ar-**H**), 2.25 (m, 1H, -C**H**-CH_3), 0.87 (d, *J* = 6.9 Hz, 6 H, -CH-(C**H**$_3$)$_2$). ^{13}C NMR (400 MHz, $CDCl_3$): δ 191.8 (1C, CO-Ar), 173.1 (1C, O-CO-O), 164.2 (1C=N), 135.9 (1C, Ar), 134.9 (1C, Ar), 132.0 (1C, Ar), 130.5 (1C, Ar), 129.3 (2C, Ar), 129.1 (2C, Ar), 128.8 (2C, Ar), 127.8 (2C, Ar), 32.8 (1C , -**C**H-CH_3), 14.4 (2C, -CH–(**C**H_3)$_2$). IR: νmax (KBr disc, cm-^{1}): 2966 (C-H), 1766 (C=O), 1679 (C=N), 1235 (O-C) and 962 (N-O). HRMS (ESI+, 70 eV) calculated for $C_{18}H_{17}NO_3Na$ (M+Na+): 318.1100, Found: 318.1101. Found C, 73.09; H, 5.76; N, 4.41 (Required for $C_{18}H_{17}N\ O_3$: C, 73.20; H,5.80; N, 4.74).

1-{[(*Z*)-(1,2-Diphenylethylidene)amino]oxy}propan-1-one (24)

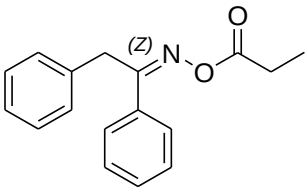

The reaction was carried out according to general procedure B using (1*Z*)-*N*-hydroxy-1,2-diphenylethanimine (0.10 g, 0.47 mmol, 1 eq) and propionylchloride (0.05 mL, 0.52 mmol, 1.1 eq). The crude product was chromatographed [SiO_2; 10% diethyl ether in n-hexane] to give compound **24** (0.023 g, 18 %) as clear pale-yellow oil. ^{1}H NMR (400 MHz, $CDCl_3$): δ 7.94-7.18 (m, 10H, Ar-**H**), 4.33(s, 2H, Ar-C**H**$_2$), 2.28 (q, *J* = 7.1 Hz, 2H, -C**H**$_2$-CH_3), 1.35 (t, *J* = 7.1 Hz, 3H -CH_2- C**H**$_3$). ^{13}C NMR

(400 MHz, $CDCl_3$): δ 168.8 (1C,C=O), 161.5 (1C, C=N), 135.4 (1C, Ar) 134.6 (1C, Ar), 131.2 (1C, Ar), 129.9 (2C, Ar), 129.4 (2C, Ar), 128.7 (2C, Ar), 128.5 (2C, Ar), 125.4 (1C, Ar), 41.2 (1C, **C**H_2-Ar), 25.3 (1C, -**C**H_2-CH_3), 9.1 (1C, -CH_2-**C**H_3). IR: νmax (ATR)/cm^{-1}: 2987 (C-H), 1688 (C=O), 1680 (C=N), 1228 (O-C) and 954 (N-O). HRMS (ESI+, 70eV) calculated for $C_{17}H_{17}NO_2$: 267.3233, Found: 267.3233.

1-{[(*E*)-(1,2-Diphenylethylidene)amino]oxy}propan-1-one (25)

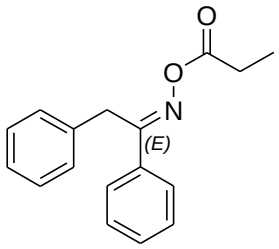

The reaction was carried out according to general procedure B using (1*E*)-*N*-hydroxy-1,2-diphenylethanimine (0.10 g, 0.47 mmol, 1 eq) and propionylchloride (0.05 mL, 0.52 mmol, 1.1 eq). The crude product were chromatographed [SiO_2; 10% diethyl ether in *n*-hexane] to give compound **25** (0.02 g, 21%) as a yellow oil. ^{1}H NMR (400 MHz, $CDCl_3$): δ 7.96-7.19 (m, 10H, Ar-**H**), 4.35 (s, 2H, Ar-C**H**$_2$), 4.26 (q, *J* = 7.2 Hz, 2H, O -C**H**$_2$-CH_3), 1.36 (t, *J* = 7.2 Hz, 3H, O-CH_2- C**H**$_3$). ^{13}C NMR (400 MHz, $CDCl_3$): δ 168.9 (1C, O-CO-O), 161.6 (1C, C=N), 135.5 (1C, Ar) 134.7 (1C, Ar), 131.3 (1C, Ar), 130.0. (2C, Ar), 129.5 (2C, Ar), 128.8 (2C, Ar), 128.6 (2C, Ar), 125.5 (1C, Ar), 34.3 (1C -**C**H_2-Ar), 25.8 (1C, -**C**H_2-CH_3), 9.4 (1C, -CH_2-**C**H_3). IR: νmax (ATR)/cm^{-1} : 2953 (C-H), 1687 (C=O), 1641 (C=N), 1282 (O-C) and 933 (N-O). HRMS (ESI+, 70 eV) calculated for $C_{17}H_{17}NO_2$: 267.3233, Found: 267.3233. Found C, 68.76; H, 6.04; N, 5.32 (Required for $C_{17}H_{17}O_2$ N; C,72.07; H,6.05; N, 4.94).

Chapter 4:References

Abbott, C., McCaughan, G. and Gorrell, M. (1999). Two highly conserved glutamic acid residues in the predicted beta propeller domain of DPP-IV are required for its enzyme activity. *Federation of the European Biochemical Societies Letters,* **458**(3): 278-284.

Aertgeerts, K., Ye, S., Tennant, M., Kraus ,L., Rogers, J., Sang ,C., Skene ,J. , Webb, R. and Prasad, S. (2004). Crystal structure of human dipeptidyl peptidase IV in complex with a decapeptide reveals details on substrate specificity and tetrahedral intermediate formation. *Protein Science*, **13**(2): 412-421.

Ahn, J., Kim, J., Kim, H., Kwon, H., Huh, S., Rhee, S., Kim, K., Yang, S., Park, S., Lee, J., Kim, S. and Cheon, H. (2005). Synthesis and evaluation of pyrazolidine derivatives as dipeptidyl peptidase IV (DPP-IV) inhibitors. *Bioorganic and Medicinal Chemistry Letters,* **15**(5): 1337-1340.

Ahren, B., Pacini,G., Foley, JE. and Schweizer, A. (2005). Improved meal related β-cell function and insulin sensitivity by DPP-IV inhibitor vildagliptin in metformin treated patients with type 2 diabetes over 1 year. *Diabetes Care*, **28**: 1936–1940.

American Diabetes Association. (2007). All about diabetes. Available from <http://www.diabetes.org/aboutdiabetes. jsp> accessed July 5, 2010.

Augeri,D., Robl, J., Betebenner, D., Magnin, D., Khanna, A., Robertson, J., Wang, A., Simpkins, L., Taunk, P., Huang, Q., Han, S., Abboa-Offei, B., Cap, M., Xin, L., Tao, L., Tozzo, E., Welzel, G., Egan, M., Marcinkeviciene, J.,Chang, S., Biller, S., Kirby, M., Parker, R. and Hamann, L. (2005). Discovery and preclinical profile of saxagliptin (BMS-477118): a highly potent, long-acting, orally active dipeptidyl peptidase IV inhibitor for the treatment of type 2 diabetes. *Journal of Medicinal Chemistry*, **48**: 5025–5037.

Augustyns, K., Van der Veken, P., Senten, K. and Haemers, A. (2005). The therapeutic potential of inhibitors of DPP-IV and related praline-specific aminopeptidases. *Current Topics in Medicinal Chemistry*, **12**: 971–998.

Brubaker, P. and Drucker, D. (2002). Structure-Function of the Glucagon Receptor Family of G protein–coupled Receptors: The glucagon, GIP, GLP-1, and GLP-2 receptors. *Receptors and Channels*, **8**: 179–188.

Burkey, B., Hoffmann, P., Hassiepen, U., Trappe, J, Juedes, M. and Foley, J. (2008). Adverse effects of dipeptidyl peptidases 8 and 9 inhibition in rodents revisited**.** *Diabetes Obesity and Metabolism*, **10** (11**)**: 1057-1059.

Chien, C., Huang, H., Chou, C., Chen, S., Han, Y., Chang, G., Liang, H. and Chen, X. (2004). One site mutation disrupts dimer formation in human DPP-IV proteins. *Journal of Biological Chemistry*, **279** (50): 52338-52345.

Covington, MB. (2001). Traditional Chinese medicine in the treatment of diabetes. *Diabetes Spectrum*, **12** (3): 155-159.

Creutzfeldt, W. (1979). The incretin concept today. *Diabetologia*, **16**: 75–85.

Demuth, H., Baumgrass, R., Schaper, C., Fischer, G. and Barth, A. (1988). DPP-IV inactivation with N-peptidyl-O-aroyl hydroxylamines. *Journal of Enzyme Inhibition*, **2** (2): 129-42.

Ding, W., Renstrom, E., Rorsman, P., Buschard, K. and Gromada, J. (1997). GLP-1and glucose-dependent insulinotropic polypeptide stimulates Ca2+-induced secretion in rat alpha-cells by a protein kinase A mediated Mechanism. *Diabetes*, **46**: 792-800.

Drucker, D. (2003). GLP-1 and the islet ß-cell: Augmentation of cell proliferation and inhibition of apoptosis. *Endocrinology*, **144**: 5145-5148.

Edmondson, S., Mastracchio, A., Mathvink, R., He, J., Harper, B., Park, Y., Beconi, M., Di Salvo, J, Eiermann, G. J, He, H., Leiting, B., Leone, J., Levorse, D., Lyons, K., Patel, R., Patel, S., Petrov, A., Scapin, G., Shang, J., Sinh Roy, R., Smith, A., Wu, J. , Xu, S., Zhu, B., Thornberry, N. and Weber, A. (2007). *Journal of Medicinal Chemistry*, **49**: 3614-3618.

Engel, M., Hoffmann, T., Manhart, S., Heiser, U., Chambre, S., Huber, R., Demuth, H. and Bode,W. (2006). Rigidity and Flexibility of DPP- IV: Crystal Structures of and Docking Experiments with DPIV Crystal Structures of and Docking Experiments with DPIV. *Journal of Biological Chemistry*, **355**: 768–783.

Engel, M., Hoffmann, T., Wagner, L., Wermann, M., Heiser, U., Kiefersauer, R., Huber, R., Bode, W., Demuth, H.U. and Brandstetter, H. (2003). The crystal structure of DPP-IV (CD26) reveals its functional regulation and enzymatic mechanism**,** *Proceedings of the National Academy of Sciences,* **100**: 5063–5068.

Farooqi, H., Khan, H., Gupta, R., Habib, A., Akhtar, P., Mir, S. and Naquvi, K. (2010). New trends of diabetes therapy type 2 of the animal model. *International Journal of Pharmaceutical and Clinical Research*, **2** (2): 80-89.

Flatt, P., Bailey, C. and Green, B. (2008). DPP-IV and related molecules in type 2 diabetes. *Frontiers in Bioscience*, **13**: 3648-3660.

Geldern, T. and Trevillyan, J. (2006). "The Next Big Thing" in diabetes: clinical progress on DPP-IV inhibitors. *Drug Development Research*, **67**: 627–642.

Goke, R., Fehmann, H., Linn, T., Schmidt, H., Krause, M., Eng, J. and Goke, B. (1993). Exendin-4 is a high potency agonist and truncated exendin-(9-39)-amide an antagonist at the glucagon-like peptide 1-(7-36)-receptor of insulin-secreting cells. *Journal of Bioloigcal Chemistry*, **268** (26): 19650-19655.

Green, B., Flatt, P. and Bailey, C. (2006). DPP-IV inhibitors: a newly emerging drug class for the treatment of type 2 diabetes. *Diabetes and vascular disease research*, **3** (3): 159–165.

Green, P. and Doherty, J. (1979). Patent Specification 1537 921.

Gromada, J., Holst, J. and Rorsman, P. (1998). Cellular regulation of islet hormone secretion by the incretin hormone GLP-1. *European Journal of Physiology*, **435**: 583-594.

Guillausseau,P., Meas, M., Virally, M., Laloi-Michelin, V., Médeau,V. and Kevorkian, J. (2008). Abnormalities in insulin secretion in type 2 diabetes mellitus. *Diabetes* and *Metabolism*, **34**: 43-48.

Haffner,C., McDougald, D., Randhawa, A., Reister, S., and Lenhard, J. (2003). World Patent Application no WO 2003002531.

Havale, S., and Pal, M. (2009). Medicinal chemistry approaches to the inhibition of dipeptidyl peptidase-4 for the treatment of type 2 diabetes. *Bioorganic* and *Medicinal Chemistry*, **17**: 1783–1802.

Hiramatsu, H., Kyono, K., Higashiyama, Y., Fukushima, C., Shima, H., Sugiyama, S., Inaka, K.,Yamamoto, A. and Shimizu, R.(2003). The structure and function of human dipeptidyl peptidase IV, possessing a unique eight-bladed -propeller fold. *Biochemical and Biophysical Research Communications*, **302**: 849–854.

Hirashima ,S., Suzuki, T., Ishida ,T., Noji, S., Yata, S., Ando, I., Komatsu, M., Ikeda, S. and Hashimoto, H. (2006). Benzimidazole derivatives bearing substituted biphenyls as hepatitis C virus NS5B RNA-dependent RNA polymerase inhibitors: Structure-activity relationship studies and identification of a potent and highly selective inhibitor JTK-109. *Journal of Medicinal Chemistry*, **49**(15): 4721-4736.

Holt, R., and Hanley, N. (2007). *Essential: Endocrinology and Diabetes* (5th ed.). Oxford: Blackwell Publishing.

Huang, S., and Czech, M. (2007). The GLUT4 Glucose Transporter. *Cell Metabolism***, 5** (4): 237- 252.

Idris, I. and Donnelly, R. (2007). Dipeptidyl peptidase-IV inhibitors: a major new class of oral antidiabetic drug. *Diabetes, Obesity and Metabolism*, **9**: 153–165.

Iglesias, E. and Williams, D. (1989). Carbanion nitrosation: Reaction of malononitrile with nitrous acid. *Chemical Society, Perkin Transactions*, **2**(4): 343-346.

Kieffer, T. and Habener, J. (1999). The Glucagon-Like Peptides. *Endocrine Reviews*, **20**: 876-913.

Kileinspehn, G., Jung ,J, and Studiahze,S. (1967). The chemical shift of the hydroxyl proton of oximes in dimethyl Sulfoxide. *Journal of Organic Chemistry*, **32**(2): 460–462.

Kim, K., Rhee, S. and Kim, H. (2005). KR-62436, 6-(2-[5- cyano-4,5-dihydropyrazol-1-yl)-2-oxoethylamino]ethylamino) nicotinonitrile, is a novel dipeptidyl peptidase-IV (DPP-IV) inhibitor with antihyperglycaemic activity. *European Journal of Pharmacology*, **518**: 63–70.

Kong, M., Ngai, M. and Krische, R. (2006). Highly enantioselective direct reductive coupling of conjugated alkynes and α-ketoesters via rhodium-catalyzed asymmetric hydrogenation. *Journal of the American Chemical Society*. **128:** 718-719.

Koo, D., Kim, J., Sungsub, K., Kyoung, H., Hong, Y., Hur, C., Yim, J., Geun, T., Oon, H., Kwon, O., Kwon, S. and Lee, S. (2007). Synthesis, SAR, and Xray strucure of novel potent DPP-IV inhibitors: Oxadiazolyl ketones. *Bioorganic and Medicinal Chemistry letters*, **17**: 4167-4172.

Kowalchick, J., Leiting, B., Pryor, K., Marsilio, F., Wu, J., He, H., Lyons, K., Eiermann,G., Petrov, A., Scapin, G., Patel, R., Thornberry, N., Weber, A. and Kim, D. (2007). Design, synthesis, and biological evaluation of triazolopiperazine-based beta-amino amides as potent, orally active dipeptidyl peptidase IV (DPP-IV) inhibitors. *Bioorganic and Medicinal Chemistry Letters* , **17**: 5934-5939.

Kurukulasuriya, R., Rohde, J., Szczepankiewicz, B., Basha, F., Lai,C., Jae, H., Winn,M., Stewart ,K., Longenecker, K., Lubben, T., Ballaron, S., Sham, H. and Geldern, T. (2006). Xanthine mimetics as potent DPP-IV inhibitors. *Biooragnaic and Medicinal Chemistry Letters*, **16:** 6226-6230.

Lambeir, A., Durinx, C., Scharpe, S. and De Meester, I. (2003). DPP-IV from bench to bedside: an update on structural properties, functions, and clinical aspects of the enzyme DPP-IV. *Critical Reviews Clinical Laboratory Sciences*, **40**: 209-94.

Liang, G., Qian, X.,Biftu, T., Singh, S., Gao, Y., Scapin, G., Patel, S., Leiting,B., Patel, R., Wu, J., Zhang, X., Thornberry, N. and Weber, A. (2008). *Bioorganic* and *Medicinal Chemistry Letters*, **18**: 3706.-3711.

Luca, L., Giacomelli, M. and Taddei, J. (2001). An Easy and Convenient Synthesis of Weinreb Amides and Hydroxamates. *Organic Chemistry*, **66**: 2534-2537.

Ludvik, B., Neuffer, B. and Pacini, G. (2004). Efficacy of Ipomoea batatas (Caiapo) on diabetes control in type 2 diabetes subjects treated with diet. *Diabetes Car*e, **27** (2): 436-40.

Luna, B. and Felinglos, M. (2001). Oral Agents in the Management of Type 2 Diabetes Mellitus. *American Family Physician*, **63** (9): 1747-1757.

Magnin, D., Robl, J., Sulsky, R., Augeri, D., Huang, Y., Simpkins, L., Taunk, P., Betebenner, D., Robertson, J., Abboa-Offei, B.,Wang, A., Cap, M., Xin, L., Tao, L., Sitkoff, D., Malley, M., Gougoutas, J., Khanna, A., Huang, Q., Han, S., Parker, R. and Hamann, L. (2004). Synthesis of novel potent DPP-IV inhibitors

with enhanced chemical stability: Interplay between the N-terminal amino acid alkyl side chain and the cyclopropyl group of alpha-aminoacyl-L-*cis*-4, 5-methanopralinenitrile-based inhibitor. *Journal of Medicinal Chemistry*, **47**: 2587-2598.

Mest, H. and Mentlein, R. (2005). Dipeptidyl peptidase inhibitors as new drugs for the treatment of type 2 diabetes. *Diabetologia,* **48**(4): 616-20.

Metzler, W., Yanchunas, J., Weigelt, C., Kish, K., Klei, H.E., Xie, D., Zhang, Y., Corbett, M., Tamura, J.K., He, B., Hamann, L.G., Kirby, M.S. and Marcinkeviciene, J. (2008). Involvement of DPP-IV catalytic residues in enzyme-saxagliptin complex formation. *Protein Science*, **17**(2): 240-250.

Miller, S., Onge, E. and Taylor, J. (2008). DPP-IV inhibitors: A review of sitagliptin, vildagliptin, alogliptin, and saxagliptin. *Formulary*, **43**: 4-5.

Morrison, R. and Boyde, R. (1983). *Organic Chemistry* (5th ed.). New Jersey: Prentice Hall, Englewood Cliffs.

Mulakayala, N., Reddy, U., Iqbal, J. and Pal, M. (2010). Synthesis of DPP-IV inhibitors: a brief overview. *Tetrahedron*, **66**: 4919-4938.

Nauck, M., Meininger, G., Sheng, D., Terranella, L. and Stein, P. (2007). Efficacy and safety of the DPP-IV inhibitor, sitagliptin, compared to the sulphonylurea glipizide in patients with type 2 diabetes inadequately controlled on metformin alone: a randomised, double-blind, non-inferiority trial. *Diabetes and Obesity Metabolism*, **9**: 194–205.

Nordhoff, S., Cerezo-Gálvez, S., Feure,r A., Hill, O., Matassa, VG., Metz, G., Rummey, C., Thiemann, M. and Edwards, PJ. (2006). The reversed binding of beta-phenethylamine inhibitors of DPP-IV: X-ray structures and properties of novel fragment and elaborated inhibitors. *Bioorganic* and *Medicinal Chemistry Letters*, **16**(6): 1744-8.

Oefner, C., Arcy, A., Mac Sweeney, A., Pierau, S., Gardiner, R. and Dale, G. (2003). High-resolution structure of human apo dipeptidyl peptidase IV/CD26 and its complex with 1-[([2-[(5-iodopyridin-2-yl)amino]-ethyl]-amino)-acetyl]-2-cyano-(S)-pyrrolidine. *Acta-crystallographica. Section D, Biological Crystallography*, **59**: 1206-1212.

Ogata,S., Misumi, Y., Tsuji, E., Takami, N., Oda,K. and Ikehara,Y. (1992). Identification of the active site residues in DPP- IV by affinity labeling and site-directed mutagenesis. *Biochemistry*, **31**(9): 2582-2587.

Ooi, T., Takahashi, M., Doda, K. and Maruoka, K. (2002). Supporting information for symmetric induction in sulfonate under phase-transfer conditions: experimental evidence for the participation of an anionic pathway. *Journal of American Chemical Society*, **124** (26): 7640–7641.

Peters, J. (2007). 11 years of cyanopyrrolidines as DPP-IV Inhibitors. *Current topics in Medicinal Chemistry*, **7**: 579-595.

Pospisilik, A., Martin, J., Doty, T., Eases, J., Pamir, N., Lynn, S., Piteau, H., Demuth, C., McIntosh, C. and Pederson, R. (2003). DPP- IV inhibitor treatment stimulates β-cell survival and islet neogenesis in streptozotocin-induced diabetic rats. *Diabetes*, **52**: 741-750.

Prisant, LM. (2004). Preventing type II Diabetes Mellitus. *Journal of Clinical Pharmacology*, **44**: 406-413.

Ramajayama, R., Giridhar, R., Yadav, M., Balaraman, R., Djaballah , H., Shum,D. and Radu, C. (2008). Synthesis, antilekemic and antiplelte activities of 2, 3-diaryl-6.7-dihydro-5H-1,4 diazepines. *European Journal of Medicinal Chemistry*. **43**: 2004-2010.

Rasmussen, H., Branner, S., Wiberg, F. and Wagtmann, N. (2003). Crystal structure of human DPP- IV/CD26 in complex with a substrate analog. *Nature Structural Biology,* **10**: 19-25.

SanMartín, R., Olivera, R., Marigorta, E. and Dominguez, E. (1995). A New General Method for the Synthesis of 4-Hydroxylated 3-Arylterahydroisoquinoline. *Tetrahedr*on, **51**: 5361-5368.

Senten, K., Daniëls, L., Ven der Veken, P., De Meester, I., Lambeir, A., Scharpe, S., Haemers, A. and Augustyns, K. (2003). Rapid parallel synthesis of dipeptide diphenyl phosphonate esters as inhibitors of dipeptidyl peptidases. *Journal of Combinatorial Chemistry*, **5** (3): 336-344.

Shoichet, B. (2004). Virtual screening of chemical libraries. *Nature*, **432** (19): 862-865.

Shubrook, J., Colucci, R. and Schwartz, F. (2009). Exploration of the DPP-4 inhibitors with a focus on saxagliptin. *Expert Opinion in Pharmacother*, **10** (17): 2927-2934.

Snow, R., and Bachovchin, W. (1995). Boronic acid inhibitors of DPP-IV: a new class of immunosuppressive agents. *Advances in Medicinal Chemistry*, **3**: 149-152.

Sorbera, L., Revel, L. and Castaner, J. (2001). P32/ 98. Antidiabetic and DPP- IV inhibitor. *Drugs of Future*, **26** (9): 859-860.

Thoma, R., Loffler, B., Stihle, M., Huber, W., Ruf, A. and Hennig, M. (2003). Structural basis of praline-specific exopeptidase activity as observed in DPP-IV. *Structure*, **11:** 947-959.

Thornberry, N., and Gallwitz, R. (2009). Mechanism of action of inhibitors of DPP-IV. *Best Practice and Research Clinical Endocrinology and Metabolism*, **23**: 479-486.

Tsai, T., Coumar, M., Hsu, T., Hsieh, H., Chien, C., Chen, C., Chang, C, Lo, Y., Wu, S., Huang, C., Huang, Y., Wang, M., Wu, H., Lee, H., Chen, X., Chao, Y. and Jiaang, W. (2006). *Bioorganic and Medicinal Chemistry Letters*, **16**: 3268-3270.

Unger, R. and Eisentraut, A. (1969). Entero-insular axis. *Archives of Internal Medicine*, **123** (3): 261-266.

Villhauer, E., Brinkman, J., Naderi, G., Burkey, B., Dunning, B., Prasad, K., Mangold, B., Russel, M. and Hughes, T. (2003). 1-[[(3-Hydroxy-1-adamantyl) amino] acetyl]-2-cyano-(*S*)-pyrrolidine: a potent, selective, and orally bioavailable dipeptidyl peptidase IV inhibitor with antihyperglycemic properties. *Journal of Medicinal Chemistry, **46**:* 2774- 2789.

Vilsbøll, T. and Knop, K. (2007). DPP-IV inhibitors - current evidence and future directions. *The British Journal of Diabetes and Vascular Disease*, **7**: 9-74.

Wiedeman, P. (2007). DPP-IV Inhibition: Promising therapy for the treatment of type 2 diabetes. *Progress in Medical Chemistry,* **45**: 71-73.

Wu, J., Chen, Y., Shi, X. and Gu, W. (2009). DPP- IV inhbitors: a novel emerging target class for the treatment of type2 diabetes. *Jouranl of Nanjing Medical University*, **23**(4): 228-235.

Yip, R. and Wolfe, M. (2000). GIP biology and fat metabolism. *Life Science*, **66**: 91-103.